

tijdschrift voor
**NUCLEAIRE
GENEESKUNDE**



Special issue

Cardiovascular Imaging
A dynamic field

LUTATHERA®

INTRODUCING GEP-NETs' NEW HUNTER



▼ Dit geneesmiddel is onderworpen aan aanvullende monitoring. Daardoor kan snel nieuwe veiligheidsinformatie worden vastgesteld. Beroepsbeoefenaren in de gezondheidszorg worden verzocht alle vermoedelijke bijwerkingen te melden via het nationale meldsysteem:
Nederlands Bijwerkingen Centrum Lareb:
www.lareb.nl

Naam van het geneesmiddel:
Lutathera 370 MBq/ml oplossing voor infusie

Farmaceutische vorm:
Oplossing voor infusie. Heldere, kleurloze tot lichtgele oplossing.

De kwalitatieve en kwantitatieve samenstelling van werkzame bestanddelen:
Eén ml oplossing bevat 370 MBq lutetium (¹⁷⁷Lu)-oxodotreotide op de datum en het tijdstip van kalibratie. De totale hoeveelheid radioactiviteit per injectieflacon voor éénmalig gebruik is 7.400 MBq op de datum en het tijdstip van de infusie.

LUTATHERA® is geïndiceerd voor de behandeling van niet-resecreerbare of gemetastaseerde, progressieve, goed gedifferentieerde (G1 en G2), somatostatinereceptor-positieve gastro-entero-pancreatische neuroendocriene tumoren (GEP-NET's) bij volwassenen. www.lutathera.com

Dosering en wijze van toediening: Lutathera mag uitsluitend worden toegediend door personen die bevoegd zijn om radiofarmaceutica te hanteren in aangewezen klinische omgevingen en na evaluatie van de patiënt door een gediplomeerde arts. Alvorens de behandeling met Lutathera op te starten, moet beeldvorming van somatostatinereceptoren (scintigrafie of positronemissietomografie [PET]) de overexpressie van deze receptoren in het tumorweefsel bevestigen, waarbij de opname door de tumor ten minste even hoog moet zijn als de normale opname in de lever (tumornamescore ≥ 2). Daarnaast zijn vóór elke toediening en tijdens de behandeling, biologische tests vereist om de toestand van de patiënt opnieuw te beoordelen en het behandelprotocol indien nodig aan te passen (dosis, infusieinterval, aantal infusies). Zie de volledige SmPC voor meer informatie. Het aanbevolen behandelingsschema voor Lutathera bij volwassenen bestaat uit 4 infusies van elk 7.400 MBq. Het aanbevolen interval tussen elke toediening is 8 weken, hetgeen kan worden verlengd tot 16 weken in geval van toxiciteit waarvoor de dosis moet worden aangepast (DMT, dose modifying toxicity). Om de nieren te beschermen moet een aminozuroplossing intraveneus worden toegediend. Zie de volledige SmPC voor meer informatie. Gezien de vaste volumetrische activiteit van 370 MBq/ml op de datum en het tijdstip van kalibratie, is het volume van de oplossing aangepast tussen 20,5 ml en 25,0 ml om de vereiste hoeveelheid radioactiviteit op de datum en het tijdstip van de infusie te verschaffen. Lutathera moet worden toegediend via een langzame intraveneuze infusie gedurende ongeveer 30 minuten, tegelijk met een aminozuroplossing, via een contralaterale intraveneuze infusie (aparte intraveneuze katheter en gestart 30 minuten vóór de infusie van Lutathera). Het geneesmiddel mag niet als bolus worden geïnjecteerd. Premedicatie met anti-emetica dient 30 minuten voor de aanvang van de infusie van de aminozuroplossing te worden geïnjecteerd. De aanbevolen infusiemethode voor de toediening van Lutathera is de zwaartekraftmethode. Tijdens de toediening dienen de aanbevolen voorzorgsmaatregelen te worden genomen. Lutathera dient rechtstreeks vanuit de oorspronkelijke container te worden geïnfuseerd. De injectieflacon mag niet worden geopend en de oplossing mag niet worden overgebracht naar een andere container. Tijdens de toediening mag uitsluitend wegwerkmaterialen worden gebruikt. Het geneesmiddel dient te worden geïnfuseerd via een intraveneuze katheter die uitsluitend voor de infusie van dit geneesmiddel in deader is geplaatst. Zie de volledige SmPC voor meer informatie over opslag, ruimte en benodigdheden alsmede de gedetailleerde toedieningsprocedure. In sommige omstandigheden kan het noodzakelijk zijn om de behandeling met Lutathera tijdelijk stop te zetten, de dosis na de eerste toediening aan te passen of de behandeling zelfs te staken. **Contra-indicaties:** Contra-indicaties zijn overgevoeligheid voor de werkzame stof of voor een van de hulstoffen, vastgestelde of vermoede zwangerschap of wanneer een zwangerschap niet is uitgesloten en nierfalen met een creatinineklaring van $< 30 \text{ ml/min}$.

Bijzondere waarschuwingen en voorzorgen bij gebruik: Bijzondere voorzorgen moeten worden genomen bij patiënten met morfologische afwijkingen van de nieren of urinewegen, urine-incontinentie, lichte tot matige chronische nierziekte met een creatinineklaring van $\geq 50 \text{ ml/min}$, hematologische toxiciteit hoger dan of gelijk aan graad 2 (CTCAE) voor de behandeling anders dan lymfopenie, botmetastase of die eerder chemotherapie hebben ontvangen. Laat optredend myelodysplastisch syndroom (MDS) en acute leukemie (AL) zijn waargenomen na behandeling met Lutathera. Factoren zoals leeftijd > 70 jaar, verminderde nierfunctie, cytopenieën bij aanvang, eerder aantal behandelingen, eerdere blootstelling aan chemotherapeutische middelen (in het bijzonder alkylerende middelen) en eerdere radiotherapie worden aangegeven als mogelijke risico's en/of voorstellende factoren voor MDS/AL. Crises als gevolg van overmatige afgifte van hormonen of biologisch actieve stoffen kunnen optreden na behandeling met Lutathera, daarom dient in sommige gevallen een nacht observatie van patiënten in het ziekenhuis te worden overwogen. Regels voor bescherming tegen radioactieve straling dienen te worden gevolgd, waaronder bijzondere voorzorgsmaatregelen in het geval van extravasatie en urine-incontinentie. Zie de volledige SmPC voor meer informatie of maatregelen voor de bescherming tegen radioactieve straling. Dit geneesmiddel bevat maximaal 3,5 mmol (81,1 mg) natrium per dosis. Hiermee dient rekening te worden gehouden bij patiënten met een natriumarm dieet. **Bijwerkingen:** Vaak voorkomende bijwerkingen zijn beenmergtoxiciteit met trombocytopenie, lymfopenie, anemie of pancytopenie. Nefrotoxiciteit met hematurie, nierfalen, proteinurie. Bloedcreatineïne verhoogd, misselijkheid, braken, vermoeidheid, elektrocardiogram QT verlengd, hypertensie, overmatig blozen, hypotensie, dyspneu, abdominale distensie, diarree, abdominale pijn, constipatie, dyspepsie, gastritis, hyperbilirubinemie, alopecia, skeletspiertelselpijn, spierspasmen, acuut nierletsel, verhoogde leverfunctietesten.

Farmacotherapeutische Groep:

Overige therapeutische radiofarmaca, ATC-code: V10XX04

Houder van de vergunning voor het in de handel brengen:

Advanced Accelerator Applications

20 rue Diesel 01630 Saint Genis Pouilly Frankrijk

Nr. van de vergunning voor het in de handel brengen:

EU/1/17/1226/001

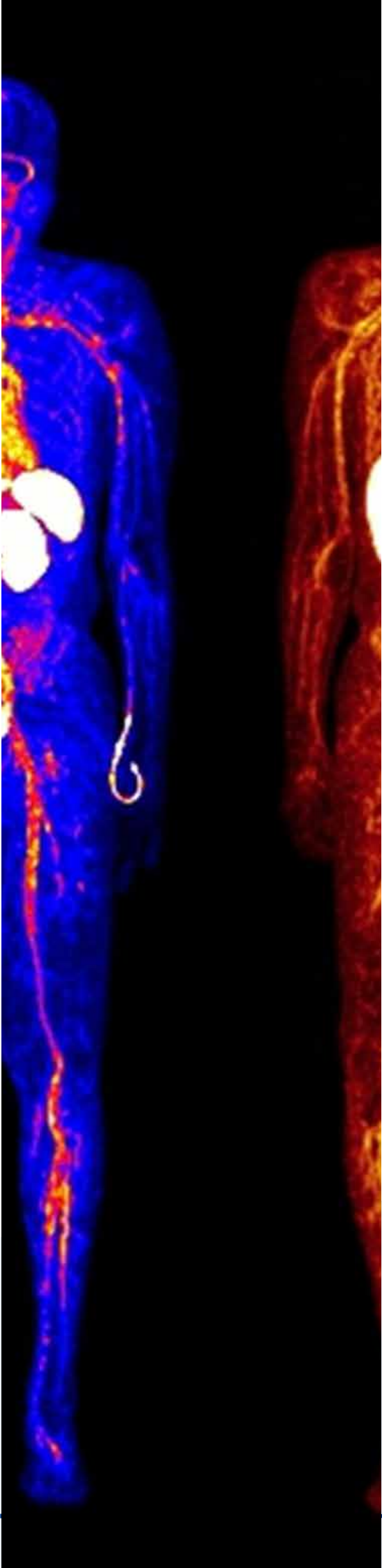
Algemene indeling voor de aflevering:

UR

Datum product informatie:

Oktober 2017





Inhoud

VOORWOORD

Cardiovascular imaging, A dynamic field

R.H.J.A. Slart, MD, PhD

1808

Implementation of a new non-invasive diagnostic strategy in the diagnosis of coronary artery disease

F.M. van der Zant, MD, PhD

1810

Rubidium-82 myocardial perfusion PET/CT

A.M. Scholtens, MD

1817

Pitfalls in myocardial blood flow quantification with rubidium-82 PET

J.D. van Dijk, MSc, PhD

1822

Nieuwe ontwikkelingen op het gebied van cardiovasculaire CT

A.M. den Harder, MD, PhD

1830

Ervaringen van de complementaire radioloog en nucleair geneeskundige

N.H.J. Prakken, MD, PhD

1836

Imaging cardiac sympathetic innervation: current clinical status

B.F. Bulten, MD, PhD

1839

Recommendation on imaging in cardiac sarcoidosis: a summary

R.H.J.A. Slart, MD, PhD

1845

¹⁸F-FDG PET/CT with clinical impact in infective endocarditis

A. Gomes, MD

1848

Diagnostic workup of giant cell arteritis; role of imaging

E. Brouwer, MD, PhD

1853

Diagnose en behandeling geïnfecteerde vaatprothesen, handvatten voor de kliniek

M. Wouthuyzen-Bakker, MD, PhD

1861

Future perspective: where is cardiovascular nuclear imaging heading?

F.M. Bengel, MD, FAHA

1868

CURSUS- EN CONGRESAGENDA

1870

CARDIOVASCULAR IMAGING

A dynamic field

Back in 2007, I was honoured to be guest-editor of the December special issue, entitled "Nucleair geneeskundige beeldvorming van het hart: stand van zaken nu en een blik in de toekomst." Now, 10 years later, I was once again asked to be guest-editor of the yearly Special Issue. I accepted this proposal promptly, as this was an ideal opportunity to look back at the changes in the field of cardiovascular imaging during the past 10 years.

In light of the developments of the last decade and in order to provide a view of the future, this special issue reflects on the current possibilities in *cardiac imaging*, which now also includes *vascular imaging*. The reader will notice the rapidity of clinical implementation of new techniques and applications. Cardiovascular imaging is a dynamic part of our profession.

Further developments have provided the bridge from cardiac to vascular imaging, as described in the article on clinical applications of FDG PET/CT in vascular graft infection detection. Subsequently, visualizing large vessel vasculitis (LVV) is the initial step towards meeting the huge unmet need for a fast diagnostic work-up including state-of-the-art imaging in LVV. Also a new application of FDG PET/CT as recommended by the ESC guidelines for the detection of endocarditis and distance septic embolism plays an important role in clinical practice, and is shared with you in this special issue. The new procedural recommendation of imaging in cardiac sarcoidosis, a successful joint initiative of several societies, is summarized, including some helpful flow-charts in the work up in cardiac sarcoidosis.

The transformation of our landscape of SPECT-CT roads for quantification of myocardial perfusion to PET/CT cardio-streets is very exciting. This change is discussed by the imaging groups of Alkmaar (¹³N-ammonia PET), Amersfoort and 's-Hertogenbosch (⁸²Rb PET). This is followed by a detailed description of how to deal with the pitfalls of ⁸²Rb PET, which have important clinical consequences.

We should not forget the current use of CT in nuclear cardiology. CT is applied in clinical practice for beneficial attenuation correction, including coronary calcium scoring and (hybrid) CT coronary angiography systems. New developments of CT, such as myocardial perfusion CT, are also ongoing and are described in this Special Issue.

The unique cross-over training for radiologists and nuclear medicine physicians in the Netherlands has also been launched in the Cardiovascular track, and experiences of two colleagues in Nuclear Medicine and Radiology are shared with you. We hope this is an example of how cross-over has synergistic effects on the collaboration between Nuclear Medicine and Radiology.

Thus far cardiac MIBG imaging has mainly been evaluated for the assessment of cardiovascular events (i.e. ADMIRE trial), but new applications of imaging the autonomic heart function with MIBG appear on the horizon, such as in cardiac amyloidosis, or for the assessment of cardiac toxicity in patients receiving severe chemotherapeutic regimens.

Finally, future perspectives in the field of cardiovascular imaging are provided by our internationally respected colleague Prof. dr. Frank Bengel, from the Medical School in Hannover, department of Nuclear Medicine in Germany.

Today, (nuclear) cardiovascular imaging is a dynamic field with a promising future, but as changes occur very rapidly, the new technical possibilities should be picked up and implemented by those active in the field. Collaboration with Radiology will promote the development of novel and existing imaging techniques, but the freedom and flexibility of research in the two domains should be respected.

I hope to meet you again in 10 years, to share with you the newest developments, and to look back on our progress.
I wish you all a prosperous 2018!

**Riemer H.J.A. Slart, MD, PhD,
UMC Groningen & University of Twente
Editor-in-chief of this Special issue**

Cover: Example of ^{18}F -interleukine-2 (^{18}F -IL2) whole body PET. Interleukin-2 (IL2) binds with high affinity to IL2 receptors overexpressed on activated T lymphocytes in various pathological conditions, including cardiovascular diseases, for instance atherosclerosis.



Implementation of a new non-invasive diagnostic strategy in the diagnosis of coronary artery disease

F.M. van der Zant, MD, PhD¹; R.J.J. Knol, MD, PhD¹; J.H. Cornel, MD, PhD²; V.A. Umans, MD, PhD²; S.V. Lazarenko, MSc, PhD¹; M. Wondergem, MD², PhD¹

Departments of ¹Nuclear Medicine and ²Cardiology, Noordwest Ziekenhuisgroep, Alkmaar, the Netherlands

Abstract

Due to technological developments and increasing availability of PET/CT systems and positron emitting isotope producing equipment, a shift from conventional myocardial perfusion scintigraphy (MPS) towards other types of non-invasive cardiac imaging is being observed. In our hospital, ^{99m}Tc-sestamibi MPS was replaced by cardiac CT and ¹³N-ammonia myocardial perfusion PET/CT in 2011 and 2013, respectively, after a gradually declining clinical interest in MPS in the preceding years. This report aims to describe the process of implementation of this renewed non-invasive diagnostic strategy for patients with chest pain in our institution, the effects it has on patient radiation burden and patient satisfaction concerning these types of cardiac imaging.

The diagnostic strategy for patients with chest pain was successfully implemented, replacing conventional MPS by more sophisticated techniques with substantially lower radiation burden. Today, both cardiac CT and ¹³N-ammonia myocardial perfusion PET/CT are used routinely and efficiently for these patients. Both types of non-invasive cardiac imaging are well tolerated and highly valued by our patients.

Introduction

Cardiac non-invasive imaging in coronary artery disease (CAD) has evolved rapidly in the past decades. Although conventional myocardial perfusion scintigraphy (MPS) using tracers such as ^{99m}Tc-tetrofosmin, ^{99m}Tc-sestamibi or ²⁰¹Thallium are still widely available and commonly used in clinical practice, hospitals that have access to a cyclotron or ⁸²Rubidium generator are gradually migrating towards myocardial perfusion Positron Emission Tomography/Computed Tomography (PET/CT), which requires ⁸²Rubidium (⁸²Rb), ¹⁵O-water ($H_2^{15}O$) or ¹³N-ammonia (¹³NH₃). Additionally, myocardial perfusion PET/CT may be combined with Calcium Scoring (CaSc) and/or Coronary Computed Tomography Angiography (CCTA) studies generated by the same system.

The diagnostic performance of both myocardial perfusion PET/CT and CCTA are claimed to outperform that of conventional MPS. Reported sensitivities and specificities for detection of CAD are 91% (_{95%}CI 83-100%) and 89% (_{95%}CI 73-100%) for PET/CT [1], and 98% (_{95%}CI 96-99%) and 85% (_{95%}CI 81-89%) for CCTA [2,3], respectively. For conventional MPS with attenuation correction, a recent meta-analysis demonstrated a sensitivity of 0.84 (_{95%}CI, 0.79-0.88) and a specificity is 0.80 (_{95%}CI, 0.74-0.85) [4] for conventional MPS with attenuation correction. Moreover, both CCTA and myocardial perfusion PET/CT can be performed in a more time-efficient manner compared to conventional MPS, while the radiation burden of both imaging procedures is typically

substantially lower than that of MPS. In the Northwest Clinics, equipped with an on-site cyclotron facility, a project was initiated to replace the conventional MPS with CCTA and ¹³N-ammonia PET/CT by collaboration between the departments of cardiology, nuclear medicine and radiology. The aim of the present report is to describe the implementation of this new non-invasive diagnostic strategy in the diagnosis of CAD.

Methods

Northwest Clinics (Noordwest Ziekenhuisgroep) is a collection of hospitals and outpatient clinics situated in the northwestern part of The Netherlands. The department of nuclear medicine is located in the large regional teaching hospital in Alkmaar and has a regional function for PET/CT imaging. The department of cardiology is equipped with a percutaneous coronary intervention (PCI) unit. In Alkmaar, a cyclotron facility was deployed mid-2012. Although this cyclotron is primarily meant for and financed by the production of the isotope fluor-18 for a variety of PET tracers such as ¹⁸F-fluorodeoxyglucose (¹⁸F-FDG), the isotope nitrogen-13 is also produced and used for ¹³N-ammonia, enabling myocardial perfusion PET/CT. In recent years, this has led to optimization of the non-invasive diagnostic strategy in the diagnosis of CAD.

Orientation phase

A committee with participants from the departments of cardiology, nuclear medicine and radiology gathered

regularly and was asked to develop a new non-invasive diagnostic strategy for the diagnosis of CAD, initially based on personal professional experience in cardiac imaging. Members of the committee then visited several, for the most part academic hospitals in both Europe and the United States. All acquired information and experiences from those visits were shared and discussed in several meetings and related to the latest available scientific literature on the topic.

Development phase

During the orientation phase it was acknowledged that essentially two clinically relevant questions in the diagnosis of CAD should be answered by the new imaging strategy. First and foremost, the imaging strategy should be able to discriminate between presence or absence of CAD. Second, an estimation of the myocardial blood flow (MBF) and coronary flow reserve (CRF) should be obtained to quantify the effects of obstructive CAD.

A combination of CaSc and CCTA was determined as the tool of interest to rule out CAD. Although CCTA can diagnose obstructive CAD, its accuracy in diagnosing obstructive CAD may be hampered by larger calcified plaques, which produce blooming artefacts, while the technique is also vulnerable to other kinds of artefacts. Although attempts have been reported in the literature [5] CT provides no widely accepted methods to determine MBF or CFR, nor does Magnetic Resonance Imaging (MRI). For MBF and CFR measurements, myocardial perfusion PET/CT has proven to be valuable and it has been used for this purpose for many years in institutions with access to a cyclotron.

Dose consideration

Due to improvements in CT-scanning equipment, the effective radiation dose of CCTA has declined over the years and can now be below 1 mSv, for instance by using dual source flash techniques and/or iterative reconstruction techniques

[6]. The effective doses resulting from myocardial perfusion PET are generally more favourable compared to MPS. While the effective dose for MPS ranges from 5.2 mSv for a single ^{99m}Tc-tetrofosmin exercise study up to 16 mSv for ²⁰¹Thallium, the equivalent dose for PET varies from 1.5 mSv to 2.1 mSv and 3.8 mSv for ¹³N-ammonia and, ¹⁵O-Water and ⁸²Rubidium, respectively [7].

¹³N-ammonia was chosen in our institution as the tracer for myocardial perfusion PET/CT since nitrogen-13 has favourable imaging characteristics, relatively low radiation burden, and a half-life of 9.96 min, which is long enough for preparation of the tracer and transportation between our cyclotron facility and PET/CT system before it is administered to the patient. It was estimated that 7 to 8 runs of the cyclotron would be sufficient to produce the necessary amount of ¹³N-ammonia to cover the envisioned patient population.

Clinical considerations

All patients who present to the cardiac outpatient clinic or cardiac emergency room receive a Duke cardiac risk score assessment. Based on this risk score the appropriate technique is chosen [8]. Symptomatic patients with low to intermediate risk for coronary disease, are considered eligible for CaSc and CCTA according to appropriate use criteria [9], whereas pregnant and lactating patients are considered not eligible. Patients allergic to intravenous radiocontrast can be scanned with caution after proper pretreatment with prednisone and clemastine. Coronary calcification can cause blooming artefacts, which may result in non-interpretable CCTA [9,10]. It has been suggested not to perform a CCTA when CaSc is exceeding 400-1000, although this particular cut-off range has not been validated [11,12]. In our current practice (see flowchart in figure) patients with CaSc > 400 are being transferred to ¹³N-ammonia PET/CT for further coronary evaluation. Patients with non-diagnostic CCTAs, for instance due to artefacts, may pro-

ceed to ¹³N-ammonia PET/CT to determine MBF and CFR, whereas patients with obstructive CAD may proceed to either ¹³N-ammonia PET/CT or CAG, depending on symptoms. Furthermore, patients are referred for ¹³N-ammonia PET/CT according to appropriate use criteria for myocardial perfusion PET [13].

Patient preparation

Patients are not allowed to smoke or to use coffee on the day of the CCTA and/or ¹³N-ammonia PET/CT acquisition. Patients are also asked to fast for 4 hours before the procedure, although water is allowed. Patients are instructed to discontinue Metformin from the day of the CCTA until 48 hours after the scan, in case of estimated glomerular filtration rate (eGFR) <60 ml/min (this value will be adjusted in the near future to comply with the upcoming revisited consensus). Also, sildenafil is disallowed within 24 hours before CCTA. On the day of the CCTA, an 18 gauge intravenous line is placed in preferably the right antecubital fossa. For ¹³N-ammonia PET/CT an intravenous line is placed in each arm. Blood pressure is recorded and an electrocardiogram (ECG) is obtained. Also, patients are asked about allergies, pregnancy, lactation, severe chronic obstructive pulmonary disease or asthma and medication use. Prior to CCTA, 100 mg atenolol is given orally when the heart rate exceeds 60 bpm and no contraindications exist. Additionally, up to 30 mg of metoprolol is administered intravenously directly before CCTA in an attempt to decrease the heart rate when a rate of <60 bpm is not accomplished after administration of atenolol, and two doses of 0.4 mg nitroglycerin are given sublingually [14]. For ¹³N-ammonia PET/CT acquisition is performed in rest and followed by a pharmacologically induced stress acquisition, using either adenosine (0.14 mg/kg/min) or 400 µg regadenoson. The imaging protocol was described in more detail in a previous report [15].

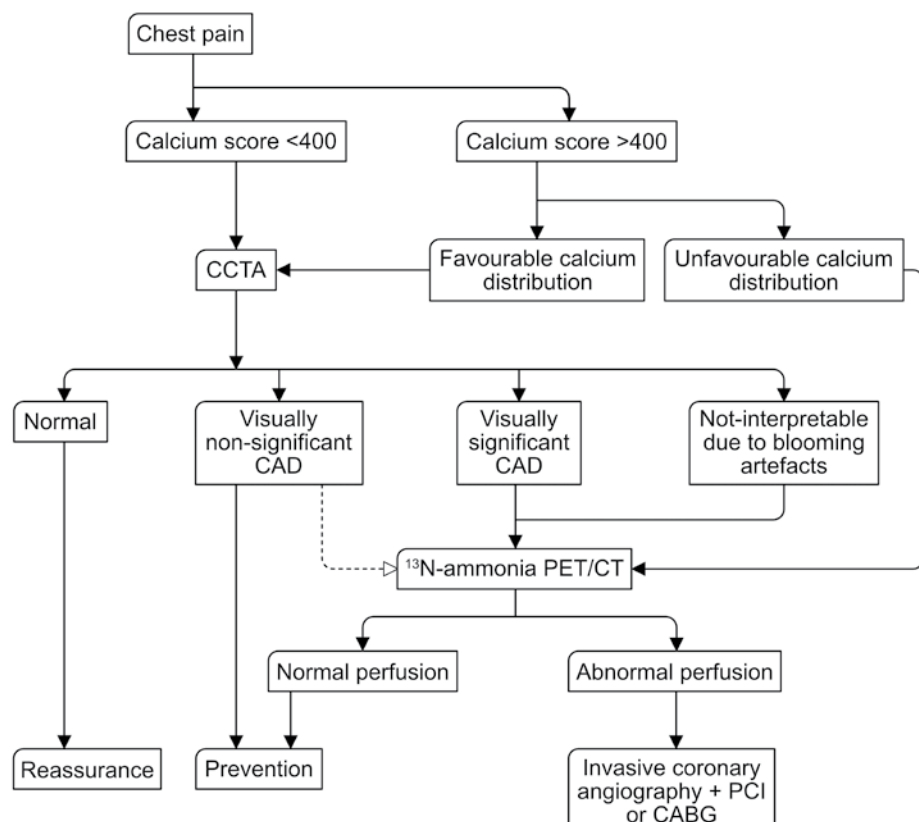


Fig. Flow chart for patients with chest pain.

Local logistics

For CCTA, a Siemens Somatom Definition Flash (Siemens Medical Systems, Erlangen, Germany) system is used on our department of nuclear medicine with a nearby patient preparation room. Directly adjacent to the department, a Cyclone® 18 Twin cyclotron is situated (IBA Cyclotron Solutions, Louvain-la-Neuve, Belgium). A total of three PET/CT scanners are present, of which two are of the Biograph TP16 type (Siemens Medical Systems, Erlangen, Germany) and these are used simultaneously when myocardial perfusion PET/CT is performed. An additional Biograph2 is used incidentally for myocardial perfusion PET/CT when necessary. A consultation room is present in the department of nuclear medicine. A cardiologist discusses the scan results with each patient directly after the CCTA procedure, and treatment adjustments are made during this consultation. Furthermore, a training facility is offered to

cardiology, radiology and nuclear medicine residents. Standardized reports are used for CaSc, CCTA and ¹³N-ammonia PET/CT studies.

Training and quality control

The technologists were trained extensively by the vendor of the scanning equipment, experienced technicians from other institutions and the local medical staff in order to acquire expertise in image acquisition, software applications and the medical background of these procedures. Cardiologists, radiologists and nuclear medicine physicians participated in a variety of cardiac CT and cardiac PET/CT courses. Several physicians, including nuclear medicine physicians, obtained level 2 certification for cardiac CT. Daily, weekly, monthly and annual quality control (QC) tests are performed in order to maintain high image quality and proper scanner performances. All results are automatically analysed and

reported. QC tests for the Somatom Definition Flash include CT check-up and calibration (daily), noise and CT number of water (weekly), light marker, topogram position and MTF (monthly) and dose calibration with CTDI phantom (annually). The quality tests of the Biograph TP16 PET/CT system include a daily PET quality test of homogeneity using a ⁶⁸Ge phantom, a daily CT check-up procedure and weekly CT quality measurements using the Siemens CT quality phantom. Moreover, maintenance is scheduled every 6 months and performed by qualified and authorized service engineers from Siemens.

The cyclotron facility (Cyclotron MCA BV) harbours the pharmacy which produces positron-emitting radiopharmaceuticals for PET/CT and prepares gamma-emitting radiopharmaceuticals for use in conventional nuclear medicine procedures. All procedures are carried out according to the European Union Guidelines to GMP (Good Manu-

factoring Practice) Eudralex Volume 4 [16]. Quality control of these radiopharmaceuticals is performed according to the European Pharmacopoeia.

Implementation

In our institution, CCTA has been operational since December 2011 and ^{13}N -ammonia myocardial perfusion PET/CT was started in September 2013. Almost all patients provided written informed consent for usage of their anonymous data for scientific use, teaching and quality assessment. Several variables are prospectively collected in a database including the scan type, age, gender, Duke Clinical Score, cardiac risk factors, scan results, estimation of the total radiation dose delivered and changes in patient management, among others.

Year-to-year trends in non-invasive cardiac imaging

In order to obtain insight in the trends in referral for the various types of non-invasive cardiac imaging studies that are performed at our department, the year-to-year numbers of scans were retrieved from the hospital database from 2007 to 2015. The total number of conventional myocardial perfusion scintigraphs, myocardial perfusion PET/CTs and CCTAs were scored for each of the study types mentioned.

Estimation of radiation dose

After each cardiac CT procedure, the radiation dose delivered to the patient

is automatically calculated and reflected as the CT dose index (CTDI_{vol}) and dose length product (DLP).

CTDI_{vol} represents the average radiation dose over a specific scanned volume. DLP equals CTDI_{vol} multiplied by scan length. The effective dose of each scan is estimated by multiplying the DLP by 0.014 mSv/mGy·cm as proposed by the European Working Group for Guidelines on Quality Criteria in CT, however the International Commission on Radiological Protection (ICRP) proposed a k-factor of 0.028 mSv/mGy·cm. [17] The total dose of topogram, test bolus tracking, CaSc, and CCTA is used to estimate the effective radiation dose for each patient. For ^{13}N -ammonia PET/CT, the effective dose is generated by multiplying the administered dose (in MBq) by 2.0×10^{-3} mSv/MBq [7]. For $^{99\text{m}}\text{Tc}$ -sestamibi the radiation dose can be estimated by multiplying the administered dose in MBq by 9.0×10^{-3} and 7.9×10^{-3} mSv/MBq for resting state and exercise according to the International Commission on Radiation Protection (ICRP) and by 1.3×10^{-2} and 9.5×10^{-3} mSv/MBq for resting state and exercise according to the Radiation Internal Dose Information Center (RIDIC), respectively [7].

The estimated effective dose was calculated for two large cohorts of patients that were referred to either cardiac CT (from 2011 until 2015) or ^{13}N -ammonia PET/CT (from 2013 until 2016), and related to the effective dose typical for $^{99\text{m}}\text{Tc}$ -sestamibi studies.

Patient satisfaction surveys

Patient satisfaction for cardiac CT was measured with a standardized survey in 2012-2013 and for ^{13}N -ammonia PET/CT in 2015. For both surveys, a series of consecutive patients were given a questionnaire directly after the procedure and questions were asked about various subjects such as the quality of the information provided, preparation prior to CCTA or ^{13}N -ammonia PET/CT and about the procedure itself. Patients were also asked to share their opinion on the fast diagnostic track of CCTA.

Statistics

Statistical Package for Social Sciences version 20 was used for descriptive statistics (percentage, median, mean and standard deviation (SD)). The one sample Kolmogorov-Smirnov test was used to test continuous data for normal distribution.

Results

Number of non-invasive imaging procedures

Table 1 displays the number of non-invasive cardiac imaging procedures; MPS, CCTA and ^{13}N -ammonia PET/CT, respectively. The number of MPS declined from 1241 in 2007 to 510 in 2013. An explanation for the decline in referral for MPS could be an increased use of coronary angiography with and without fractional flow reserve (FFR) measurements. At the end of 2013, ^{13}N -ammonia PET/CT was introduced and 90 procedures were performed in

Table 1. Year-to-year number of non-invasive imaging procedures in the Northwest Clinics from 2007-2015.

	2007	2008	2009	2010	2011	2012	2013	2014	2015
MPS*	1241	1106	1036	855	820	638	510	0	0
CCTA**	-	-	-	-	-	1056	1051	1060	790
^{13}N -ammonia PET/CT	-	-	-	-	-	-	90	747	755

*MPS = Myocardial Perfusion Scintigraphy, **CCTA = Coronary Computed Tomography Angiography

the last months of that year. In 2014 and 2015, a total of 747 and 755 myocardial perfusion PET/CTs were performed, respectively. The numbers for CCTA including CaSc are 1056, 1051, 1060 and 790 for the years 2012, 2013, 2014 and 2015, respectively. The decline of CCTAs in 2015 is the result of a temporary shortage in staff and was restored to previous levels in 2016. Over the years, in 136 patients a CaSc >400 was detected which led directly to referral for ^{13}N -ammonia PET/CT or directly to invasive coronary angiography, without performing a CCTA. The reasons for the latter were that on second thoughts these patients were re-categorized as high-risk patients by the cardiologist after the CaSc, usually due to presence of typical chest pain. Besides CCTA and CaSc, cardiac CT is also used for pulmonary vein visualization prior to ablation in patients with atrial fibrillation and incidentally for triple rule out scanning.

Patients and estimated radiation dose

From December 2011 until December 2015, a total of 3562 patients (2079 women and 1483 men, mean \pm SD age 57 \pm 10.6 years) were prospectively included in a database. Of these, 2273 received CCTA using a high-pitch helical Flash protocol in best diastolic phase, whereas 870 were scanned using prospective ECG triggering in either diastolic or systolic phase and 59 were scanned using retrospective ECG-triggering. Eight patients were scanned using a triple rule out protocol, 136 patients received CaSc without further CCTA and 208 patients were referred for pre-ablation pulmonary vein evaluation. Data on scan type or estimated radiation dose was missing in 7 patients. The mean \pm SD estimated dose for the above-mentioned cardiac CT procedures are 1.7 \pm 0.8 mSv, 4.7 \pm 2.9 mSv, 6.4 \pm 2.7 mSv, 4.8 \pm 1.7 mSv, 0.7 \pm 0.7 mSv and 3.2 \pm 1.9 mSv, respectively.

From September 2013 to March 2016 1489 patients referred for ^{13}N -ammonia PET/CT were prospectively included

in the database (710 women and 779 men, mean \pm SD age 67 \pm 9.9 years). As 300 MBq and 400 MBq ^{13}N -ammonia is used in our institution for rest state and pharmacological stress myocardial perfusion PET/CT, respectively, an effective dose of $700 \text{ MBq} \times 2.0 \times 10^{-3} \text{ mSv}/\text{MBq} = 1.4 \text{ mSv}$ is estimated for all patients receiving this type of non-invasive cardiac imaging. In 931 patients the DLP of the low dose CT for attenuation correction was registered. Of these, the mean \pm SD was $80 \pm 36 \text{ mGy} \cdot \text{cm}$ for DLP and $1.1 \pm 0.5 \text{ mSv}$ for the effective radiation dose. Previously, 700 MBq $^{99\text{m}}\text{Tc}$ -mibi for resting state MPS and 700 MBq for exercise MPS was used, resulting in an effective dose of 11.8 mSv according to ICRP and 15.7 mSv according to RIDIC, respectively.

Patient survey results

Cardiac CT survey. A total of 123/150 questionnaires were returned (M/F 27%/73%, age 36-70y, mean 60.6y, median 61y). Thirty-one percent had received no (14%) or only little (17%) information about the procedure by the referring cardiologist. However, patients graded the information provided in the brochure as largely (12%) or entirely clear (88%). All patients were satisfied with the information provided by CT-technicians before the procedure and all patients stated that the procedure had occurred entirely or largely as expected. Six percent of the patients had experienced a delay before scanning. Thirteen percent of the responders classified the administrated agents (nitroglycerin, beta-blockers or contrast agents) as inconvenient, although no severe side effects were encountered. Ninety-six percent of the patients were largely or very satisfied regarding the total duration of the fast track. On a scale of 1 to 10 (from low to high satisfaction), responders rated the fast diagnostic track with an 8.7 ± 0.84 (mean \pm SD).

^{13}N -ammonia myocardial perfusion PET/CT survey. A total of 250 questionnaires were distributed to patients

referred for ^{13}N -ammonia PET/CT from March until October 2015. Of these 250 questionnaires 117 questionnaires (60 women and 57 men) were filled out on the internet. Seventy-seven percent of patients felt they were informed adequately about the procedure by the referring cardiologist, while 15% of the patients experienced the information as inadequate and 8% did not get any information. The additional information given by the technologist prior to the procedure was judged as adequate in 97%. During adenosine or regadenoson infusion 49% experienced dyspnea, 33% chest pain and 15% nausea. The administration of ^{13}N -ammonia was not noticed by 88% of the patients. On a scale of 1 to 10 (from low to high satisfaction) 22% scored a 10, 33% a 9, 40% a 8, 4% a 7 and 1% a 6, respectively.

Discussion

Worldwide, CAD is increasing due to the rising prevalence of diabetes mellitus, obesity, and an aging patient population [18]. Non-invasive cardiac evaluation procedures for detection and follow up of CAD include exercise ECG, MPS or myocardial perfusion PET/CT, stress echocardiography, cardiac MRI, or anatomical imaging by cardiac CT. In our institution, we successfully replaced MPS by ^{13}N -ammonia and CCTA, with the aim to improve the diagnosis with less radiation burden for patients of certain categories, such patients with a low-to-intermediate risk for significant CAD. Especially in women, CAD can lead to atypical symptoms and non-invasive techniques that can accurately rule out CAD are warranted in this patient category [19].

Between 2007 and 2011, before the introduction of ^{13}N -ammonia myocardial perfusion PET/CT, a gradual decline in MPS was noticed. While more invasive studies (coronary angiography including flow measurements) were performed in patients during those years, cardiologists, nuclear medicine physicians and radiologists teamed up

as a taskforce to plan a less invasive clinical pathway for patients with suspected CAD or to rule out CAD. After implementation of CCTA and ¹³N-ammonia myocardial perfusion PET/CT, locally known as the 'cardiac street', an increase in usage has been observed, with the exception of the year 2015, for earlier mentioned reasons. In particular, the number of ¹³N-ammonia PET/CTs performed has increased in 2016 and 2017.

Both CCTA and ¹³N-ammonia PET/CT are tolerated well and appreciated by patients, especially the fast diagnostic track for CCTA in which patients receive a diagnosis and treatment plan from a cardiologist directly after performing the CT and the associated analysis. Although both adenosine and regadenoson produce temporary side-effects, patients are generally satisfied concerning the ¹³N-ammonia myocardial perfusion PET/CT, which is done within half an hour (both rest state and stress acquisitions), and which has been shown to have a better diagnostic performance compared to conventional MPS, while the exposure to ionizing radiation to patients is substantially lower.

Before implementation of CCTA and ¹³N-ammonia PET/CT, our department used 700 MBq ^{99m}Tc-sestamibi for resting MPS and 700 MBq for exercise MPS, resulting in an effective dose of 11.8 mSv according to ICRP and 15.7 mSv according to RIDIC. Using the newer, non-invasive techniques the effective radiation dose has been reduced to 1.4 mSv (¹³N-ammonia) plus 1.1±0.5 mSv (attenuation CT) for myocardial perfusion PET/CT and to 1.7±0.8 mSv, 4.7±2.9 mSv, 6.4±2.7 mSv for CCTA plus CaSc plus topogram for high pitch Flash, prospective CCTA and retrospective CCTA. Medical imaging examinations are estimated to produce a stochastic extrapolated lifetime 1 in 2000 risk of developing fatal cancer when an effective dose of 10 mSv is delivered, which is >10-fold lower than the lifetime risk of dying in a motor vehicle accident (in the USA) and also substantially lower

than dying in a pedestrian accident or by drowning [20]. Although these estimations, which are based on the linear non-threshold model as proposed in the BEIR VII report, have been a matter of debate for low effective doses [21-23], it still makes sense to hold on to the ALARA (as low as reasonably achievable) principle in non-invasive cardiac imaging, especially in younger patients and women with low risk for significant CAD.

Conclusion

A new diagnostic strategy for patients with chest pain was successfully implemented in our department, replacing conventional MPS by more sophisticated techniques with substantially lower radiation burden. Today, both cardiac CT (CCTA and CaSc) and ¹³N-ammonia myocardial perfusion PET/CT are used routinely and efficiently for these patients. Both types of non-invasive cardiac imaging are well tolerated and highly valued by our patients.

Acknowledgments

The authors wish to thank Jackeline Sombroek-Appel for her assistance in the patient satisfaction surveys.

f.m.vander.zant@nwz.nl ♦

References

1. Naya M, Di Carli MF. Myocardial perfusion PET/CT to evaluate known and suspected coronary artery disease. *Q J Nucl Med Imaging* 2010;54(2):145-56.
2. Hulten EA, Carbonaro S, Petrillo SP, Mitchell JD, Villines TC. Prognostic value of cardiac computed tomography angiography a systematic review and meta-analysis. *J Am Coll Cardiol* 2011;57(10):1237-47.
3. Ollendorf DA, Kuba M, Pearson SD. The diagnostic performance of multi-slice coronary computed tomography angiography: a systematic review. *J Gen Intern Med* 2011;26(3):307-16.
4. Huang JY, Huang CK, Yen RF et al. Diagnostic Performance of Attenuation-Corrected Myocardial Perfusion Imaging for Coronary Artery Disease: A Systematic Review and Meta-Analysis. *J Nucl Med* 2016 dec; 57(12):1893-98.
5. Choi AD, Joly JM, Chen MY, Weigold WG. Physiologic evaluation of ischemia using cardiac CT: current status of CT myocardial perfusion and CT fractional flow reserve. *J Cardiovasc Comput Tomogr* 2014 Jul-Aug;8(4):272-81.
6. Duarte R, Bettencourt N, Costa JC, Fernandez G. Coronary computed tomography angiography in a single cardiac cycle with a mean radiation dose of approximately 1 mSv: initial experience. *Rev Port Cardiol* 2010 Nov;29(11):1667-76.
7. Stabin MG. Radiopharmaceuticals for nuclear cardiology: radiation dosimetry, uncertainties and risk. *J Nucl Med* 2008;49:1555-63.
8. Umans V, Knol R, van der Zant FM, Cornel JH. Effectiever behandelen door precisiediagnose. *Medisch Contact* 2016 jun;22:18-20
9. Taylor AJ, Cerqueira M, Hodgson JM, et al. ACF/SCCT/ACR/AHA/ASE/ASNC/NASCI/SCAI/SCMR 2010 Appropriate Use Criteria for Cardiac Computed Tomography. A Report of the American College of Cardiology Foundation Appropriate Use Criteria Task Force, the Society of Cardiovascular Computed Tomography, the American College of Radiology, the American Heart Association, the American Society of Echocardiography, the American Society of Nuclear Cardiology, the North American Society for Cardiovascular Imaging, the Society for Cardiovascular Angiography and Interventions, and the Society for Cardiovascular Magnetic Resonance. *J Cardiovasc Comput Tomogr*

- 2010;4:407.e1-33.
10. Cordeiro MA, Miller JM, Schmidt A, et al. Non-invasive half millimetre 32 detector row computed tomography angiography accurately excludes significant stenoses in patients with advanced coronary artery disease in high calcium scores. *Heart* 2006;92:589-97.
 11. Pundziute G, Schuijf JD, Jukema JW, et al. Impact of coronary calcium score on diagnostic accuracy of multislice computed tomography coronary angiography for detection of coronary artery disease. *J Nucl Cardiol* 2007;14:36-43.
 12. Abbara S, Arbab-Zadeh A, Callister TQ et al. SCCT guidelines for performance of coronary computed tomographic angiography: A report of the Society of Cardiovascular Computed Tomography Guidelines Committee. *Cardiovasc Comput Tomogr* 2009;3:190-204.
 13. http://www.snm.org/docs/PET_PROS/ardiacPracticeGuidelinesSummary.pdf. Accessed Sept 11th 2017.
 14. Bogaard K, van der Zant FM, Knol RJ et al. High-pitch prospective ECG-triggered helical coronary computed tomography angiography in clinical practice: image quality and radiation dose. *Int J Cardiovasc Imaging* 2015 Jan;31(1):125-33.
 15. Kan H, Knol RJ, Lazarenko SV et al. Occurrence of typical perfusion defects attributed to jailed or occluded side branch after ramus descendens anterior stenting in a patient cohort referred for $^{13}\text{NH}_3$ myocardial PET/CT. *Nucl Med Commun.* 2016 May;37(5):480-6.
 16. http://ec.europa.eu/health/documents/eudralex/vol-4/index_en.htm. Accessed Sept 11th 2017.
 17. Christner JA, Kofler JM, McCollough CH. Estimating effective dose for CT using dose-length product compared with using organ doses: Consequences of adopting International Commission on Radiological Protection publication 103 or dual-energy scanning. *AJR Am J Roentgenol* 2010;194:1404.
 18. Okrainec K, Banerjee DK, Eisenberg MJ. Coronary artery disease in the developing world. *Am Heart J* 2004;148:7e15.
 19. Mosca L, Mochari-Greenberger H, Dolor RJ, et al. Twelve year follow-up of American women's awareness of cardiovascular disease risk and barriers to heart health. *Circ Cardiovasc Qual Outcomes* 2010;3:120-127.
 20. Meinel FG, Nance JW, Harris BS, et al. Radiation risks from cardiovascular imaging tests. *Circulation* 2014;130:442-445.
 21. National Research Council, Committee to Assess Health Risks from Exposure to Low Levels of Ionizing Radiation. Health risks from exposure to low levels of ionizing radiation:BEIR VII phase 2. Washington, DC: National Academies Press, 2006.
 22. American Association of Physicists in Medicine. AAPM position statement on radiation risks from medical imaging procedures (policy number PP 25-A; 2011). Available at <https://www.aapm.org/org/policies/details.asp?id=318&type=PP> Accessed Sept 11th 2017.
 23. Health Physics Society. Radiation risk in perspective: Position statement of the Health Physics Society. July 2010. Available at http://hps.org/documents/risk_ps010-2.pdf Accessed Sept 11th 2017.

Rubidium-82 myocardial perfusion PET/CT

A.M. Scholtens, MD¹; P.C. Barneveld, MD²

Departments of Nuclear Medicine of ¹Meander Medical Center, Amersfoort, the Netherlands, and ²Jeroen Bosch Hospital, 's-Hertogenbosch, the Netherlands

Summary

Scholtens AM, Barneveld PC. Rubidium-82 myocardial perfusion PET/CT.

Myocardial perfusion imaging (MPI) with Technetium-based compounds is the mainstay for nuclear cardiology in the Netherlands based primarily on its availability, with PET MPI only performed in certain hospitals with cyclotron-generated radiopharmaceuticals such as N-13 ammonia or O-15 water. In recent years, Rubidium-82 (a generator-based positron emitter) PET has become the standard modality for MPI in two hospitals in the Netherlands: the Jeroen Bosch Hospital and the Meander Medical Center. In this article we describe the general aspects of imaging with this tracer.

Introduction

Historically and into the present day, single photon emission computed tomography (SPECT) and more recently SPECT/CT have been the workhorse modality for nuclear myocardial perfusion imaging (MPI). It is a widely available and validated non-invasive test to diagnose coronary artery disease, stratify risk, predict outcomes, guide patient management, and control costs (1-5). Positron emission tomography (PET) MPI has thus far been constrained to a limited number of centres, mostly due to the need for a cyclotron to produce the necessary short-lived radiotracers: N-13 ammonia ($^{13}\text{NH}_3$) and O-15 water (H_2^{15}O).

Recently, the generator-based radio-

tracer Rubidium-82 (^{82}Rb) has been of increasing interest in the Netherlands as PET-based imaging, with its intrinsically preferable properties compared to SPECT in general and in the setting of MPI in particular, becomes attractive even in non-academic centres. ^{82}Rb has been in use as the standard MPI at the Jeroen Bosch Hospital since 2012 with an automatic-operating-generator constructed by dr. R.A.M.J Claessens and in the Meander Medical Center since 2014 using the commercially available Bracco generator.

Tracer aspects

The rubidium-generator (figure 1) contains accelerator-produced strontium-82 (^{82}Sr) adsorbed on stannic oxide in a lead-shielded column and provides a means for obtaining solutions of ^{82}Rb in the chemical form of rubidium chloride ($^{82}\text{RbCl}$). ^{82}Sr decays to ^{82}Rb with a ^{82}Sr half-life of 25 days (600 hrs). The ^{82}Sr is produced in an accelerator by proton spallation of molybdenum, Mo (p, spall) ^{82}Sr or by the reaction ^{85}Rb (p, 4n) ^{82}Sr . The ^{82}Sr produced

has no carrier added. ^{82}Rb in turn decays by positron emission and associated gamma emission with a physical half-life of 75 seconds.

Compared to the other PET-tracers available, ^{82}Rb has a high-energy positron with considerably longer maximum and mean ranges before annihilation occurs (table 1). As spatial resolution degrades as the kinetic energy increases (6), ^{82}Rb has the lowest spatial resolution of the commonly available PET-tracers. Nevertheless, its spatial resolution still outperforms common SPECT imaging and this lower spatial resolution means that there is less of a learning curve when moving from SPECT MPI to ^{82}Rb PET MPI; compared to $^{13}\text{NH}_3$ images, where regional differences in myocardial thickness (especially near the apex) are more pronounced, ^{82}Rb images are "SPECT-like" in appearance (figure 2) but at a decidedly higher image quality (7,8).

Stress testing and acquisition

Due to the short half-life of ^{82}Rb and the need to image the influx-phase



Figure 1. Rubidium infusion system next to the PET camera in the Meander Medical Center.

Table 1. Properties of available PET MPI tracers.

pharmaceutical	isotope	half-life	production	physiology	positron range (mm in H ₂ O)	
					mean	
					max.	
rubidium	⁸² Rb	76 seconds	generator	extracted/retained	5.9	17.0
water	¹⁵ O	122 seconds	cyclotron	freely diffusible	3.0	8.4
ammonia	¹³ N	10 minutes	cyclotron	diffusible/retained	1.8	5.5
acetate	¹¹ C	20 minutes	cyclotron	extracted/metabolized	1.2	4.2

from the blood pool into the myocardium for flow measurements, all aspects of ⁸²Rb PET MPI need to be performed inside the PET camera. As patients need to remain as motion-free as possible, ergometric stress testing is not feasible and patients are stressed through pharmacological means. The most common protocols employ either adenosine or regadenoson, both vasodilating agents. The largest advantage of adenosine is its low cost and the large body of experience using it as a pharmacological stressor. Downsides are the need for constant infusion during the stress test, necessitating two IV lines (one for adenosine, one for ⁸²Rb infusion) and side-effects, most notably advanced conduction blocks and hyperreactivity in asthma patients. Due to the short biological half-life of approximately ten seconds, such side-effects are usually self-limiting after cessation of adenosine administration.

Regadenoson is a selective A2A adenosine receptor agonist which elicits fewer side-effects and can be administered as a slow bolus, making it feasible to perform the stress test with only one IV line. Its greatest drawback is its cost, approximately fifty times that of adenosine. That cost is partially recovered through reduced costs for other materials and an increase in scan-time efficiency.

Acquisition

Acquisition protocols for ⁸²Rb MPI are outlined in figure 3.

Using adenosine a stress-rest protocol can be used because of the shorter half-life of adenosine. With regadenoson, acquisition starts with the rest perfusion scan. In short, a topogram is acquired to ascertain the position of the heart, followed by a non-triggered low dose CT for attenuation correction. Rest perfusion images are acquired directly

after, over a period of seven minutes. Three minutes later, when the generator has generated sufficient ⁸²Rb and the rest activity has decayed sufficiently, the pharmacological stressor is administered and stress imaging begins. During these acquisitions the low dose CT can be checked for errors such as breathing artefacts, and if judged inadequate for attenuation correction a second CT can be acquired at the end of the protocol.

There is no stress-only protocol as the combined radiation dose of the stress and rest ⁸²Rb dose together is approximately 2.8 mSv, nearly half of the radiation dose of a stress-only ^{99m}Tc SPECT examination, and the entire stress-rest or rest-stress protocol can be performed within 45 minutes as opposed to common two-day protocols for SPECT MPI, with each visit taking up to three hours.

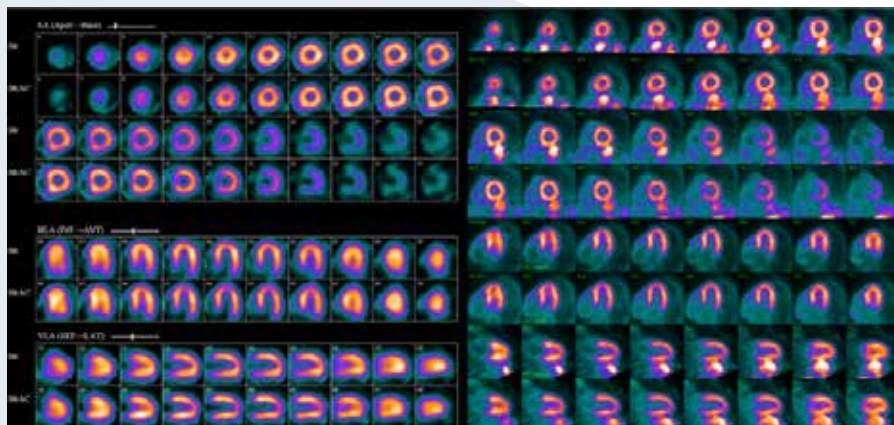


Figure 2. Comparison of stress-only ^{99m}Tc-tetrofosmin SPECT (without and with attenuation correction, left) and stress-rest ⁸²Rb PET MPI in the same patient. Although spatial resolution of the PET images is better, the images are essentially comparable.

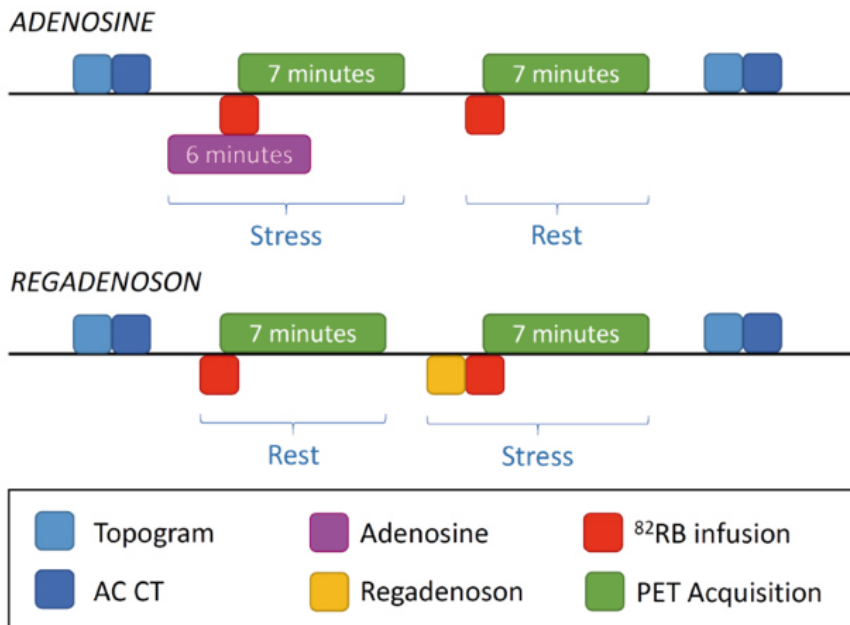


Figure 3. Acquisition protocols for ^{82}Rb PET MPI.

Reconstruction

7-minute list mode acquisitions of both the rest and the stress images are reconstructed into multiple subsets:

- A dynamic subset for flow quantification of the first five minutes, reconstructed as one 10 second frame, eight 5 second frames, three 10 second frames, two 20 second frames and three 60 second frames
- Static perfusion images containing the information from 2.5 - 7 minutes
- Gated images containing the information from 1.5 - 7 minutes

All images are attenuation corrected, with an additional non-corrected reconstruction of the static images.

Quantification of flow

The technical aspects of PET/CT perfusion quantification will be discussed in detail in the article by Van Dijk et al. elsewhere in this issue. Briefly, by measuring the input function at the level of the left ventricle lumen, measuring uptake into the myocardium and taking into account the single-compartment model for ^{82}Rb , blood flow at the level of the myocardium can be calculated in millilitres per gram per minute (mL/g/

min). Normal ^{82}Rb -values for rest flow are between 0.8 and 1.2 mL/g/min after correction for the rate pressure product, the product between the systolic blood pressure and heart rate, which should be normalised to 8000. During vasodilation, flow should increase to at least 2.0 mL/g/min, with coronary flow reserve (CFR, expressed as stress flow/ rest flow) preferably above 2.5.

Clinical implementation

With greater image quality and robust flow quantification, the interpretability of ^{82}Rb PET MPI is superior to standard SPECT MPI. A meta-analysis by McArdle et al. (8) showed superior diagnostic accuracy for ^{82}Rb PET over $^{99\text{m}}\text{Tc}$ SPECT MPI. Even though contemporary, state-of-the-art SPECT studies with attenuation correction were included for the analysis and ^{82}Rb imaging did not include flow quantification, ^{82}Rb PET still outperformed $^{99\text{m}}\text{Tc}$ SPECT with a pooled sensitivity of 90% versus 85%, pooled specificity of 88% versus 85%, and an area under the summary receiver-operating characteristic curve of 0.95 versus 0.91. Although SPECT MPI performed better under these stringent inclusion criteria than in many

larger meta-analyses, it could not match ^{82}Rb PET.

Additionally, a meta-analysis by Jaarsma et al. which included SPECT, MRI and PET imaging for coronary artery disease concluded that PET as a modality had the highest accuracy and area under the curve (3).

As visual and semi-quantitative analyses (both for SPECT MPI and ^{82}Rb PET MPI) are based on the relative regional differences between areas of the left ventricle in a (stress or rest) scan, and differences in regional distribution between rest and stress images, they are prone to underdiagnose diffuse flow abnormalities as these are normalised in the scale. Through absolute quantification of flow, this confounding factor is neutralised. However, as measurements are performed on the level of the myocardium, it is not possible to differentiate multivessel epicardial disease which requires invasive treatment from microvascular disease that will not benefit from epicardial procedures. It seems justified that these patients receive coronary angiography to exclude significant epicardial coronary disease, at which point microvascular disease may be set

Table 2. Radiation dose for adults in cardiac nuclear imaging with technetium-compounds and rubidium.

tracer	half-life	procedure	effective dose ($\mu\text{Sv}/\text{MBq}$)	dose, MBq	effective dose, mSv
$^{99\text{m}}\text{Tc}$ -sestamibi	6 h	rest	9.0	700-900	6.3-8.1
		stress	7.9	700-900	5.5-7.1
$^{99\text{m}}\text{Tc}$ -tetrofosmin	6 h	rest	7.6	700-900	5.3-6.8
		stress	7.0	700-900	4.9-6.3
^{82}Rb	76 s	rest/stress	1.25	1100-1500	1.4-1.9

as the final diagnosis.

Quantitative perfusion analysis adds prognostic information, also in patients without perfusion abnormalities (9). Additionally, even if ischaemia is visible by visual and semi-quantitative means, flow measurements may show abnormalities in visually normal flow territories (figure 4), essentially "upgrading" patients from single vessel to multivessel disease with its concomitant adverse effect on prognosis (10). Parkash et al. reported larger defect sizes in 3-vessel disease with quantification ($69 \pm 24\%$) as opposed to relative analysis ($44 \pm 18\%$, $p=0.008$) (11).

Another advantage of PET MPI is that gated acquisition is performed at stress and rest. Although this is mostly a vasodilation stress, information of the contractile function both at peak stress and

in rest are obtained. This provides extra information in the same study.

Ziadi et al. demonstrated that ^{82}Rb -based CFR measurement was an independent predictor of 3-vessel disease which showed a higher diagnostic sensitivity for multivessel involvement (88%) than combined other risk factors such as reduced ejection fraction at peak stress, trans ischaemic dilatation and ECG changes (60%) (12).

When convenient, acquisition can easily be extended with a calcium score CT or even a coronary angio CT to provide even more information.

Radiation exposure

As mentioned earlier, ^{82}Rb PET has a lower radiation burden than common $^{99\text{m}}\text{Tc}$ SPECT imaging (table 2), although dose reduction in SPECT MPI is a field

in motion with lower possible doses reported through the use of dedicated camera types such as multi-pinhole cadmium zinc telluride camera systems. The entire rest-stress protocol performed with $2 \times 1110 \text{ MBq}$ ^{82}Rb and low dose CT for attenuation correction can be performed at a radiation dose of approximately $2.8 + 0.4 = 3.2 \text{ mSv}$ as opposed to doses upwards of 12-14 mSv for common comparable SPECT/CT protocols (5,13,14).

Additionally, as the maximum dose is delivered during the scan itself and dissipates quickly due to the short half-life of ^{82}Rb , the total dose per examination for the imaging technicians is also significantly reduced (15).

Future perspectives

The current gold standard for ob-

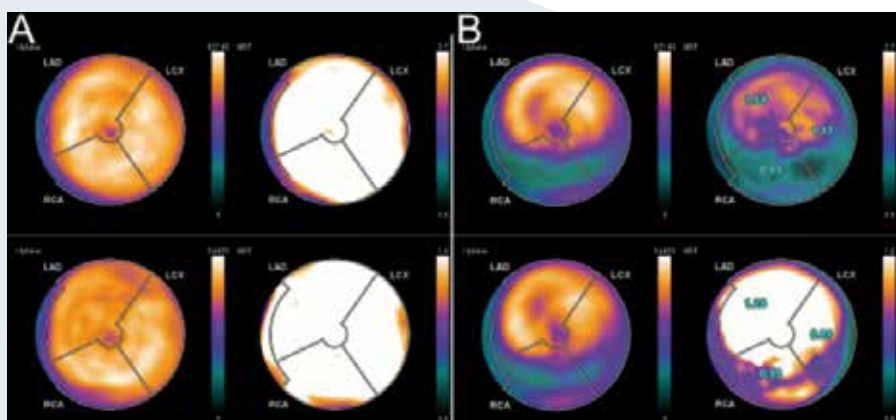


Figure 4. A: Normal perfusion on relative (left) and quantitative (right) bull's eye plots. B: Relative images indicate inferior wall infarction with minimal ischaemia, but quantitative analysis shows diffuse hypoperfusion of the entire left ventricle during stress, indicative of significant three vessel disease. Upper row: stress images, lower row: rest images.

structive coronary disease is invasively measured fractional flow reserve (FFR) which measures the decrease in pressure over a single stenotic lesion. As PET flow measurements are performed at the level of the myocardium, they take into account all flow reducing stenoses in the course of a coronary vessel. It is possible that consecutive lesions that, each on their own, only show moderate abnormalities on FFR may together produce a significant flow reduction at the level of the myocardium. Currently no conclusive data on this phenomenon exists but when flow measurements become more widely available further research regarding the relation between PET flow measurements and FFR measurements could and should be performed.

Conclusion

^{82}Rb PET MPI outperforms SPECT MPI in image quality, diagnostic accuracy and both time and radiation burden for the patient and personnel, without the need for a cyclotron on-site. It allows for quantitative measurement of myocardial blood flow, which has additional clinical value over visual and semi-quantitative analysis alone.

a.scholtens@meandermc.nl ♦

References

- International Atomic Energy Agency. Nuclear cardiology: Its role in cost effective care. Vienna: International Atomic Energy Agency; 2012
- Hachamovitch R, Hayes SW, Friedman JD, Cohen I, Berman DS. Comparison of the short-term survival benefit associated with revascularization compared with medical therapy in patients with no prior coronary artery disease undergoing stress myocardial perfusion single photon emission computed tomography. *Circulation*. 2003;107:2900-7
- Jaarsma C, Leiner T, Bekkers SC, et al. Diagnostic performance of non-invasive myocardial perfusion imaging using single-photon emission computed tomography, cardiac magnetic resonance, and positron emission tomography imaging for the detection of obstructive coronary artery disease: A meta-analysis. *J Am Coll Cardiol*. 2012;59:1719-28
- Metz LD, Beattie M, Hom R, et al. The prognostic value of normal exercise myocardial perfusion imaging and exercise echocardiography: A meta-analysis. *J Am Coll Cardiol*. 2007;49:227-37
- Ghotbi AA, Kjaer A, Hasbak P. Review: Comparison of PET rubidium-82 with conventional SPECT myocardial perfusion imaging. *Clin Physiol Funct Imaging*. 2014;34:163-70
- Beanlands RS, Youssef G. Diagnosis and prognosis of coronary artery disease: PET is superior to SPECT: Pro. *J Nucl Cardiol*. 2010;17:683-95
- Bateman TM, Heller GV, McGhie AI, Friedman JD, Case JA, Bryngelson JR, et al. Diagnostic accuracy of rest/stress ECG-gated rb-82 myocardial perfusion PET: Comparison with ECG-gated tc-99m sestamibi SPECT. *J Nucl Cardiol*. 2006;13:24-33
- Mc Ardle BA, Dowsley TF, de-Kemp RA, Wells GA, Beanlands RS. Does rubidium-82 PET have superior accuracy to SPECT perfusion imaging for the diagnosis of obstructive coronary disease?: A systematic review and meta-analysis. *J Am Coll Cardiol*. 2012;60:1828-37
- Farhad H, Dunet V, Bachelard K, et al. Added prognostic value of myocardial blood flow quantitation in rubidium-82 positron emission tomography imaging. *Eur Heart J Cardiovasc Imaging*. 2013;14:1203-10
- Saraste A, Kajander S, Han C, Nesterov SV, Knuuti J. PET: Is myocardial flow quantification a clinical reality? *J Nucl Cardiol*. 2012;19:1044-59
- Parkash R, deKemp RA, Ruddy TD, et al. Potential utility of rubidium 82 PET quantification in patients with 3-vessel coronary artery disease. *J Nucl Cardiol*. 2004;11:440-9
- Ziadi MC, Dekemp RA, Williams K, et al. Does quantification of myocardial flow reserve using rubidium-82 positron emission tomography facilitate detection of multivessel coronary artery disease? *J Nucl Cardiol*. 2012;19:670-80
- Senthamiczhelvan S, Bravo PE, Lodge MA, et al. Radiation dosimetry of ^{82}Rb in humans under pharmacologic stress. *J Nucl Med*. 2011;52:485-91
- Di Carli MF, Murthy VL. Cardiac PET/CT for the evaluation of known or suspected coronary artery disease. *Radiographics*. 2011;31:1239-54
- Tout D, Davidson G, Hurley C, et al. Comparison of occupational radiation exposure from myocardial perfusion imaging with Rb-82 PET and Tc-99m SPECT. *Nucl Med Commun*. 2014;35:1032-7

Pitfalls in myocardial blood flow quantification with rubidium-82 PET

J.D. van Dijk, MSc, PhD¹; P.L. Jager, MD, PhD¹; J.A. van Dalen, MSc, PhD²

Departments of ¹Nuclear medicine and ²Medical physics, Isala hospital, Zwolle, the Netherlands

Abstract

Absolute myocardial blood flow (MBF) quantification with rubidium-82 (⁸²Rb) PET is increasingly used and is of clear added value in clinical practice. However, in order to achieve its full potential and to produce consistent and accurate results, users should be aware that for example the type of PET system, dynamic sampling, and image reconstruction and post-processing settings can all significantly influence the MBF measurements. These influences limit the comparability of MBF measurements across centres. And although the other important parameter, the coronary flow reserve (CFR), is less influenced by such variability, the test-retest variability is still imperfect and creates a grey area around the CFR threshold. In this manuscript we highlight the most important choices, underlying assumptions and technical pitfalls when performing ⁸²Rb PET imaging and place the MBF measurements into clinical context.

Introduction: added value of myocardial PET quantification

The use of positron emission tomography with computed tomography (PET/CT) for myocardial perfusion imaging (MPI) including absolute myocardial blood flow (MBF) quantification is increasing (1, 2). This increase is not only due to better temporal and spatial resolution of PET as compared to SPECT but also to the increased availability of PET/CT systems and introduction of strontium-82/rubidium-82 (⁸²Sr/⁸²Rb) generators (3-5). These generators allow PET MPI without a cyclotron, as is required when using nitrogen-13 ammonia (¹³NH₃), oxygen-15 (¹⁵O) water, or possibly in the near future fluor-18 labelled flurpiridaz (6). MBF quantification provides relevant clinical information which can increase the diagnostic accuracy (7, 8). However, in order for absolute MBF quantification to achieve its full clinical potential, it must be well understood and standardized so that consistent and accurate results can be routinely produced across different

centres (9). There are multiple pitfalls when adopting PET based MBF quantification into clinical practice. In this manuscript we focus on MBF quantification with ⁸²Rb PET. First we provide a technical background and then highlight the most important choices and pitfalls. Finally, we place the MBF quantification with ⁸²Rb PET into clinical context.

Technical background

The MBF can be calculated in absolute terms (millilitre blood per gram myocardial tissue per minute) by acquiring a dynamic PET scan of the myocardium, followed by reconstructions of multiple images using different time frames. The acquisition is initiated upon administration of the activity and reconstructed data are used as an input for a kinetic model. To calculate the MBF, the model requires at least two inputs: the tracer activity concentration in the left ventricle (blood pool) and the tracer concentration in the myocardium over time. These inputs are typically derived

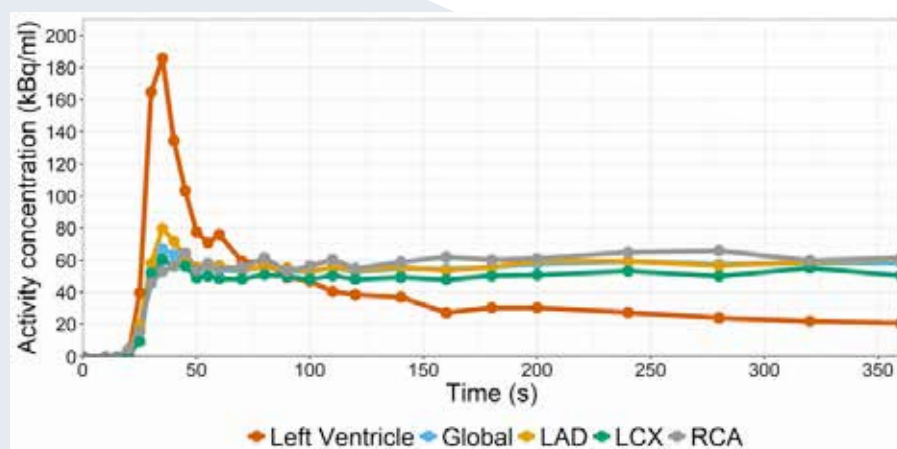


Figure 1. Example of a decay corrected time-activity curve of a dynamic stress ⁸²Rb PET examination showing the activity concentration in the left ventricle (blood pool), in the whole myocardial wall (global) and the three vascular trajectories: left anterior descending (LAD), left circumflex (LCX) and right coronary artery (RCA). The activity bolus, indicating the first-pass, is clearly visible in the left ventricle around 40s post injection and this peak is also visible in the myocardium. Next, the activity in the left ventricle decreases whereas the activity is retained by the myocardium.

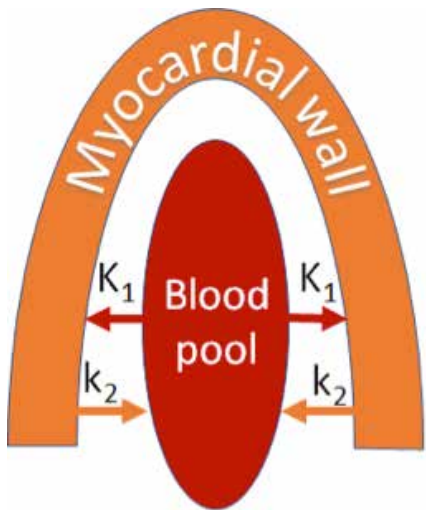


Figure 2. Schematic representation of a one-compartment model with the blood pool as arterial input, the myocardial wall as compartment, K₁ explaining the tracer uptake in the myocardial wall and k₂ the washout from the myocardial wall to the blood.

from the reconstructed images by measuring the activity concentrations in the left ventricle and myocardium in each time frame using a region of interest (ROI). These measurements lead to time activity curves (TACs) of the blood pool and (a segment of) the myocardium, as illustrated in figure 1.

Kinetic modelling

The most commonly used kinetic model for ⁸²Rb MBF quantification is the one-tissue compartment model, as illustrated in figure 2. This model uses the activity concentrations in the blood pool (in kBq/mL) and myocardium (in kBq/g) as input and is used to derive two parameters: K₁, which indicates the tracer uptake from the blood pool (ventricle) to the myocardium, and k₂, the washout from the myocardium to the blood. Both parameters can be derived by fitting the model to the TACs. The MBF can be derived from K₁ when correcting for the tracer- and model-specific extraction fraction. ⁸²Rb is not a perfect flow tracer as it does not accumulate in the myocardium

linearly proportional to perfusion. The extraction of ⁸²Rb from the blood decreases curvilinear with increasing flow rates and is around 40% for MBF>2 mL/g/min, as shown in figure 3. This is commonly known as the roll-off phenomenon. The MBF is therefore always underestimated with increasing flows when not correcting for this phenomenon. Furthermore, one should also correct for the limited resolution of the PET systems. The main correction is for partial volume effects (illustrated in figure 4): the loss of apparent activity in small regions or on edges because of the limited resolution of the PET scanner, the large positron range of ⁸²Rb and respiratory and cardiac motion. A geometrical correction model can be used to compensate for this effect. This correction model assumes that the myocardial wall has a fixed thickness and the arterial input is accurately known. However,

as the thickness of the myocardial wall differs between patients and the blood pool activity concentration measurements can be hampered by noise, partial volume correction also introduces additional variation to the MBF quantification. This geometrical correction model also compensates for the spillover effect (also illustrated in figure 4): where there is a gain in apparent activity in small regions or on edges which have a much lower uptake than the surrounding tissue. Due to this spillover effect one can already observe activity in the edges of the myocardium during the early stages of the dynamic scans which is spillover from the activity in the blood pool. Another factor which is unrelated to the limited resolution of the PET system but which is occasionally mistaken for spillover, is the arterial blood in the coronary arteries within the myocardium. The activity in the

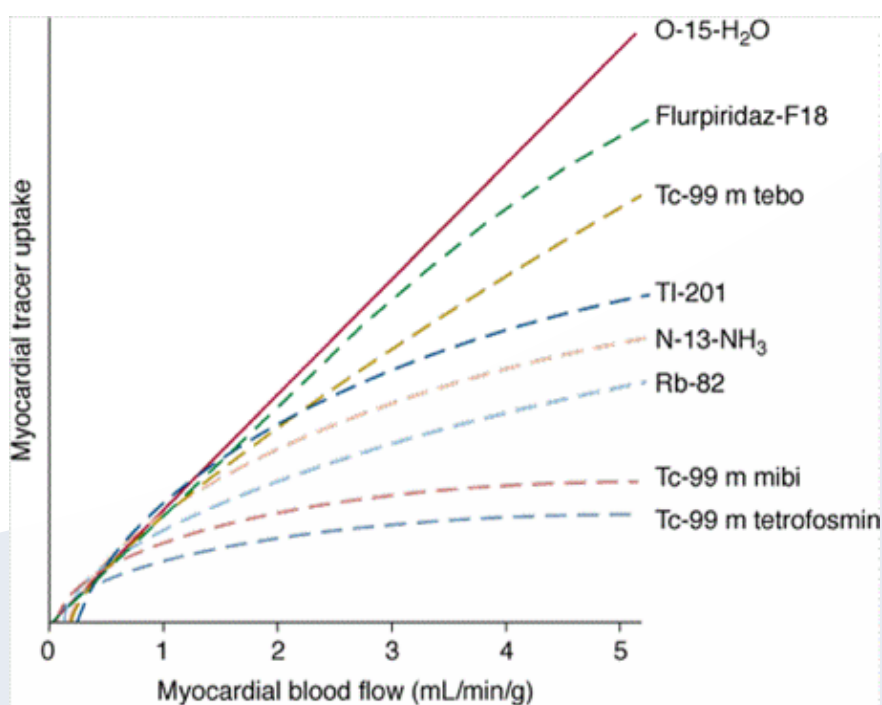


Figure 3. Relationship between myocardial blood flow and the myocardial tracer uptake, K₁, showing the roll-off phenomena for multiple cardiac tracers. From Fuster et al. (32).

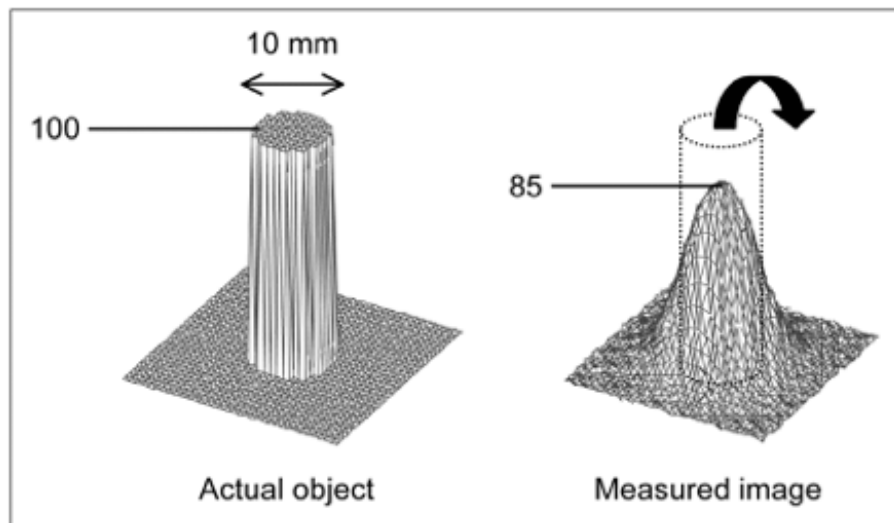


Figure 4. Illustration showing the partial volume and spillover effect with on the left side the actual circular activity source and on the right side the observed activity in which a part of the signal is observed outside the actual source (spillover) resulting in a decrease in the observed activity (partial volume). From: Soret et al. (33)

coronaries is falsely attributed to the myocardial tissue uptake, automatically changing the measured MBF. However, the geometrical correction as applied for partial volume and spillover effects often also corrects for this effect. One should note that all corrections that are and need to be applied differ between the different available models and induce uncertainties in MBF measurements (10-13).

MBF and CFR

The MBF in rest is derived by using the dynamic data that are acquired in rest.

The MBF in stress, the hyperaemic flow, is derived from the dynamic stress acquisition. By dividing the MBF in stress by that of the MBF in rest, the coronary flow reserve (CFR) is obtained:

$$\text{CFR} = \frac{\text{MBF}_{\text{stress}}}{\text{MBF}_{\text{rest}}}$$

In addition to calculating the MBF or CFR for the whole myocardium, one can also obtain the MBF or CFR for each of the 17 segments or per vascular trajectory. However, one should keep in mind that choosing a smaller region of interest will automatically induce a higher variability in the measured activity concentration and will therefore result in less reliable MBF or CFR values.

Pitfalls

Count rate capability PET scanner

The PET acquisition for MBF quantification is simultaneously started with the injection of activity and therefore has to

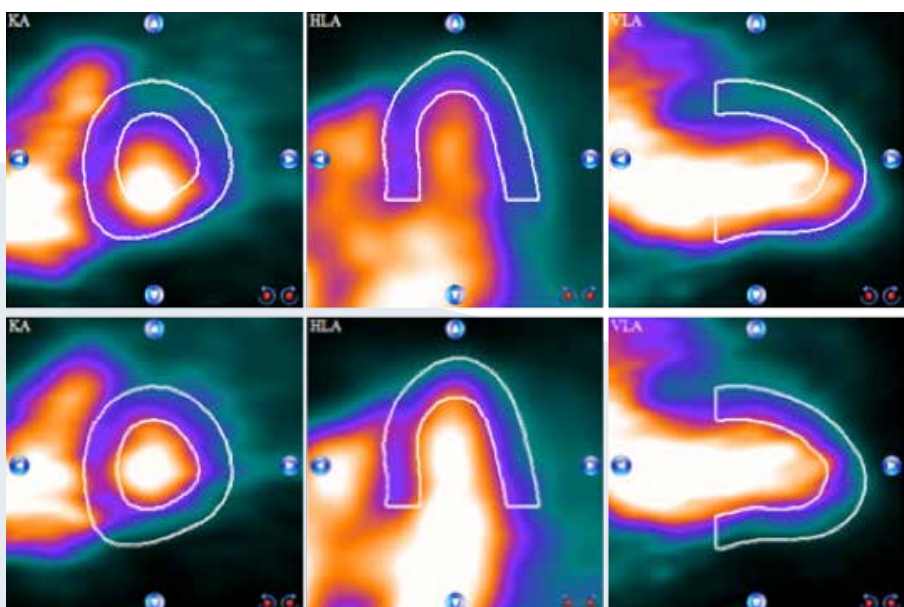
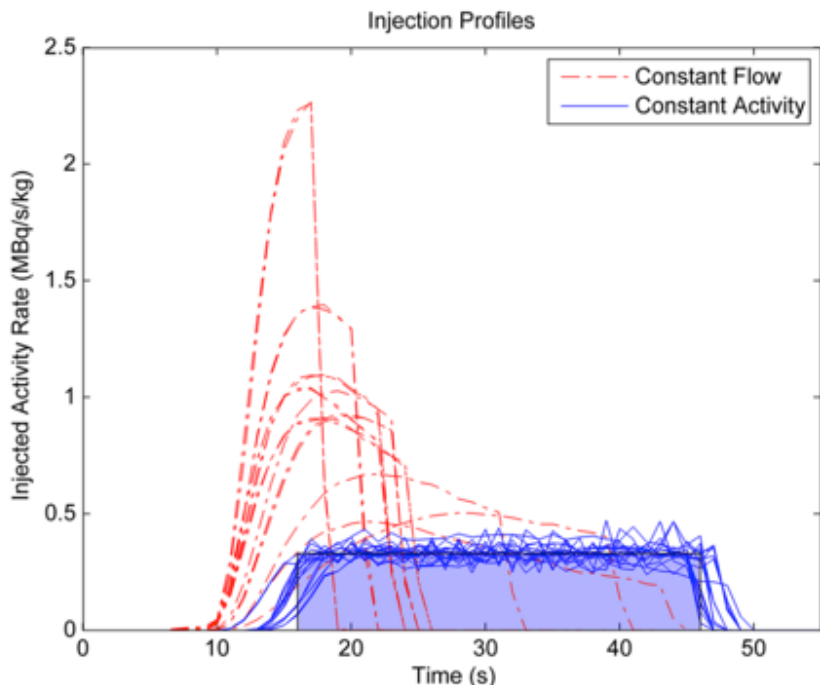


Figure 5. Example of a typical PET acquisition using the 5th (25-30s) time frame showing in the top row an upward creep of the myocardium indicated by the white contours. The contours of the myocardium are based on the data acquired between 150-420 s. This contour is manually corrected using dedicated software in the second row. From left to right the corresponding short axis, vertical long axis, and horizontal long-axis slices are shown.

Figure 6. ^{82}Rb infusion profiles for a constant activity (blue) and constant flow (red) in a test-retest cohort. The constant activity infusion profile is recognized by the 'square-wave' whereas the activity administration varies over time when using a constant flow injection profile. From: Klein et al. (22).



cope with very high count rates. Moreover, when using tracers with a short half-life such as ^{82}Rb , high activities of 1100–1500 MBq are recommended to obtain sufficient image quality (14, 15). High count rates can result in detector saturation, extreme dead time effects and loss of resolution and contrast (16). A PET system with a poor count rate performance can therefore negatively impact the reliability of MBF. Hence, it is important to make sure that a PET system is suitable for MBF quantification with ^{82}Rb (16).

Pharmacological stress and patient motion

The ^{82}Rb administration and induction of stress have to be performed in the PET room to be able to visualize the first-pass and ^{82}Rb uptake in the myocardium. Hence, pharmacological stress is often applied when patients are lying inside the PET camera. Adenosine and dipyridamole are commonly used as a stress agent, mainly due to their low costs. However, they are also associated with more side-effects, discomfort and patient motion compared

to regadenoson (17–19). As patient motion can severely impact image quality and MBF quantification (20), regadenoson could be preferred over adenosine or dipyridamole despite its higher costs. Yet regadenoson seems associated with cardiac motion. In a recent study, we observed an upward motion (creep) of the myocardium in almost 50% of our patients during stress imaging using regadenoson (21). This upward motion is likely caused by an increased diaphragmatic excursion and lung volume and a lower position of the diaphragm at the start of the acquisition as a result of the pharmacological stress. As the depth of respiration decreases during the acquisition, a repositioning of the diaphragm and myocardium occur in this post-pharmacological exercise period (21). In this way a mismatch arises between the presumed location of the myocardium and the PET data in the first minutes of the acquisition. As a result, the myocardium perfused by the right coronary artery often appears to be located at the position of the left atrium in the first time frames. This can result in artificially

high MBF values, especially in the right coronary artery (RCA) area. However, motion correction using post-processing software can resolve this issue, as shown in figure 5.

In addition to a possible upward creep, it is important to pay attention to the time between administration of regadenoson and ^{82}Rb , as this delay can influence the MBF measurements. Johnson et al. showed that the optimal time delay between starting the regadenoson and administration of ^{82}Rb is 55 s (19).

Accurate activity infusion

Besides the use of a PET system with sufficient count rate capability, one should also be aware of the influence of the type of ^{82}Rb activity bolus delivered by the $^{82}\text{Sr}/^{82}\text{Rb}$ generator. When using a flow dependent injection profile, a longer activity bolus will be required when the $^{82}\text{Sr}/^{82}\text{Rb}$ generator becomes older, as shown in figure 6. However, a constant activity injection profile prevents lengthening of this bolus as a constant activity per second is administered, independent of gene-

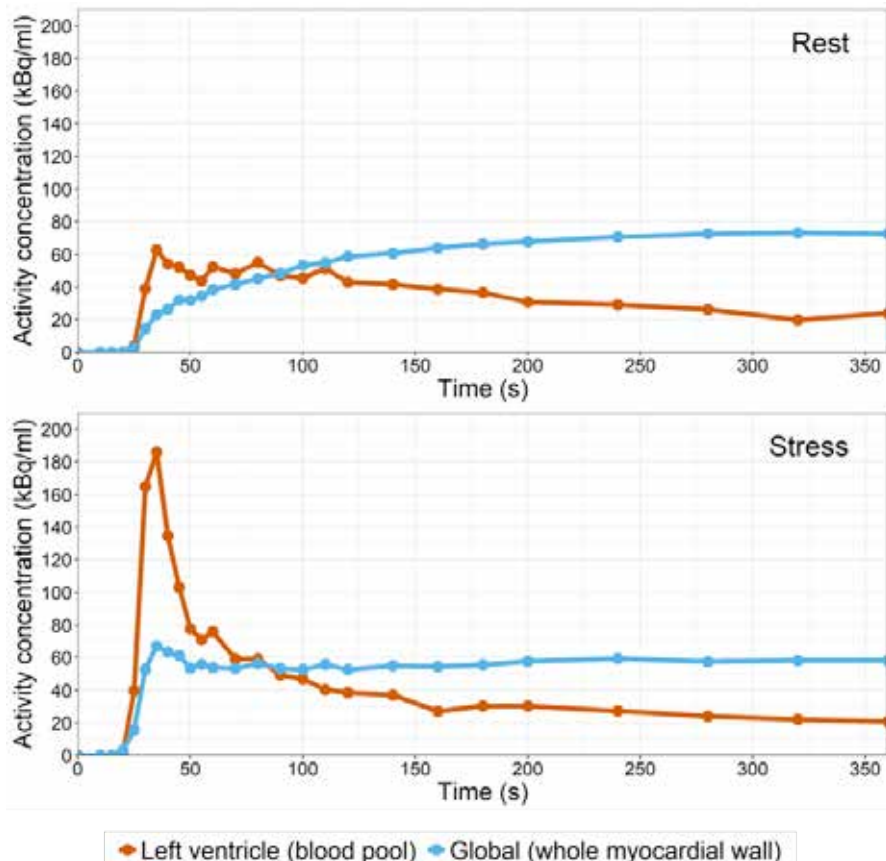


Figure 7. Top figure shows the time-activity curve of a rest ^{82}Rb PET examination in which the activity did not reach the myocardium as a bolus, probably due to a pinched vein. This resulted in an underestimation of the blood flow. However, this effect was not observed during the stress acquisition (bottom figure).

rator age. Klein et al. recently reported that a constant activity instead of a flow-depending injection profile resulted in a higher test-retest repeatability and, hence, less variance (22). As not all generators are able to provide an activity depending flow, an alternative is to explore the use of lower activities which are easier to produce by the generator and which will limit the lengthening of the bolus.

Furthermore, it is important to pay attention that the administered activity reaches the myocardium as a bolus. In our institute, we observe in 1 to 2% of our patients that the activity does not reach the myocardium as a bolus, as shown in figure 7. Although the generator is still able to inject the activity without any pressure alarms, the activity is not properly distributed into the main blood circulation. This phenomenon occurs in both rest and stress studies independently and we there-

fore assume it may be due to a pinched vein. It can be recognized when assessing the TACs, which show a clear absence of a sharp ventricular blood pool peak, i.e. a bolus, in addition to a slowly increasing activity concentration in the myocardium. Occurrence of this phenomenon makes the MBF and CFR values of that particular study unreliable.

Reconstruction and data processing

Attenuation correction

CT based attenuation correction (AC) is commonly applied to the PET reconstruction to reduce the image noise, artefacts, and distortion due to the attenuated photons. Misregistration of the AC-CT with the PET data can result in under- or overestimation of tracer activities in the PET images and therefore hamper MBF quantification. It is therefore essential to check and correct possible misalignments of the

CT-AC and PET images. Only the PET data acquired after the blood pool phase is generally used to check for possible misalignments, as these data contribute to the visualization of the myocardial contours. However, possible motion during the blood pool phase, such as an upward creep of the myocardium, is therefore not visible during this registration process and misregistration in these early time frames may occur. Although the effect of misregistration in the early time frames is still unknown, some centres already match the AC-CT for each individual time frame prior to the PET reconstruction to overcome this possible issue.

Dynamic sampling

The dynamic scans are reconstructed from the list-mode data by reconstructing multiple images containing data acquired at different times. Both the number and length of the time frames are

crucial. Aliasing can occur when fitting TACs using time frames that are relatively long. This can result in undersampling and, hence, underestimation of the left-ventricle blood pool concentration. However, time frames that are too short may result in high statistical variation in the measured activity concentrations, resulting in less reliable results. A recent study of Lee et al. showed that the use of 24 x 5s time frames during the blood pool phase and 2x 120s for the second phase optimally samples the TAC (23). However, less time frames may provide similar results and could be beneficial as the computation time needed for the reconstructions increases with the number of time frames and can take up to more than an hour for a complete rest-stress study.

PET image reconstruction

Besides the number and length of the time frames, the reconstruction settings can also influence the reconstruction speed. Time of flight (TOF) reconstruction typically doubles the time required for the reconstructions. Although TOF improves inconsistencies in PET corrections for attenuation, scatter and detector normalization (9), its effect on the MBF measurements seems limited (24). Suda et al. described that the MBF in rest using TOF reconstructions was systematically 5% higher compared to the MBF based on non-TOF reconstructions, but this effect was not observed for stress MBF (24). Centres with a high patient throughput can therefore decide to only reconstruct the static and gated images with TOF, as TOF does improve the visual image quality but has only limited impact on quantification.

In addition to TOF, one can also adjust the image filtering which is usually turned on by default when using iterative reconstructions such as ordered subsets expectation maximization (OSEM) reconstructions. Chilra et al. recently reported that the influence of the width of a Gaussian filter (4, 6 or 8 mm), the number of iterations and subsets (2x24, 2x16, 3x16 or 4x16) or turning

on resolution recovery, also known as modelling of the point spread function (PSF), does not affect the MBF (25). However, Armstrong et al. did observe differences in MBF when applying resolution recovery, although they did not find any differences in CFR measurements (26). Hence, one should be aware that variation may occur when using different filter settings.

Post-processing software

The final step of the MBF quantification is the post-processing of the data to calculate the MBF and CFR. There are multiple software packages with a variety of different kinetic models, relations between K1 and MBF in them and, hence, different settings and assumptions to correct for e.g. the extraction fraction, partial volume and spillover effects. Software packages may also differ in the way of reorienting the left ventricle to short-axis orientation and the identification of the boundaries of the myocardium. Calculated MBF values can therefore differ with different software by over 20%, even when using the same kinetic model and kinetic relations (27, 28). It is therefore important to be cautious when comparing the MBF across software packages. However, calculated CFR values seem more comparable with different software (27, 28). This is probably due to the fact that the variation in the different correction factors on the absolute MBF values in rest and stress cancel each other out.

Clinical (un)certainty

Although physicians always desire one cut-off threshold that can classify the absence or presence of disease or classify the severity of the disease, the uncertainty of the measured MBF values makes this impossible. A recent study by Kitkungvan et al. highlights this by reporting the test-retest reproducibility using ⁸²Rb PET (29). Whereas the coefficient of variance of the same-day reproducibility of MBF was ±10%, this became ±21% when the test was reperformed after a few days.

This biological and methodological variability, both explaining about 10% of the variation, indicates the grey area surrounding the desired cut-off to describe the physiological severity. In addition, the exact MBF threshold will depend on reconstruction settings, kinetic model settings and the software package that is used. Generalized MBF thresholds suitable for all centres can therefore not be defined. However, in contrast to MBF values, it seems that the CFR values are relatively safe to compare across centres (22–24, 26–28). Although a CFR cut-off for ⁸²Rb has not been established in the same rigorous way as with ¹⁵O (30), the cut-off value is commonly chosen to be around 2.0 (31). Hence, when incorporating the biological and methodological variability into this CFR threshold, this means that physicians should be careful in drawing conclusions when CFR values are between 1.6 and 2.4.

Conclusion

The possibility to provide quantitative MBF and CFR data based on ⁸²Rb PET imaging is of clear added value in clinical practice. However, all readers should be aware of the underlying assumptions and technical pitfalls. Differences in equipment, acquisition and reconstruction settings and processing software can result in varying MBF values which makes standardized MBF thresholds practically impossible. And although the other important parameter, CFR, is less influenced by practical variances, the methodologic and biologic variability still induces a grey area around the threshold influencing the determination and the classification of the disease.

j.d.vandijk@isala.nl ♦

References

- Orton EJ, Al Harbi I, Klein R, et al. Detection and severity classification of extracardiac interference in ⁸²Rb PET myocardial perfusion imaging.

- Med Phys. 2014;41:102501.
2. Ghobti AA, Kjaer A, Hasbak P. Review: comparison of PET rubidium-82 with conventional SPECT myocardial perfusion imaging. *Clin Physiol Funct Imaging* 2014;34:163-70
 3. Bateman TM, Heller G V, McGhie AI, et al. Diagnostic accuracy of rest/stress ECG-gated Rb-82 myocardial perfusion PET: Comparison with ECG-gated Tc-99m sestamibi SPECT. *J Nucl Cardiol.* 2006;13:24-33
 4. Bengel FM, Higuchi T, Javadi MS, Lautamäki R. Cardiac Positron Emission Tomography. *J Am Coll Cardiol.* 2009;54:1-15
 5. Arumugam P, Tout D, Tonge C. Myocardial perfusion scintigraphy using rubidium-82 positron emission tomography. *Br Med Bull.* 2013;107:87-100
 6. Clinicaltrials.gov. A Phase 3 Multi-center Study to Assess PET Imaging of Flurpiridaz F 18 Injection in Patients With CAD. Available at: <https://clinicaltrials.gov/ct2/show/results/NCT01347710?sect=X01256#all>. (Accessed on: August 24, 2017)
 7. Mc Ardle BA, Dowsley TF, DeKemp RA, et al. Does Rubidium-82 PET have superior accuracy to SPECT perfusion imaging for the diagnosis of obstructive coronary disease? *J Am Coll Cardiol.* 2012;60:1828-37
 8. Majmudar MD, Murthy VL, Shah R V., et al. Quantification of coronary flow reserve in patients with ischaemic and non-ischaemic cardiomyopathy and its association with clinical outcomes. *Eur Heart J Cardiovasc Imaging.* 2015;16:900-9
 9. Moody JB, Lee BC, Corbett JR, et al. Precision and accuracy of clinical quantification of myocardial blood flow by dynamic PET: A technical perspective. *J Nucl Cardiol.* 2015;22:935-51
 10. Lortie M, Beanlands RSB,
 - Yoshinaga K, et al. Quantification of myocardial blood flow with ⁸²Rb dynamic PET imaging. *Eur J Nucl Med Mol Imaging.* 2007;34:1765-74
 11. Klein R, Beanlands RSB, DeKemp RA. Quantification of myocardial blood flow and flow reserve: Technical aspects. *J Nucl Cardiol.* 2010;17:555-70
 12. Waller AH, Blankstein R, Kwong RY, Di Carli MF. Myocardial blood flow quantification for evaluation of coronary artery disease by positron emission tomography, cardiac magnetic resonance imaging, and computed tomography. *Curr Cardiol Rep.* 2014;16:483
 13. Hsu B. PET tracers and techniques for measuring myocardial blood flow in patients with coronary artery disease. *J Biomed Res.* 2013;27:452-9
 14. Dilsizian V, Bacharach SL, Beanlands RS, et al. ASNC imaging guidelines/SNMMI procedure standard for positron emission tomography (PET) nuclear cardiology procedures. *J Nucl Cardiol.* 2016;23:1187-226
 15. Hesse B, Tägil K, Cuocolo A, et al. EANM/ESC procedural guidelines for myocardial perfusion imaging in nuclear cardiology. *Eur J Nucl Med Mol Imaging* 2005;32:855-897.
 16. Renaud JM, Yip K, Guimond J, et al. Characterization of 3-Dimensional PET Systems for Accurate Quantification of Myocardial Blood Flow. *J Nucl Med.* 2017;58:103-9
 17. Memmott MJ, Tonge CM, Saint KJ, Arumugam P. Impact of pharmacological stress agent on patient motion during rubidium-82 myocardial perfusion PET/CT. *J Nucl Cardiol.* 2017;1-10
 18. Cerqueira MD. The future of pharmacologic stress: selective A2A adenosine receptor agonists. *Am J Cardiol.* 2004;94:33D-40D
 19. Johnson NP, Gould KL. Regadenoson versus dipyridamole hyperemia for cardiac PET imaging. *JACC Cardiovasc Imaging.* 2015;8:438-47
 20. Hunter CRRN, Klein R, Beanlands RS, deKemp RA. Patient motion effects on the quantification of regional myocardial blood flow with dynamic PET imaging. *Med Phys.* 2016;43:1829-40
 21. Koenders S, Van Dijk JD, Jager PL, et al. Need for Correction of Myocardium Movement during Dynamic Rubidium-82 Stress PET for Accurate Myocardial Blood Flow Quantification. *Oral Abstr.* Present. at 28th annual Congress of the European Association of Nuclear Medicine (EANM), Vienna, Austria, 25 Oct. 2017
 22. Klein R, Ocneanu A, Renaud JM, et al. Consistent tracer administration profile improves test retest repeatability of myocardial blood flow quantification with ⁸²Rb dynamic PET imaging. *J Nucl Cardiol.* 2016;1-13
 23. Lee BC, Moody JB, Weinberg RL, et al. Optimization of temporal sampling for ⁸²rubidium PET myocardial blood flow quantification. *J Nucl Cardiol.* 2017;24:1517-29
 24. Suda M, Onoguchi M, Tomiyama T, et al. The reproducibility of time-of-flight PET and conventional PET for the quantification of myocardial blood flow and coronary flow reserve with ¹³N-ammonia. *J Nucl Cardiol.* 2016;23:457-72
 25. Chilra P, Gnesin S, Allenbach G, et al. Cardiac Rb-82 PET/CT: Optimization of image acquisition and reconstruction parameters. *Nuklearmedizin.* 2014;53:A120.
 26. Armstrong IS, Tonge CM, Arumugam P. Impact of point spread function modeling and time-of-flight on myocardial blood

- flow and myocardial flow reserve measurements for rubidium-82 cardiac PET. *J Nucl Cardiol.* 2014;21:467-74
27. Tahari AK, Lee A, Rajaram M, et al. Absolute myocardial flow quantification with ^{82}Rb PET/CT: comparison of different software packages and methods. *Eur J Nucl Med Mol Imaging.* 2014;41:126-35
28. Slomka PJ, Alexanderson E, Jácome R, et al. Comparison of clinical tools for measurements of regional stress and rest myocardial blood flow assessed with ^{13}N -ammonia PET/CT. *J Nucl Med.* 2012;53:171-81
29. Kitkungvan D, Johnson NP, Roby AE, et al. Routine Clinical Quantitative Rest Stress Myocardial Perfusion for Managing Coronary Artery Disease. *JACC Cardiovasc Imaging.* 2017;10:565-77
30. Danad I, Uusitalo V, Kero T, et al. Quantitative assessment of myocardial perfusion in the detection of significant coronary artery disease: Cutoff values and diagnostic accuracy of quantitative $[^{15}\text{O}]\text{H}_2\text{O}$ PET imaging. *J Am Coll Cardiol.* 2014;64:1464-75
31. Ziadi MC, Dekemp RA, Williams KA, et al. Impaired myocardial flow reserve on rubidium-82 positron emission tomography imaging predicts adverse outcomes in patients assessed for myocardial ischemia. *J Am Coll Cardiol.* 2011;58:740-8
32. Fuster V, Walsh R, Harrington R. *Hurst's the heart*, 13th ed. McGraw Hill Professional; 2011.
33. Soret M, Bacharach SL, Buvat I. Partial-volume effect in PET tumor imaging. *J Nucl Med.* 2007;48:932-45

Nieuwe ontwikkelingen op het gebied van cardiovasculaire CT

**A.M. den Harder, MD, PhD; R.W. van Hammersveld, MD; R.A.P. Takx, MD, PhD;
M.J. Willemink, MD, PhD; T. Leiner MD, PhD**

Universitair Medisch Centrum Utrecht, afdeling Radiologie, Utrecht, Nederland

Summary

In the past years, several developments in the field of cardiovascular computed tomography (CT) have emerged. The radiation dose associated with cardiovascular CT has decreased tremendously due to technical advancements such as iterative reconstruction and prospective ECG triggering. Furthermore, the measurement of fractional flow reserve (FFR) on CT data has showed the potential to replace FFR measured with invasive angiography. Dynamic stress induced CT perfusion enables the evaluation of myocardial ischaemia. Lastly, new generation spectral CT systems offer improved tissue separation due to the discrimination between different energy levels.

renden een bepaalde fase van de hartcyclus met de volledige stroomsterkte gescand, en wordt de stroomsterkte buiten deze fase gereduceerd of uitgezet (2). Hierdoor kan de stralingsdosis aanzienlijk worden verlaagd (3). Prospective ECG triggering wordt daarom vandaag de dag in het merendeel van de patiënten toegepast. Een tweede manier om de dosis te reduceren is het gebruiken van een hoge pitch bij *dual source* CT-scanners. Hierbij wordt het gehele hart in één hartslag gescand. De delen die gemist worden door de hoge pitch worden opgevuld door de tweede detector waardoor alsnog een diagnostisch beeld ontstaat. Ook zijn er zogenaamde volume CT-scanners die, door een groot detectoroppervlak, in één rotatie het gehele hart kunnen afbeelden (4). Met bovenstaande technieken wordt er gedurende één hartcyclus gescand, in plaats van twee of meer. Ten derde heeft de introductie van iteratieve reconstructietechniek geleid tot een aanzienlijke reductie in de stralingsdosis (5). Een reconstructietechniek is noodzakelijk om de data die door een CT-scanner wordt geproduceerd om te zetten in beelden. Een veelgebruikte, relatief eenvoudige, reconstructietechniek is *filtered back projection* (FBP). Iteratieve reconstructie is een alternatief voor FBP en zorgt voor een reductie in de hoeveelheid ruis. Hierdoor is het mogelijk om met een lagere dosis toch voldoende beeldkwaliteit te krijgen (6,7). Hoewel iteratieve reconstructie al decennia wordt toegepast in de nucleaire geneeskunde, was dit tot voor kort niet mogelijk bin-

nen de radiologie vanwege een gebrek aan rekenkracht. Iedere fabrikant heeft een of meerdere iteratieve reconstructie algoritmes op de markt gebracht, en deze worden in toenemende mate toegepast in de kliniek. Ten vierde kan de stralingsdosis worden verlaagd door de spanning en de stroomsterkte automatisch aan te passen aan het te scannen lichaamsgebied; op nieuwere CT-scanners is het tevens mogelijk om op een buisspanning van 70 kVp te scannen. Tot slot kan de opkomst van *dual energy* CT-scanners mogelijk bijdragen aan een verlaging van de stralingsdosis. Doordat het hierbij mogelijk is om een virtuele blanco scan te reconstrueren uit een CT-scan met jodiumhoudend contrast, kan de blanco CT-scan voor het bepalen van de calciumscore mogelijk achterwege worden gelaten.

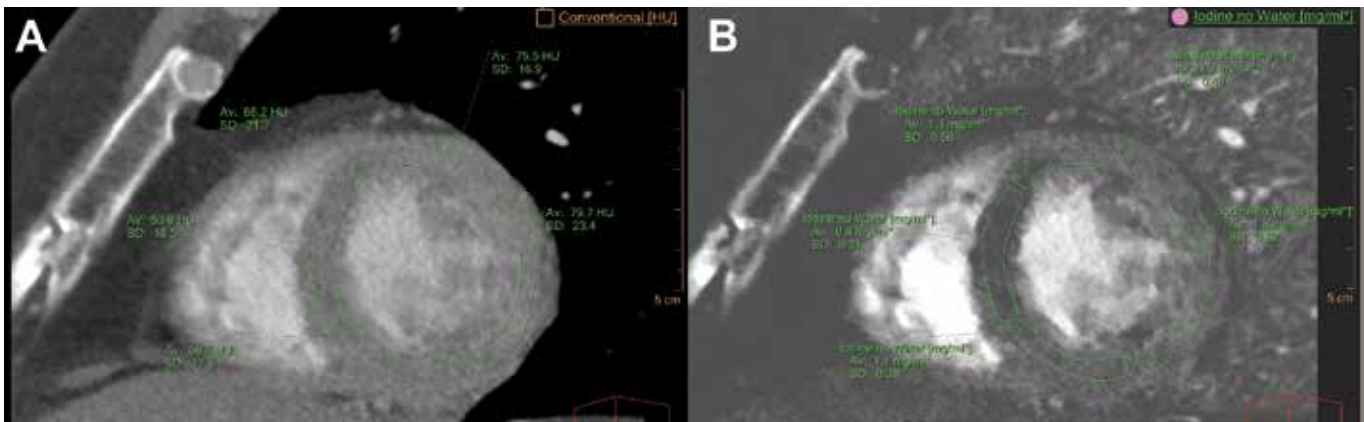
De stralingsdosis van een CT-hart is door toepassing van deze nieuwe technieken aanzienlijk gereduceerd. Een rapport van de European Society of Cardiology rapporteerde dat inmiddels 66% van de cardiale CT-scans wordt gemaakt met een stralingsdosis onder de 2 mSv, en dat de mediane stralingsdosis tussen 2010 en 2013 met meer dan 90% is gedaald (8).

FFRCT

CT-angiografie heeft een uitstekende negatieve voorspellende waarde voor het uitsluiten van coronaire hartziekten (9). De positieve voorspellende waarde voor het detecteren van hemodynamisch significant coronair lijden is echter suboptimaal, vooral omdat de

Verlaging van de stralingsdosis

Het aantal CT-scans dat jaarlijks in Nederland wordt gemaakt is enorm toegenomen van 400 duizend in 1991 naar 1,4 miljoen in 2014 (1). CT-scans van het hart gaan gepaard met een relatief hoge stralingsdosis. Diverse technische ontwikkelingen hebben het echter mogelijk gemaakt de stralingsdosis substantieel te verlagen. Allereerst kan er gebruik gemaakt worden van prospectieve ECG triggering. Vooreerst werd het hart gescand met 100% stroomsterkte (*amperage*) gedurende de gehele hartcyclus. Bij prospectieve ECG triggering wordt er alleen gedu-



*Dual energy statische CT-perfusie scan van een patiënt met significante stenose in de LAD ($FFR<0.8$). **A.** Conventioneel beeld met subtiële hypoattenuatie mid-en inferoseptaal; **B.** Weefselspecifiek beeld voor jodiumhoudend contrast waarbij de hoeveelheid jodiumhoudend contrast in het myocard is gekwantificeerd. Septaal en inferoseptaal is er een lagere hoeveelheid jodiumhoudend contrast zichtbaar waardoor het perfusiedefect beter zichtbaar is.*

stenosegraad geen goede voorspeller is (10,11). Recente vooruitgang in de computervloeistofdynamiek maakt het mogelijk om hemodynamische significantie van coronairlijden te bepalen, gebruik makend van CT-datasets. Dit levert een fractional flow reserve CT (FFRCT) waarde op, waarbij een waarde kleiner dan 0,80 wordt beschouwd als afwijkend en passend bij een hemodynamisch significante coronaire hartziekte. Er is recent veel onderzoek gedaan naar de waarde van FFR op basis van CT-beelden. Ten eerste heeft de techniek een vergelijkbare diagnostische waarde als bij invasief gemeten FFR (12). De analyse kan worden uitgevoerd door een extern bedrijf waarvoor de CT-beelden dienen te worden geüpload (HeartFlow, Redwood City, Californië, Verenigde Staten van Amerika) of de analyse kan worden uitgevoerd op een lokaal werkstation (Siemens Healthineers, Forchheim, Duitsland), waarbij een vereenvoudigd model wordt toegepast. Tevens hebben twee studies een analyse verricht naar de kosten van FFRCT, waarin lagere kosten worden geprojecteerd (30-32% lager) en een verbeterde uitkomst (12-19% minder cardiovasculaire gebeurtenissen na 1 jaar) door patiënten adequater te selecteren voor een dotterbehandeling (13,14). Recentelijk zijn de resultaten van de PLATFORM-studie (Prospective Longitudinal Trial of FFRct: Outcome

and Resource iMPact) gepubliceerd (15). In deze prospectieve studie wordt aangetoond dat FFRCT een geschikt alternatief biedt voor invasieve angiografie, waarbij in 61% van de gevallen naar aanleiding van de CT/FFRCT resultaten invasieve angiografie werd afgezegd. Er zijn echter verschillende hindernissen die nog moeten worden overwonnen voordat FFRCT in de standaard klinische praktijk kan worden geïmplementeerd. Ten eerste zijn er geen gerandomiseerde studies uitgevoerd die het gebruik van FFRCT onderzoeken. Ten tweede zijn kwalitatief goede CT-beelden zonder aanzienlijke artefacten nodig om de FFR waarde te berekenen hetgeen relatief nieuwe CT-hardware vereist. In een studie werd 13% van de CT-scans beschouwd als van onvoldoende kwaliteit (16). Ten derde zijn de berekeningen gebaseerd op aannames en modellering en mogelijk kunnen afwijkingen in de berekende FFR waarde optreden bij bijvoorbeeld patiënten met bloedarmoede. Ten slotte is het niet bekend of er per scan betaald moet worden of per licentie, en om welke bedragen het gaat.

Samengevat kan FFRCT in de toekomst een poortwachtersrol gaan vervullen vanwege de toename in specificiteit vergeleken met CT-angiografie. De meeste van de eerder besproken beperkingen kunnen mogelijk in de nabije toekomst worden overwonnen met verdere aan-

passingen van het algoritme en vooruitgang in computertechnologie.

Myocard CT-perfusie

Een CT-scan van het hart is een sterk diagnostisch hulpmiddel voor het aantonen of excluderen van coronaire hartziekten (17,18). Echter, bij aanwezigheid van een stenose, is het beoordelen van de stenosegraad een relatief slechte voorspeller voor de mate van ischemie (18). Dit geldt met name voor ernstig verkalkte coronairarteriën en bij de aanwezigheid van een stent. Om de mate van ischemie te beoordelen worden deze patiënten daarom vaak verwezen naar een functionele test (zoals nucleaire stress test of MRI). Door recente (technische) ontwikkelingen van stress-geïnduceerde CT-perfusie is er nu de mogelijkheid om de mate van ischemie te beoordelen met behulp van CT. Met CT-perfusie kan ischemie in het myocard worden gedetecteerd door de distributie van jodiumhoudend contrast tijdens de ‘first-pass’ te beoordelen. Omdat de distributie van het contrast wordt bepaald door bloedtoevoer naar het myocard kunnen ischemische perfusiedefecten worden geïdentificeerd als gebieden met hypoattenuatie (zie figuur). Bij dynamische CT-perfusie worden er na toediening van jodiumhoudend contrast meerdere CT-scans van het hart gemaakt gedurende een vooraf ingestelde periode (ongeveer

30 seconden). Op deze manier worden er beelden verkregen van de volledige eerste passage van het contrastmiddel en kunnen meerdere kwantitatieve analyses van de bloedstroom in het myocard (*myocardial blood flow*) worden uitgevoerd. Voor anatomische evaluatie van onder andere de coronairarteriën, wordt er naast een dynamische stress CT-perfusie ook een CT-hart in rust gemaakt. Een belangrijk voordeel van CT-perfusie is het feit dat er zowel anatomische als functionele informatie beschikbaar is binnen één onderzoek, perfusiedefecten kunnen zo gecorreleerd worden aan desbetreffende aanvoerende coronairarteriën of andere extra-luminale structuren. Een nadeel van dynamische CT-perfusie betreft de hoge stralingsdosis, een combinatie van CT-hart in rust en dynamische stress CT-perfusie komt al snel uit op 15-20 mSv (19). Eerder beschreven technieken, zoals gebruik van lage kVp en iteratieve reconstructie, in combinatie met nieuwe technieken, zoals het combineren van een dynamische stress CT-perfusie met een CT-hart in rust, hebben de potentie deze dosis te verlagen en worden momenteel onderzocht (20). Een andere manier om dosis te besparen betreft een static stress CT-perfusie, hierbij wordt onder stress een CT-hart (dit kan zowel een retrospectief als prospectief ECG geleide scan zijn) op één tijdstip verkregen gedurende de vroeg arteriële fase. Er is een optimaal tijdframe van ongeveer acht seconden om ischemische en niet-ischemische gebieden van elkaar te differentiëren (21,22), een goede timing is daarom van groot belang. Perfusiedefecten kunnen zowel visueel als (semi-) kwantitatief worden beoordeeld door hypoattenuatie van ischemische gebieden te analyseren en door middel van de transmurale perfusieratio (ratio tussen subendocardiale en subepicardiale attenuatie)(23). Een nadeel van de static CT-perfusie techniek is dat, doordat er maar één stress CT-hart beeld verkregen wordt, deze gevoeliger is voor artefacten (zoals *beam hardening*) en dat bij een suboptimale timing de optimale

fase voor ischemiedetectie gemist kan worden. Een relatief nieuwe ontwikkeling in het veld is het gebruik van dual energy CT voor het maken van de *static* CT-perfusie scan. Door gebruik te maken van dual energy CT kan beam hardening worden gereduceerd en kunnen naast de conventionele beelden ook weefselspecifieke beelden voor jodiumhoudend contrast worden gereconstrueerd. Hierdoor kan op het moment van de scan de hoeveelheid jodiumhoudend contrast in het myocard worden gekwantificeerd, hetgeen een semi-kwantitatief surrogaat is voor myocard-perfusie (24). Een combinatie van zowel verlaging van de stralingsdosis, als toepassing van *dual energy* CT en *static* CT-perfusie zullen naar verwachting binnen afzienbare tijd leiden tot implementatie van myocard CT-perfusie in de dagelijkse klinische praktijk.

Dual energy en spectrale CT

Ondanks het overweldigende succes van de CT-scan, heeft deze techniek nog steeds belangrijke nadelen. Ten eerste de blootstelling van patiënten aan röntgenstraling: zoals eerder beschreven kan de stralingsdosis worden verminderd, maar dit resulteert in andere problemen zoals ruis en artefacten in CT-beelden. Ten tweede kan met CT slecht onderscheid worden gemaakt tussen pathologisch en gezond weefsel omdat het contrast tussen verschillende weke delen relatief slecht is. Qua weefseldifferentiatie is CT momenteel inferieur ten opzichte van andere modaliteiten zoals MRI. In de klinische praktijk wordt dit deels aangepakt door toediening van contrastmiddelen, maar dat brengt ons bij de derde limitatie- jodiumhoudend contrast dat wordt gebruikt voor CT kan schadelijk zijn voor de nieren en jodiumallergie komt relatief vaak voor. Ten slotte worden CT-pixelwaarden weergegeven in Hounsfield units (HU), welke afhankelijk zijn van de spanning van de röntgenbuis en de omliggende anatomie, waardoor CT-beeldpixels geen werkelijke contrastconcentraties weergeven en daardoor soms moei-

lijk te interpreteren zijn. Dit probleem kan theoretisch worden verholpen met *dual energy* CT (25), een techniek die weefselspecifieke beelden kan reconstrueren. Helaas is de scheiding tussen hoog- en laagenergetische röntgenfotonen (spectrale scheiding) suboptimaal met huidige *dual energy* CT-scanners. Het gebruik van meer dan twee energielevels kan theoretisch resulteren in betere weefselspecifieke beelden, wat kan resulteren in CT-beelden met absolute kwantitatieve betekenis.

Alle genoemde nadelen van de conventionele CT-scan kunnen theoretisch worden verholpen met spectrale CT. Een van de belangrijkste kenmerken van spectrale CT is het vermogen om attenuatieverschillen tussen weefsels weer te geven bij verschillende energielevels. Dit kan op twee manieren, namelijk met *dual energy* CT en met *photon counting* CT. Met *dual energy* CT worden hogenergetische röntgenfotonen onderscheiden van laagenergetische röntgenfotonen. *Dual energy* CT is een techniek die klinisch toepasbaar is aangezien dual energy CT-scanners commercieel verkrijgbaar zijn. *Dual energy* CT is de eerste stap richting toekomstige CT-scanners met *photon counting* detectors. *Photon counting* CT is een opkomende techniek die de potentie heeft om een revolutie te brengen voor klinische CT-beeldvorming. *Photon counting* CT maakt gebruik van nieuwe energie-oplossende detectoren. Deze detectoren verschillen substantieel van conventionele energie-integrerende detectoren. Ideale *photon counting* CT-detectoren tellen het aantal röntgenfotonen dat de detector raakt en ook de energie van alle inkomende röntgenfotonen wordt gemeten. Dit resulteert in een hoger signaal met minder ruis, een verbeterde spatiële resolutie en verbeterde scheiding tussen de energieën van röntgenfotonen. De verbeterde spectrale scheiding geeft meer informatie dan *dual energy* CT, aangezien meer dan twee energieniveaus kunnen worden onderscheiden. Dit alles biedt de mogelijkheid om de stralingsdosis

te reduceren, beelden te reconstrueren met een hogere spatiële resolutie, beeldartefacten te verminderen (zoals *beam hardening* artefacten), het gebruik van contrastmiddelen te verbeteren en het geeft de mogelijkheid om CT-pixels volledig kwantitatief te maken. Ondanks de veelbelovende eerste resultaten is *photon counting* CT nog in ontwikkeling (26-36). Er zijn nog geen commerciële *photon counting* CT-scanners verkrijgbaar, maar het ligt in de lijn der verwachting dat dit binnen vijf tot tien jaar zal gebeuren.

Conclusie

Concluderend is de afgelopen jaren de stralingsdosis van een cardiale CT-scan van het hart substantieel verlaagd door gebruik te maken van technieken zoals prospectieve ECG triggering, hoge pitch, iteratieve reconstructie en het automatisch aanpassen van de stroomsterkte en spanning aan het te scannen lichaamsgebied. Het bepalen van de hemodynamische significantie van kransslagaderziekte met CT (FFRCT) kan potentieel invasieve angiografie vervangen. Stress-geïnduceerde CT-perfusie maakt het mogelijk om tevens de mate van ischemie te beoordelen op CT. Tot slot kan spectral CT verschillende energielevels van elkaar scheiden. Hierdoor kan de weefseldifferentiatie worden verbeterd. Hoewel de laatste drie technieken op dit moment niet name in onderzoeksverband worden toegepast, zijn de eerste resultaten veelbelovend en is het de verwachting dat deze in de komende jaren in de kliniek zullen worden geïmplementeerd.

a.m.denharder@umcutrecht.nl ♦

Referenties

- IMV, Information for the Decisions Ahead. 2016 CT Market Outlook Report. 2016; Available at: www.imvinfo.com.
- Earls JP, Berman EL, Urban BA, et al. Prospectively gated transverse coronary CT angiography versus retrospectively gated helical tech-nique: improved image quality and reduced radiation dose. *Radiology*. 2008;246(3):742-53
- Menke J, Unterberg-Buchwald C, Staab W, et al. Head-to-head comparison of prospectively triggered vs retrospectively gated coronary computed tomography angiography: Meta-analysis of diagnostic accuracy, image quality, and radiation dose. *Am Heart J*, 2013;165(2):154-63.e3.
- Di Cesare E, Gennarelli A, Di Sibio A, et al. Image quality and radiation dose of single heartbeat 640-slice coronary CT angiography: a comparison between patients with chronic atrial fibrillation and subjects in normal sinus rhythm by propensity analysis. *Eur J Radiol*. 2015;84(4):631-6
- Den Harder AM, Willemink MJ, De Ruiter QM, et al. Dose reduction with iterative reconstruction for coronary CT angiography: a systematic review and meta-analysis. *Br J Radiol*. 2016;89(1058):20150068.
- Willemink MJ, de Jong PA, Leiner T, et al. Iterative reconstruction techniques for computed tomography Part 1: technical principles. *Eur Radiol*. 2013;23(6):1623-31
- Willemink MJ, Leiner T, de Jong PA, et al. Iterative reconstruction techniques for computed tomography part 2: initial results in dose reduction and image quality. *Eur Radiol*. 2013;23(6):1632-42
- Al-Mallah MH, Aljzeeri A, Alharthi M, Alsaileek A. Routine low-radiation-dose coronary computed tomography angiography. *European Heart Journal, Supplement*. 2014;16:B12-6
- Vanhoenacker PK, Heijnenbrok-Kal MH, Van Heste R, et al. Diagnostic performance of multidetector CT angiography for assessment of coronary artery disease: meta-analysis. *Radiology*. 2007;244(2):419-28
- Rossi A, Papadopoulou SL, Pugliese F, et al. Quantitative computed tomographic coronary angiography: does it predict functionally significant coronary stenoses? *Circ Cardiovasc Imaging*. 2014;7(1):43-51
- Patel MR, Peterson ED, Dai D, et al. Low diagnostic yield of elective coronary angiography. *N Engl J Med*. 2010;362(10):886-95
- Wu W, Pan DR, Foin N, et al. Non-invasive fractional flow reserve derived from coronary computed tomography angiography for identification of ischemic lesions: a systematic review and meta-analysis. *Sci Rep*. 2016;6:29409.
- Hlatky MA, Saxena A, Koo BK, et al. Projected costs and consequences of computed tomography-determined fractional flow reserve. *Clin Cardiol*. 2013;36(12):743-8
- Kimura T, Shiomi H, Kurabayashi S, et al. Cost analysis of non-invasive fractional flow reserve derived from coronary computed tomographic angiography in Japan. *Cardiovasc Interv Ther*. 2015;30(1):38-44
- Douglas PS, Pontone G, Hlatky MA, et al. Clinical outcomes of fractional flow reserve by computed tomographic angiography-guided diagnostic strategies vs. usual care in patients with suspected coronary artery disease: the prospective longitudinal trial of FFR(CT): outcome and resource impacts study. *Eur Heart J*. 2015;36(47):3359-67
- Norgaard BL, Leipsic J, Gaur S, et al. Diagnostic performance of noninvasive fractional flow reserve derived from coronary computed tomography angiography in suspected coronary artery disease: the NXT trial (Analysis of Coronary Blood Flow Using CT Angiography: Next Steps). *J Am Coll Cardiol*. 2014;63(12):1145-55
- Budoff MJ, Dowe D, Jollis JG, et al. Diagnostic performance of 64-muli-detector row coronary computed tomographic angiography for evaluation of coronary artery stenosis in individuals without known coronary artery disease: results from the prospective multicenter ACCURA-

- CY (Assessment by Coronary Computed Tomographic Angiography of Individuals Undergoing Invasive Coronary Angiography) trial. *J Am Coll Cardiol.* 2008;52(21):1724-32
18. Meijboom WB, Van Mieghem CA, van Pelt N, et al. Comprehensive assessment of coronary artery stenoses: computed tomography coronary angiography versus conventional coronary angiography and correlation with fractional flow reserve in patients with stable angina. *J Am Coll Cardiol.* 2008;52(8):636-43
 19. Feher A, Sinusas AJ. Quantitative Assessment of Coronary Microvascular Function: Dynamic Single-Photon Emission Computed Tomography, Positron Emission Tomography, Ultrasound, Computed Tomography, and Magnetic Resonance Imaging. *Circ Cardiovasc Imaging.* 2017;10(8):10.1161/CIRCIMAGING.117.006427.
 20. Hubbard L, Ziemer B, Lipinski J, et al. Functional Assessment of Coronary Artery Disease Using Whole-Heart Dynamic Computed Tomographic Perfusion. *Circ Cardiovasc Imaging.* 2016;9(12):e005325.
 21. Pelgrim GJ, Nieuwenhuis ER, Duquay TM, et al. Optimal timing of image acquisition for arterial first pass CT myocardial perfusion imaging. *Eur J Radiol.* 2017;86:227-33
 22. Bischoff B, Bamberg F, Marcus R, et al. Optimal timing for first-pass stress CT myocardial perfusion imaging. *Int J Cardiovasc Imaging.* 2013;29(2):435-42
 23. Varga-Szemes A, Meinel FG, De Cecco CN, et al. CT myocardial perfusion imaging. *AJR Am J Roentgenol.* 2015;204(3):487-97
 24. Delgado Sanchez-Gracian C, Oca Pernas R, Trinidad Lopez C, et al. Quantitative myocardial perfusion with stress dual-energy CT: iodine concentration differences between normal and ischemic or necrotic myocardium. Initial experience. *Eur Radiol.* 2016;26(9):3199-207
 25. Alvarez RE, Macovski A. Energy-selective reconstructions in X-ray computerized tomography. *Phys Med Biol.* 1976;21(5):733-44
 26. Willemink MJ, Persson M, Pelc NJ, Fleischmann D. Photon-Counting CT: Technical Principles and Clinical Prospects. . submitted .
 27. de Vries A, Roessl E, Kneepkens E, et al. Quantitative spectral K-edge imaging in preclinical photon-counting x-ray computed tomography. *Invest Radiol.* 2015;50(4):297-304
 28. Shikhaliev PM, Fritz SG. Photon counting spectral CT versus conventional CT: comparative evaluation for breast imaging application. *Phys Med Biol.* 2011;56(7):1905-30
 29. Schlimok JP, Roessl E, Dorscheid R, et al. Experimental feasibility of multi-energy photon-counting K-edge imaging in pre-clinical computed tomography. *Phys Med Biol.* 2008;53(15):4031-47
 30. Ronaldson JP, Zainon R, Scott NJ, et al. Toward quantifying the composition of soft tissues by spectral CT with Medipix3. *Med Phys.* 2012;39(11):6847-57
 31. He P, Yu H, Thayer P, et al. Preliminary experimental results from a MARS Micro-CT system. *J Xray Sci Technol.* 2012;20(2):199-211
 32. Iwanczyk JS, Nygard E, Meirav O, et al. Photon Counting Energy Dispersive Detector Arrays for X-ray Imaging. *IEEE Trans Nucl Sci.* 2009;56(3):535-42
 33. Taguchi K, Iwanczyk JS. Vision 20/20: Single photon counting x-ray detectors in medical imaging. *Med Phys.* 2013;40(10):100901.
 34. Feuerlein S, Roessl E, Proksa R, et al. Multienergy photon-counting K-edge imaging: potential for improved luminal depiction in vascular imaging. *Radiology.* 2008;249(3):1010-6
 35. Boussel L, Coulon P, Thran A, et al. Photon counting spectral CT component analysis of coronary artery atherosclerotic plaque samples. *Br J Radiol.* 2014;87(1040):20130798.
 36. Kappler S, Hannemann T, Kraft E, et al. First results from a hybrid prototype CT scanner for exploring benefits of quantum-counting in clinical CT. . SPIE 2012;83130X.

Dank voor uw bezoek
tijdens de EANM 2017
in Wenen

bv Cyclotron VU

C Curie bvba

EuroMedical Instruments

Hoy Scandinavian ApS

M.N.T. Kwint International bv

M&I Materials Ltd

MED Nuklear-Medizintechnik Dresden GmbH

Nicesoft

Nuvia as

PI Medical Diagnostic Equipment bv

SurgicEye GmbH

VANDERWILT techniques bv



Ervaringen van de complementaire radioloog en nucleair geneeskundige

Cross-over training in de cardiovasculaire beeldvorming

N.H.J. Prakken, MD, PhD; prof. R.H.J.A. Slart, MD, PhD

Medical Imaging Center, afdelingen Radiologie en Nucleaire Geneeskunde & Moleculaire Beeldvorming, Universitair Medisch Centrum Groningen, Groningen, Nederland

Wat voorafging

In 2015 zijn cross-over trainingen en deelcertificaten geïntroduceerd als overgangsmaatregel naar de ontwikkeling van een gezamenlijke opleiding Radiologie - Nucleaire Geneeskunde (het Corona-project). Ze bieden radiologen en nucleair geneeskundigen oude stijl, jonge klaren en eenieder die er interesse in heeft, de mogelijkheid om zich – in het kader van multimodale beeldvorming – laagdrempelig tot zelfstandig niveau te bekwamen in elkaars vakgebied, met als doel een goede samenwerking te realiseren, zowel bij de training in elkaars vakgebied, alsook in de praktijk na het behalen van het certificaat.

Voor het behalen van deelcertificaten zijn door het Concilium eisen opgesteld. Uitgangspunt is dat een specialist zelfstandig een volledig onderzoek moet kunnen uitvoeren, inclusief de verslaglegging. Hiervoor is zowel praktische ervaring als theoretische onderbouwing nodig. In de basis komt het erop neer dat een specialist zich tot zelfstandig niveau bekwaamt in een deel van het andere vakgebied, door het gewenste aantal verrichtingen zelfstandig te verslaan, medeondertekend (of gesuperviseerd) door een collega van het andere specialisme. Om het deelcertificaat in het kader van samen-

werking tot een succes te maken, wordt bij de aanvraag ervan gevraagd om het andere specialisme erbij te betrekken en een bekwaamheidsverklaring af te geven. Na het behalen van het certificaat is het de bedoeling dat de radioloog en/of nucleair geneeskundige de verworven expertise ook onderhoudt, zoals dit ook geldt voor andere competenties in het kader van de wet BIG.

Cross-over training in het UMCG

De afdelingen Radiologie en Nucleaire Geneeskunde & Moleculaire Beeldvorming (NGMB) in het UMCG zijn drie jaar geleden samengegaan en omgevormd tot het Medical Imaging Center (MIC). De fusie maakte het eenvoudiger om de deelcertificering op te starten: de lijnen zijn korter, en in de praktijk kunnen radioloog en nucleair geneeskundige direct leren van elkaar techniek, waardoor de meerwaarde en ook de beperkingen ervan sneller worden ingezien. Sinds het samengaan van de afdelingen hebben een nucleair geneeskundige en twee radiologen binnen het MIC het deelcertificaat oncologie behaald.

Nucleair geneeskundige Riemer Slart en radioloog Niek Prakken zijn eind 2016 gestart met de training om respectievelijk het deelcertificaat cardiale radiologie en nucleaire cardiologie te behalen. Slart is gespecialiseerd in myocardperfusescintigrafie (MPS) SPECT en Prakken in cardiale CT en cardiale MRI. Gemiddeld kunnen ze een

halve dag per week aan de cross-over training werken. Prakken is ondertussen al in het bezit van het andere cross-over deelcertificaat FDG PET/CT whole body oncologie. Hiervoor heeft hij de benodigde 300 FDG PET-scans verslagen onder supervisie van een nucleair geneeskundige. Prakken: "Het is net even anders dan bij het deelcertificaat whole body FDG PET/CT oncologie. Deze hybride beeldvorming en verslaglegging zijn namelijk direct aan elkaar gekoppeld. Bij de cardiale beeldvorming worden de radiologische en nucleaire beeldvorming onafhankelijk van elkaar verricht. Dat betekent dat je er actief op af moet om bijvoorbeeld een CT, MRI of MPS-verslaglegging te kunnen doen."

Onderwijs

Er is een verplicht aantal scans dat verslagen moet worden: 150 MPS, 150 cardiale CT's & 150 cardiale MRI's. Na de verslaglegging worden ongeautoriseerde verslagen gezamenlijk doorgenomen en vervolgens geautoriseerd. Daarnaast wordt er onderwijs gevolgd. Het cursorisch en Beeldvormende Technieken (BVT) onderwijs voor de radioloog bestaat uit tweemaal nucleaire technieken-onderwijs, niveau 3 stralingsbescherming en een ecg-cursus. De nucleair geneeskundige volgt tweemaal cursorisch onderwijs cardiale radiologie (gezamenlijk met de aiossen), tweemaal BVT CT en viermaal BVT MRI.

Slart: "Ik zou zeker ook aanbevelen om



Niek Prakken en Riemer Slart proberen hun deelcertificaat eind 2017 af te ronden. Bij het perse komen van dit nummer wordt waarschijnlijk de champagnefles ontkorkt.

Vervolgens is het zaak om de opgedane expertise in de praktijk bij te gaan houden. Het plan is vanaf 2018 een halve tot een dag per week cross-over verslaglegging te gaan verrichten. Een verbreding binnen een subspecialisatie is dan gerealiseerd, waarmee zij beiden zelfstandig hybride verslaglegging binnen dit deelgebied kunnen uitvoeren.

mee te kijken of ingezet te worden bij het verrichten van de CT, MRI of de camera, inclusief de fietsinspanningstest en het adenosine-onderzoek. Dit geeft meer inzicht in de praktische verrichtingen en de verwerking en analyse van data, zoals dit ook het geval is bij ventrikelanalyse na het MRI-onderzoek. Maar ook hoe een afwijkende scan achteraf verklaard kan worden door bijvoorbeeld bepaalde artefacten."

Prakken en Slart adviseren om ook expertise elders op te doen, zodat je een indruk krijgt hoe de beeldvormingsprocedure buiten je eigen instituut wordt uitgevoerd. Zo heeft Slart de 'Advanced cardiale CT-cursus' aan het Erasmus MC gevuld, waarbij 100 cardiale CT's zelfstandig werden beoordeeld en gezamenlijk werden besproken. Hiervan mag hij er maximaal 50 meenemen voor de CT-cases die hij moet verzamelen in zijn verslagleggingslijst. Dat betekent dat hij 100 CT's klinisch moet verslaan en 50 uit deze database kan toevoegen om het totale aantal van 150 te kunnen bereiken. Ook heeft hij vijf dagen meegedraaid in een Hart Imaging Centrum (CNR) in Pisa/Massa, Italië, waar cardiale CT- en cardiale MRI-diagnostiek worden uitgevoerd. De verrichtingen en verslag-

legging gaven een goed beeld van de verschillende manieren van werken.

Prakken heeft in het verleden ervaring opgedaan met oncologische PET/CT-verslaglegging in het Meander Medisch Centrum in Amersfoort voor het deelcertificaat FDG whole body oncologie.

Radioloog versus nucleair geneeskundige

Welke verschillen zien Slart en Prakken tussen hun afdelingen?

Prakken: "Bij de oncologische PET/CT wordt het diagnostische CT-deel besproken/gesuperviseerd door een radioloog als de nucleair geneeskundige geen CT-certificaat heeft. Als de radioloog geen PET-certificaat heeft, voegt hij enkel een CT-deel toe. Er is geen integrale verslaglegging vanaf het eerste moment, zoals wel mogelijk is bij cross-over gecertificeerde beeldvormers."

Slart: "De nucleaire geneeskunde is een kleinschaligere afdeling dan de radiologie, waardoor de lijnen vaak korter zijn. En bij cardiale beeldvorming ligt de aandacht van de nucleair geneeskundige het meest bij functionele ischemie-(en infarct-)detectie, inclusief

het opsporen van cardiale infectie/inflammatie. Terwijl het bij de radioloog veel meer gaat over de cardiale anatomie en functie in bredere zin."

Ook is er verschil in het uitvoeren van de procedures en onderzoeken tussen de afdelingen. Als voorbeeld noemt Slart het sarcoïdosedieet bij ziekte-detectie met FDG van het hart, of de bloedsuikerspiegelbepaling bij FDG-vitaliteitonderzoek. "Voor de radiologie staat hierbij juist de nierfunctie op de voorgrond in verband met het toe te dienen intraveneuze contrast. En bij de nucleaire geneeskunde wordt vrijwel elk verslag gestructureerd uitgevoerd volgens een vaste indeling; dat is ook echt anders vergeleken met de radiologie, maar varieert wel per afdeling."

Voordelen op een rij

- Uitbreiding van vakkennis met de steeds meer toegepaste hybride beeldvormingstechnieken, waarvan PET/CT op dit moment de meest gebruikte techniek is en in de toekomst mogelijk de PET/MRI aanvullend is. De bijscholing is vooral van belang omdat het de toekomst is van het hybride beeldvormingsvak.

- Samenwerking zorgt voor een 'win-win'-situatie: door gebruik te maken van elkaars expertise over en weer, leer je van elkaars technieken. Bovendien zorgt samenwerking ervoor dat je de werkelijke meerwaarde van de technieken er ook uithaalt: $1+1>2$. Door de positieve wisselwerking die hiervan uitgaat, zal er - bij de toename van het geloof, het vertrouwen en de noodzaak in het toepassen van de meest geschikte techniek voor het beantwoorden van de hulpvraag - meer aanbod komen. Bij het MIC heeft de cross-over geleid tot verdere verbetering van de al prettige verstandhouding en een geïntensieverde samenwerking tussen radiologie en nucleaire geneeskunde. Behalve in de kliniek, zijn er ook plannen voor nog meer samenwerking in de wetenschap.
- Met de samenvoeging van de vakgebieden moeten de zittende medische-beeldvorming-specialisten ook zelf de technieken beheersen

om deze integraal bij te kunnen brengen aan de assistenten. Kruisbestuiving van elkaars expertise en nieuwe inzichten in de waarde van hybride technieken moet hiervoor eveneens verworven zijn.

- Door het samengaan van de afdelingen is het mogelijk om met één gezicht naar buiten te treden naar aanvragende klinische afdelingen. Er is ook een betere adviserende rol weggelegd voor de beeldvormende specialist. Deze heeft nu professionele kennis en overzicht over de beschikbare beeldvormingstechnieken. Vanuit dit vertrekpunt kan de beeldvormende specialist het meest geschikte onderzoek voor de patiënt aan de aanvrager adviseren.
- Er hoeft slechts één gecertificeerde beeldvormer aan te schuiven bij het cardiale MDO, waarin de uitslagen besproken worden en naast de klinische bevindingen worden gelegd. De ander houdt tijd over voor de kliniek. Een an-

der voordeel is dat de cross-over beeldvormer aanspreekpunt is voor de kliniek voor alle cardiale beeldvormingstechnieken.

Tips

- Zoek een geschikte sparringpartner en ruim hiervoor tijd in (halve tot een dag per week), waarbij eenieder voldoende aan bod komt.
- Reserveer liefst een vast moment in de week, bij voorkeur op een dag dat er voldoende aanbod is.
- Houdt rekening met de (in)planning van het cursorische onderwijs.
- Documenteer zorgvuldig wat je hebt gedaan, zodat bij indiening alles op orde is en volgens de eisen van de verenigingen kan worden aangeleverd.
- Vergeet niet regelmatig de MDO-besprekingen bij te wonen, als (extra) leermoment.

n.h.j.prakken@umcg.nl
r.h.j.a.slart@umcg.nl ♦

Imaging cardiac sympathetic innervation: current clinical status

B.F. Bulten, MD, PhD¹; W. Noordzij, MD, PhD²; D.O. Verschuren, MD, PhD³; H.J. Verberne, MD, PhD⁴

¹Department of Nuclear Medicine, Santiz, Doetinchem and Winterswijk, the Netherlands; ²Department of Radiology and Nuclear Medicine, University Medical Center Groningen, Groningen, the Netherlands; ³Department of Cardiology, Zaans Medical Center Zaandam, the Netherlands; ⁴Department of Radiology and Nuclear Medicine, Academic Medical Center, Amsterdam, the Netherlands

Abstract

Although imaging cardiac innervation has a long history, widespread clinical use has not been accomplished yet. We provide a short overview of the available SPECT and PET tracers, with ¹²³Iodine-metiodobenzylguanidine (¹²³I-mIBG) as the most important one, and the clinical indications for which they can be used, including the assessment of chronic heart failure, cardiac arrhythmias, chemotherapy induced cardiotoxicity, cardiac sarcoidosis and amyloidosis.

Introduction

Although imaging of cardiac innervation has a long history for both SPECT and PET tracers, starting with the use of ¹²³Iodine-metiodobenzylguanidine (¹²³I-mIBG) and up to the development of N-[3-bromo-4-(3-¹⁸F-fluoro-propoxy)-benzyl]-guanidine (¹⁸F-LMI1195), widespread clinical use has not been accomplished. Nonetheless, imaging cardiac innervation has some very interesting applications and can, when properly used, add valuable information in the process of clinical decision making. We will provide a short overview of the current clinical status of cardiac innervation imaging.

Cardiac innervation can be divided into the two counteracting autonomic systems, the sympathetic and parasympathetic system. For both systems radiotracers have been developed, but experience with the parasympathetic pathway is very scarce and is still a far way from clinical implementation. The sympathetic system can be further divided into a presynaptic and postsynaptic part. The postsynaptic part, in which the main imaging target is the β -adrenergic receptor, has been studied with very specific tracers, such as ¹¹Carbon-CGP-12177, but due to problems with synthesis and availability, clinical use is severely impaired. Other postsynaptic tracers have not proven their clinical value yet (1). However, experience with presynaptic cardiac imaging is extensive. Most of the tracers used are designed as analogues of norepinephrine (NE) and are taken up, concentrated and stored in the pre-synaptic nerve terminals (figure 1). Among these tracers are SPECT-based ¹²³I-mIBG, probably the most well known of all, but also newer PET-based carbon-11 labelled metahydroxyephedrine (¹¹C-mHED) and ¹⁸F-LMI1195. The latter has been developed to function as ¹²³I-mIBG, exploiting the experience with the SPECT tracer, but harvesting the

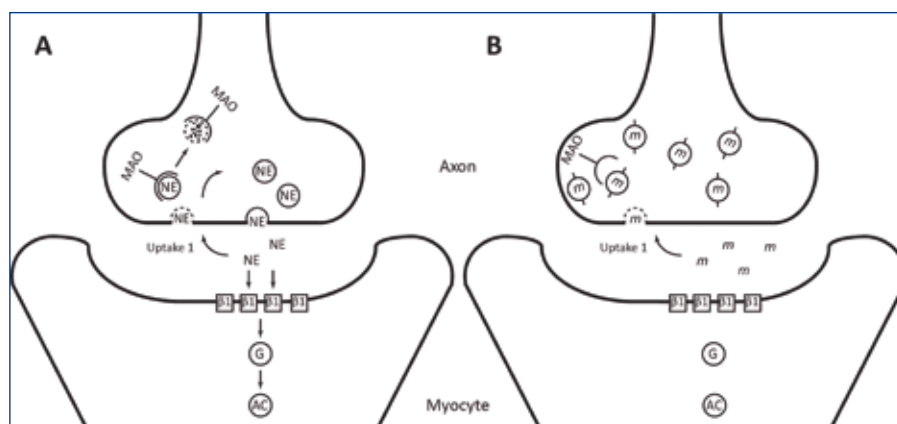


Figure 1. Schematic display of norepinephrine (NE) and ¹²³I-mIBG (m) sympathetic pathway.

A. In response to a stimulus, NE-containing vesicles are released into the synaptic cleft. There, NE binds to mainly β 1-receptors on the postsynaptic surface, which enhance adenyl cyclase (AC) activity through G protein (G) activation. NE is recycled by the uptake-1 pathway for storage or degradation by mono amine oxidase (MOA).

B. Guanethidamine, an inactive neurotransmitter that resembles NE, is chemically modified and labeled with ¹²³I, becoming ¹²³I-mIBG. When this radioactive compound is available in the circulation, it is taken up and stored in the same way as NE, but cannot be catabolised by MOA. Therefore, ¹²³I-mIBG is retained in sufficient concentrations to allow imaging with a gamma camera (39).

advantages of PET imaging in spatial resolution and quantitative analysis. The most commonly used semi-quantitative measurements of myocardial ^{123}I -mIBG uptake are the early heart-to-mediastinum ratio (HMR), derived 15 minutes post injection (p.i.) of ^{123}I -mIBG, late HMR, derived 4 hours p.i. and the ^{123}I -mIBG washout ratio (WR), calculated as the difference between early and late HMR and expressed as a percentage of the early HMR.

These tracers enable the assessment of several clinical problems, including chronic heart failure (CHF), cardiac arrhythmia, cardiotoxicity due to cancer treatment, cardiac sarcoidosis and cardiac amyloidosis.

Current clinical status

Chronic heart failure and cardiac arrhythmia

Heart failure (HF) is a life-threatening disease affecting approximately 26 million people worldwide (2). The incidence of HF in the Netherlands ranges between 28,000 and 44,000 cases per year and increases with age; the majority of HF patients are older than 75 years. Currently, there are between 100,000 and 150,000 patients with HF in the Netherlands. It is the only cardiovascular disease with both growing incidence and prevalence (3). Reasons for this trend are related to increased life expectancy, improvement

of survival after myocardial infarction and better treatment options for HF (figure 2). It is expected that the total number of HF patients in the Netherlands will increase to 275,000 in 2040.(4) As a consequence, the costs related to HF care will increase: in 2007 these costs were 455 million euro which rose to 940 million in 2011 (3). For 2025, these costs are estimated at 10 billion euros (4).

Despite the successful introduction of treatment with a combination of beta-blockers and angiotensin-converting-enzyme inhibitors or angiotensin receptor blockers together with loop diuretics, the prognosis of CHF remains unfavourable. The most recent European data (ESC-HF pilot study) demonstrate that 12-month all-cause mortality rates for hospitalised and stable/ambulatory HF patients were 17% and 7%, respectively (5). The majority of these deaths are caused by progression of HF, lethal arrhythmia and sudden cardiac death (SCD). The use of implantable devices such as implantable cardioverter defibrillators (ICD) and cardiac resynchronisation therapy (CRT) has improved the overall survival of CHF patients (6-8). Current European guidelines recommend ICD for primary prevention of fatal arrhythmias in CHF subjects with an left ventricle ejection fraction (LVEF) <35% and symptomatic HF NYHA class ≥ 2 under optimal pharmacological therapy (9). In addition, CRT is recommended in CHF patients

who remain symptomatic in NYHA class ≥ 2 under optimal pharmacological therapy, with a LVEF <35% and wide QRS complex (≥ 130 ms).

ICDs applied for primary or secondary (i.e. already proven ventricular arrhythmias) prevention reduce the relative risk of death by 20%. However, analysis of the MADIT II (Second Multicenter Automated Defibrillator Implantation Trial) has shown that the absolute reduction of fatal events was only 5.6% (19.8% to 14.2%).(7) In addition, the SCD-HeFT (Sudden Cardiac Death in Heart Failure Trial) study showed that the annual number of ICD shocks was 7.1%, of which 5.1% were appropriate, in the first year rising to 21% in the fifth year post-implantation (10). However, three years after ICD implantation for primary prevention, a remarkably high percentage of 65% had never received appropriate ICD therapy. Moreover, there is also a risk of malfunction and operative complications, e.g. inappropriate shocks, infection.

Last but not least, is the relative high cost of these devices. Therefore, it is essential, not only from a clinical but also from a socioeconomic point of view, to optimise the current selection criteria for CRT and ICD for primary prevention aimed at better identification of patients who will benefit from implantation.

Currently one of the selection criteria for CRT and ICD implantation for primary

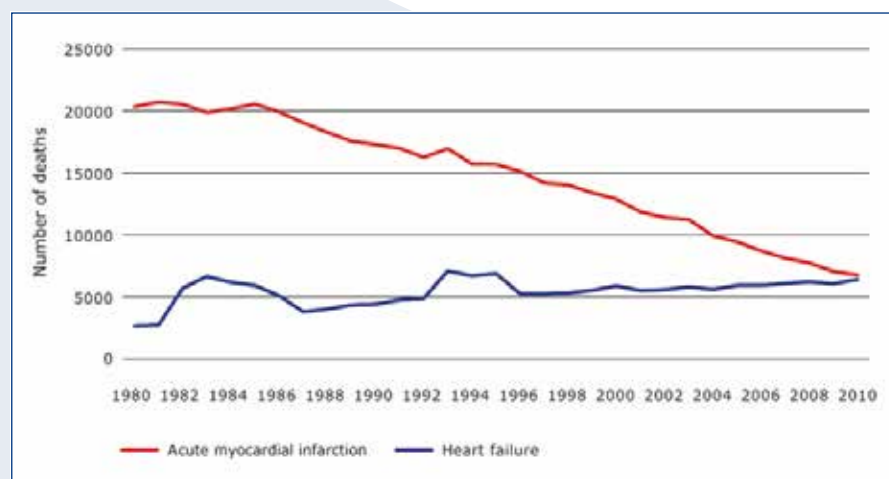


Figure 2. Number of deaths as a result of acute myocardial infarction and heart failure in the Netherlands from 1980 to 2010. The decrease in the number of deaths after myocardial infarction declines more rapidly than the increase in number of deaths due to heart failure. Source: Centraal Bureau voor de Statistiek (CBS), the Netherlands.

prevention is an LVEF <35%. However, LVEF assessed by cardiovascular magnetic resonance imaging (CMR) is significantly lower compared with echocardiography (11). Therefore, CMR would significantly increase the number of CHF patients eligible for CRT or ICD implantation. This illustrates that the method to assess LVEF has substantial impact on the selection of 'appropriate' patients for CRT and ICD implantation. The lack of uniformity among imaging modalities to assess LVEF raises the question if other parameters may be useful to better identify those patients who will benefit from CRT or ICD implantation. One of those alternative parameters might be cardiac sympathetic hyperactivity, which is related to poor prognosis and fatal arrhythmias in CHF.

The past decades, myocardial ^{123}I -mIBG scintigraphy has been shown to predict prognosis in CHF patients (12,13). A predefined LEHR (low energy high resolution) collimator derived HMR <1.6 has been suggested to be a predictor of ventricular arrhythmia (14). Furthermore, decreased ^{123}I -mIBG uptake and increased WR are associated with increased incidence of SCD or appropriate ICD therapy (15,16). Most of these studies have been conducted in various populations, both with primary and secondary prevention of SCD. In addition, extrapolation of the obtained data is hampered by the fact that these data were not corrected for differences in gamma camera-collimators use (17).

Just recently available are the results of a prospective multicentre study evaluating whether ^{123}I -mIBG scintigraphy assessed cardiac sympathetic activity could identify high-risk CHF patients most likely to undergo appropriate ICD therapy for primary prevention of SCD (18). In 135 stable CHF patients referred for prophylactic ICD implantation the combination of late HMR (HR 0.461 [0.281-0.757]) and LVEF (HR 1.052 [1.021-1.084]) was significantly associated with freedom of appropriate ICD therapy ($p<0.001$). Although this data needs to be confirmed by other studies ^{123}I -mIBG scintigraphy

seems to be helpful in selecting CHF subjects who might not benefit from ICD implantation.

Cardiotoxicity

In addition to their beneficial anticancer action, many therapies potentially exert one or more cardiotoxic effects. Anthracyclines and monoclonal antibodies such as trastuzumab are notorious for this, but the list of cardiotoxic medication is a very long one (19). Since in recent years survival of many cancer types has increased, long-term treatment complications and subsequent quality of life has received additional attention. This has led to a rise in research on cancer-treatment-induced cardiotoxicity (CIC), especially regarding the early detection of this phenomenon (20). Many patients would benefit from early stratification of patients at risk, in particular children suffering from childhood leukaemia and relatively young women who receive anthracyclines and/or trastuzumab therapy for breast cancer.

^{123}I -mIBG assessed cardiac sympathetic innervation has been proposed as a promising method to indicate which patients are at risk for developing CIC (21,22). Early experiments in rats showed a decrease in sympathetic activity in response to doxorubicin administration. Furthermore, this decrease was dose-dependent and occurred before any morphological changes or alterations in LVEF, which till date is the (clinically used) gold standard for assessment of CIC (22). A subsequent study in humans showed a concurrent decrease in sympathetic imaging and LVEF, but failed to show a strong association between the two (21). A case series by a different group showed similar results, while a recent study did not find a significant correlation between the HMR and a late decrease of LVEF (indicating CIC) in childhood cancer survivors five years post chemotherapy (23,24). This indicates that no clinically sound conclusion can be drawn yet and that will be difficult to prove since CIC can develop up to 20 years after chemotherapy, ranging from subclinical

to overt CHF. In order to conclude whether ^{123}I -mIBG assessed cardiac sympathetic activity indeed can add value to anti-cardiotoxic management, a prospective study that examines the use of HMR and WR (or comparable PET-tracers) in the early detection of CIC is therefore warranted, preferably in combination with other promising imaging methods, such as blood-drawn biomarkers, echocardiographic strain and cardiac magnetic resonance imaging.

Cardiac sarcoidosis

Cardiac involvement is a clinical predictor of morbidity and mortality in sarcoidosis patients (25). It has been shown that cardiac involvement can be identified by sympathetic imaging (26,27). Hoitsma et al. suggested that cardiac autonomic dysfunction in sarcoidosis patients depends on the presence of small fiber neuropathy (SFN), and can be sensitively detected by ^{123}I -mIBG scintigraphy (25). However, no progress has been made in implementing this into clinical practice, probably because the condition of cardiac sarcoidosis is rare. Moreover, more promising methods such as (combined) ^{18}F -FDG PET and cardiac magnetic resonance imaging have emerged and are now studied in this respect.

Cardiac amyloidosis

Patients with amyloidosis are prone to developing disturbances in autonomic innervation: dysautonomia (28). Cardiac dysautonomia can be caused by amyloid infiltration into the myocardial and conduction tissue, resulting in conduction and rhythm disorders. Cardiac dysautonomia is common in patients with transthyretin-related amyloidosis (ATTR type) and in patients with immunoglobulin light chain-derived amyloidosis (AL type) (29). More specifically, patients with the hereditary form of ATTR type amyloidosis (hATTR, formerly called familial amyloid polyneuropathy) frequently develop polyneuropathy and dysautonomia. Furthermore, cardiac dysautonomia

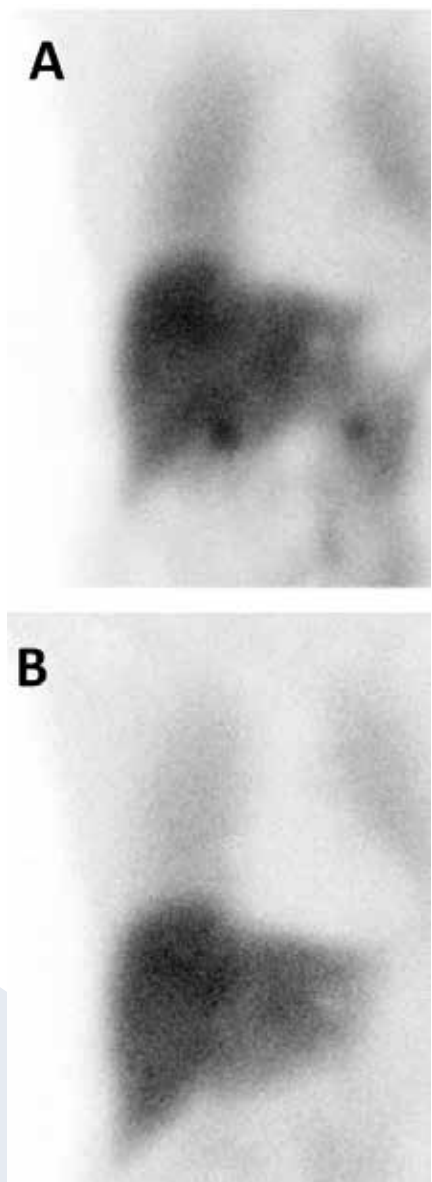


Figure 3. Example of a planar ^{123}I -mIBG scintigraphy with a medium energy collimator in a 70-year old female patient with ATTR amyloidosis based on a Val30Met mutation. A shows a planar image 15 minutes post injection (p.i.) and B shows a planar image 4 h p.i.. The calculated late HMR was 1.38 (normal value in (UMCG) laboratory: 2.0).

mia may occur independently of the presence of a typical restrictive cardiomyopathy. Amyloidosis' typical restrictive cardiomyopathy is most commonly found in patients with wild-type ATTR type amyloidosis (wtATTR, formerly called senile systemic amyloidosis). In these wtATTR patients, polyneuropathy and dysautonomia are infrequent and approximately 9% (30).

At present, actual amyloid infiltration cannot be visualised with nuclear medicine techniques. Nonetheless, semi-quantitative HMR analysis on ^{123}I -mIBG scintigraphy is assumed to provide insight in the amyloid infiltration of the sympathetic nerve system (figure 3) (31). However, when reviewing the present literature with respect to the use of ^{123}I -mIBG in patients with different types of systemic amyloidosis, due to the large overlap of late HMR ranges in ATTR and AL type amyloidosis patients, ^{123}I -mIBG scintigraphy is considered not to be able to discriminate between these amyloidosis subtypes (31).

In amyloidosis patients with impaired cardiac sympathetic innervation, decreased survival rates are established. Late HMR has been identified as an independent prognostic factor for 5-year all-cause mortality, with a 42% mortality rate for those patients with late HMR <1.60 , compared to merely 7% in patients with late HMR ≥1.60 (hazard ratio (HR) 7.2, $p<0.001$). (32) Based on the results of this study, even patients with HMR <1.60 seem to benefit from liver transplantation (because of amyloid involvement), resulting in lower long-term mortality than neurophysiological score-matched control subjects (HR 0.32, $p=0.012$). This underlines the assumption that impaired cardiac sympathetic innervation will not progress after liver transplantation, and that re-innervation cannot be detected within this duration of clinical follow-up (33). In addition, late HMR remains of prognostic importance after liver

transplantation, with larger area under the receiver-operating curve than clinical parameters and heart rate variability (AUC: 0.79 versus 0.66 and 0.52, respectively) in univariate analysis. However, multivariate analysis revealed that late HMR has no additive value to a reference model in predicting outcome (AUC 0.80 versus 0.79, respectively). (34) In the AL type population very little is known about the consequences of reduced late HMR. Follow-up of the available studies in this population is too limited to identify arrhythmogenic consequences of impaired cardiac sympathetic innervation. Data on the contribution of reduced late HMR to cardiovascular outcome measurements in patients with ATTR amyloidosis seems to be incomplete. Only one study reported the association of reduced late HMR with the presence of ventricular arrhythmia, and the progression of conduction disturbances after liver transplantation due to continuous amyloid infiltration (33). Understanding this apparent oxymoron (i.e.: the cessation of progression of cardiac innervation abnormalities despite continuous amyloid infiltration after liver transplantation) will be a challenge for future investigations.

In early studies using ^{123}I -mIBG, amyloidosis patients underwent additional (resting state) myocardial perfusion scintigraphy using thallium-201 (^{201}Tl). None of the included patients seemed to suffer from myocardial infarction, since all resting state ^{201}Tl scans were reported as normal. This perfusion - innervation mismatch is a known phenomenon in patients with ischaemic cardiomyopathy, but also occurs in patients with non-ischaemic (dilating) cardiomyopathy (35). Myocardial perfusion abnormalities are known to result in damaged sympathetic nerve terminals, leading to a larger area of impaired innervation than impaired perfusion alone. This mismatch

pattern leads to electrophysiological imbalance, which is associated with a higher risk of developing ventricular arrhythmia. The presence of structural changes (for example heterogeneous interstitial fibrosis) in combination with disturbed sympathetic stimulation due to amyloid infiltration may contribute to altered ventricular activation and contractility, and a higher risk of ventricular arrhythmia in amyloidosis patients.

In conclusion, ^{123}I -mIBG is currently the most widely used radiopharmaceutical for imaging cardiac sympathetic innervation disturbances in patients with cardiac manifestations of amyloidosis. Particularly patients with hATTR type amyloidosis show diminished late HMR's, and consequently have a higher risk of cardiac mortality.

Current challenges and future perspectives

The main problem with the use of cardiac sympathetic imaging is the lack of standardisation of acquisition protocols and the choice of relevant parameters. Many factors are of influence in determining whether cardiac sympathetic function is impaired, including collimator choice, acquisition time, placement of the region of interest and circulating catecholamines (36,37). Although big steps have been made to address these factors on cardiac ^{123}I -mIBG scintigraphy, there are still several issues that need further clarification before routine clinical use seems appropriate (36).

The development of PET-based radiopharmaceuticals to image cardiac sympathetic innervation is promising (38). For example, ^{11}C -mHED and ^{18}F -LMI1195 provide better resolution and an opportunity to evaluate quantitatively, but research on these tracers is still sparse. Furthermore, they are not yet commercially available and therefore suffer from limited availability. When this changes, the future for the sympathetic cardiac imaging depends

on these radiopharmaceuticals and a growing clinical need for them.

benbulten@gmail.com ♦

References

- Noordzij W, Slart RH. PET imaging of the autonomic myocardial function: methods and interpretation. *Clin Transl Imaging* 2015;3:365-372.
- Bui AL, Horwitz TB, Fonarow GC. Epidemiology and risk profile of heart failure. *Nat Rev Cardiol* 2011;8:30-41.
- Koopman C, Bots ML, van Oeffelen AA, et al. Population trends and inequalities in incidence and short-term outcome of acute myocardial infarction between 1998 and 2007. *Int J Cardiol* 2013;168:993-8.
- Bots ML, Van Dis I, Vaartjes F. Hart-en vaatziekten in Nederland 2015. Zoetermeer: Hartstichting; 2015.
- Maggioni AP, Dahlstrom U, Filippatos G, et al. EURObservational Research Programme: regional differences and 1-year follow-up results of the Heart Failure Pilot Survey (ESC-HF Pilot). *Eur J Heart Fail* 2013;15:808-17.
- Bristow MR, Saxon LA, Boehmer J, et al. Cardiac-resynchronization therapy with or without an implantable defibrillator in advanced chronic heart failure. *N Engl J Med* 2004;350:2140-50.
- Moss AJ, Zareba W, Hall WJ, et al. Prophylactic implantation of a defibrillator in patients with myocardial infarction and reduced ejection fraction. *N Engl J Med* 2002;346:877-83.
- Cleland JG, Daubert JC, Erdmann E, et al. The effect of cardiac resynchronization on morbidity and mortality in heart failure. *N Engl J Med* 2005;352:1539-49.
- Ponikowski P, Voors AA, Anker SD, et al. 2016 ESC Guidelines for the diagnosis and treatment of acute and chronic heart failure: The Task Force for the diagnosis and treatment of acute and chronic heart failure of the European Society of Cardiology (ESC) Developed with the special contribution of the Heart Failure Association (HFA) of the ESC. *Eur J Heart Fail* 2016;18:891-975.
- Moss AJ, Greenberg H, Case RB, et al. Long-term clinical course of patients after termination of ventricular tachyarrhythmia by an implanted defibrillator. *Circulation* 2004;110:3760-5.
- de Haan S, de Boer K, Commandeur J, et al. Assessment of left ventricular ejection fraction in patients eligible for ICD therapy: discrepancy between cardiac magnetic resonance imaging and 2D echocardiography. *Netherlands Heart Journal* 2014;22:449-55.
- Jacobson AF, Senior R, Cerqueira MD, et al. Myocardial iodine- 123 meta-iodobenzylguanidine imaging and cardiac events in heart failure. Results of the prospective ADMIRE-HF (AdreView Myocardial Imaging for Risk Evaluation in Heart Failure) study. *J Am Coll Cardiol* 2010;55:2212-21.
- Vershure DO, Veltman CE, Manrique A, et al. For what endpoint does myocardial ^{123}I -mIBG scintigraphy have the greatest prognostic value in patients with chronic heart failure? Results of a pooled individual patient data meta-analysis. *Eur Heart J Cardiovasc Imaging* 2014;15:996-1003.
- Al Badarin FJ, Wimmer AP, Kennedy KF, et al. The utility of ADMIRE-HF risk score in predicting serious arrhythmic events in heart failure patients: incremental prognostic benefit of cardiac ^{123}I -mIBG scintigraphy. *J Nucl Cardiol* 2014;21:756-62; quiz 753-55, 763-5.
- Nagahara D, Nakata T, Hashimoto A, et al. Predicting the need for an implantable cardioverter defibrillator using cardiac metaiodobenzylguanidine activity together with plasma natriuretic peptide concentration or left ventricular function. *J Nucl Med*

- 2008;49:225-33.
16. Boogers MJ, Borleffs CJ, Henneman MM, et al. Cardiac sympathetic denervation assessed with ^{123}I -iodine metaiodobenzylguanidine imaging predicts ventricular arrhythmias in implantable cardioverter-defibrillator patients. *J Am Coll Cardiol* 2010;55:2769-77.
 17. Nakajima K, Okuda K, Yoshimura M, et al. Multicenter cross-calibration of I-123 metaiodobenzylguanidine heart-to-mediastinum ratios to overcome camera-collimator variations. *J Nucl Cardiol* 2014;21:970-8.
 18. Verschure DO, de Groot JR, Mirzaei S, et al. Cardiac ^{123}I -mIBG scintigraphy is associated with freedom of appropriate ICD therapy in stable chronic heart failure patients. *Intl J Cardiol* 2017; In press.
 19. Yeh ET, Bickford CL. Cardiovascular complications of cancer therapy: incidence, pathogenesis, diagnosis, and management. *J Am Coll Cardiol* 2009;53:2231-47.
 20. Stevens PL, Lenihan DJ. Cardiotoxicity due to Chemotherapy: the Role of Biomarkers. *Curr Cardiol Rep* 2015;17:603.
 21. Carrio I, Estorch M, Berna L, et al. Indium-111-antimyosin and iodine-123-mIBG studies in early assessment of doxorubicin cardiotoxicity. *J Nucl Med* 1995;36:2044-9.
 22. Wakasugi S, Fischman AJ, Babich JW, et al. Metaiodobenzylguanidine: evaluation of its potential as a tracer for monitoring doxorubicin cardiomyopathy. *J Nucl Med* 1993;34:1283-6.
 23. Valdes Olmos RA, ten Bokkel Huinink WW, ten Hoeve RF, et al. Assessment of anthracycline-related myocardial adrenergic derangement by [^{123}I] metaiodobenzylguanidine scintigraphy. *Eur J Cancer* 1995;31A:26-31.
 24. Dos Santos MJ, da Rocha ET, Verberne HJ, et al. Assessment of late anthracycline-induced cardiotoxicity by ^{123}I -mIBG cardiac scintigraphy in patients treated during childhood and adolescence. *J Nucl Cardiol* 2017;24:256-264.
 25. Hoitsma E, Faber CG, van Kroonenburgh MJ, et al. Association of small fiber neuropathy with cardiac sympathetic dysfunction in sarcoidosis. *Sarcoidosis Vasc Diffuse Lung Dis* 2005;22:43-50.
 26. Misumi I, Kimura Y, Hokamura Y, et al. Scintigraphic detection of regional disruption of the adrenergic nervous system in sarcoid heart disease. *Jpn Circ J* 1996;60:774-8.
 27. Matsuo S, Nakamura Y, Matsui T, et al. Detection of denervated but viable myocardium in cardiac sarcoidosis with I-123 mIBG and Tl-201 SPECT imaging. *Ann Nucl Med* 2001;15:373-5.
 28. Goldstein DS. Cardiac Dysautonomia and Survival in Hereditary Transthyretin Amyloidosis. *JACC Cardiovasc Imaging* 2016;9:1442-1445.
 29. Falk RH, Comenzo RL, Skinner M. The systemic amyloidoses. *N Engl J Med* 1997;337:898-909.
 30. Pinney JH, Whelan CJ, Petrie A, et al. Senile systemic amyloidosis: clinical features at presentation and outcome. *J Am Heart Assoc* 2013;2:e000098.
 31. Noordzij W, Glaudemans AW, van Rheenen RW, et al. (123)I-Labelled metaiodobenzylguanidine for the evaluation of cardiac sympathetic denervation in early stage amyloidosis. *Eur J Nucl Med Mol Imaging* 2012;39:1609-17.
 32. Coutinho MC, Cortez-Dias N, Cantinho G, et al. Reduced myocardial ^{123}I -metaiodobenzylguanidine uptake: a prognostic marker in familial amyloid polyneuropathy. *Circ Cardiovasc Imaging* 2013;6:627-36.
 33. Delahaye N, Rouzet F, Sarda L, et al. Impact of liver transplantation on cardiac autonomic denervation in familial amyloid polyneuropathy. *Medicine (Baltimore)* 2006;85:229-38.
 34. Simoes MV, Barthel P, Matsunari I, et al. Presence of sympathetically denervated but viable myocardium and its electrophysiologic correlates after early revascularised, acute myocardial infarction. *Eur Heart J* 2004;25:551-7.
 35. Sasano T, Abraham MR, Chang KC, et al. Abnormal sympathetic innervation of viable myocardium and the substrate of ventricular tachycardia after myocardial infarction. *J Am Coll Cardiol* 2008;51:2266-75.
 36. Flotats A, Carrio I, Agostini D, et al. Proposal for standardization of ^{123}I -metaiodobenzylguanidine (mIBG) cardiac sympathetic imaging by the EANM Cardiovascular Committee and the European Council of Nuclear Cardiology. *Eur J Nucl Med Mol Imaging* 2010;37:1802-12.
 37. van der Palen RL, Bulten BF, Mavinkurve-Groothuis AM, et al. Catecholamines influence myocardial ^{123}I -mIBG uptake in neuroblastoma patients. *Nuklearmedizin* 2013;52:228-34.
 38. Slart RHJA. Autonomic innervation of the heart: role of molecular imaging. Berlin-Heidelberg: Springer-Verlag; 2015.
 39. Bulten BF. Biomarkers for the early detection of cancer treatment induced cardiotoxicity. Doctor of Philosophy, University of Twente, Enschede, The Netherlands, 2016

Recommendation on imaging in cardiac sarcoidosis: a summary

Prof. R.H.J.A. Slart, MD, PhD; A.W.J.M. Glaudemans, MD, PhD

Medical Imaging Center, Department of Nuclear Medicine and Molecular Imaging, University Medical Center Groningen, the Netherlands

Adapted from:

A Joint Procedural Position Statement on Imaging in Cardiac Sarcoidosis:

From the Cardiovascular and Inflammation & Infection Committees of the European Association of Nuclear Medicine (EANM), the European Association of Cardiovascular Imaging (EACVI), and the American Society of Nuclear Cardiology (ASNC) (Eur Heart J Cardiovasc Imag 2017 Oct 1; 18 (10): 1073-89, J Nucl Cardiol, online, 2017 Oct 17).

Abstract

This summary of the joint position paper illustrates the role and the correct use of echocardiography, radionuclide imaging with ¹⁸F-fluorodeoxyglucose positron emission tomography, radionuclide myocardial perfusion imaging and cardiovascular magnetic resonance imaging (CMR) for the evaluation and management of patients with known or suspected cardiac sarcoidosis. It will aid standardizing imaging for cardiac sarcoidosis and proposed flow charts for the work up and management of cardiac sarcoidosis are included.

Introduction

Sarcoidosis is a multisystem inflammatory granulomatous disease of unknown origin. Granulomas in sarcoidosis are compact, centrally organized collections of macrophages and epithelioid cells that are surrounded by lymphocytes. Granulomas from sarcoidosis are most often located in the lungs or its associated lymph nodes, but any organ can be affected.

Cardiac involvement may range from silent myocardial granulomas to symptomatic conduction disturbances, ventricular arrhythmias, progressive heart failure, and sudden death, accounting for 13-25% of disease-related deaths (1). The clinical course of cardiac sar-

coidosis (CS) varies from benign to life-threatening with severe heart failure and sudden cardiac death (2). The management of CS involves both immunosuppressive therapy for the treatment of sarcoidosis and cardiac-specific therapies to manage ventricular dysfunction and device therapy (pacemaker/ICD) for heart blocks and heart rhythm disturbances. The decision for drug therapy alone or the implantation of an ICD for primary prevention in the early stage of CS remains challenging. Nevertheless, it is felt that early initiation of immunosuppressive therapy may prevent progression of cardiac dysfunction and improve clinical outcomes (3). Molecular imaging of increased metabolic activity in the granulomas using ¹⁸F-fluorodeoxyglucose (FDG) positron emission tomography (PET) provides the advantages of whole heart evaluation and the ability to identify granulomas with active inflammation. Cardiovascular magnetic resonance (CMR) on the other hand is highly sensitive to detect fibrosis. The Japanese Ministry of Health, Labour and Welfare (JMHW) criteria have been widely used for the diagnosis of cardiac sarcoidosis. But, they do not include FDG PET or CMR. (4) The Heart Rhythm Society (HRS) consensus document has included FDG PET and CMR in the diagnostic criteria for cardiac sarcoidosis (5). However, procedural details of imaging are not covered in that document. This summary of the recent joint pro-

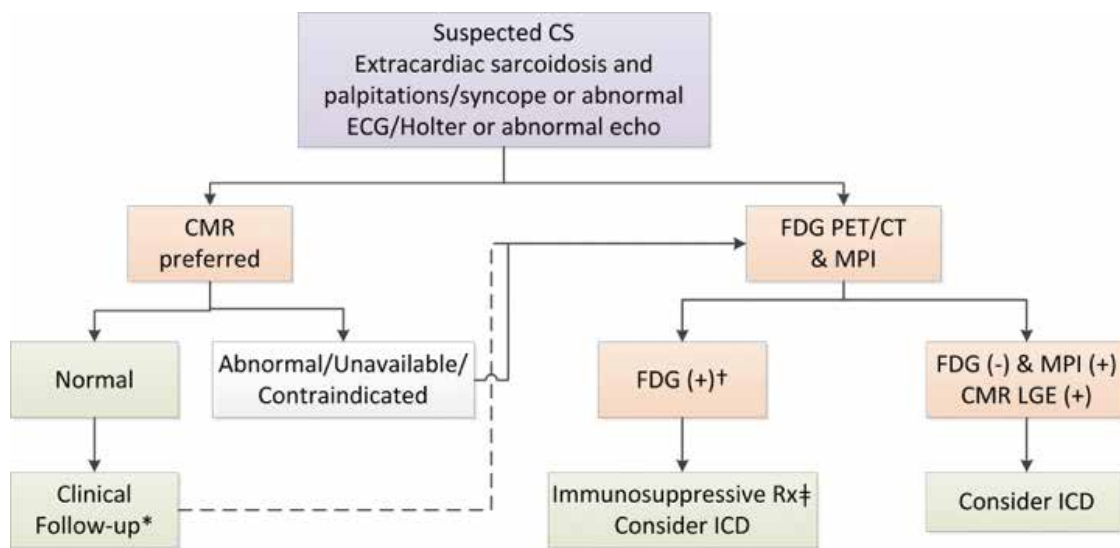
cedural position paper is to describe the work-up in patients suspected of CS with the correct use of the different imaging techniques including radionuclide imaging (FDG PET, radionuclide myocardial perfusion imaging, MPI), CMR, and echocardiography for the management of patients with known or suspected cardiac sarcoidosis.

¹⁸F-fluorodeoxyglucose positron emission tomography

In summary, FDG PET is the best clinically available tool for imaging myocardial inflammation. Careful preparation to suppress physiological myocardial glucose utilization is essential for FDG PET imaging of cardiac sarcoidosis. Combined assessment of perfusion and inflammation is necessary to provide optimal information for the diagnosis, risk assessment, and management of cardiac sarcoidosis (figure 1).

Cardiovascular magnetic resonance

In summary, CMR is a multi-parametric imaging modality that can accurately delineate cardiac morphology and function and interrogate tissue characteristics. CMR is a valuable tool for the diagnosis and risk assessment of cardiac sarcoidosis (figure 1). Whether CMR can be used to assess response to therapy is unclear, as CMR findings are limited by a relatively low specificity to distinguish scar from ac-



Abbreviations: CS = cardiac sarcoidosis; CMR = cardiovascular magnetic resonance imaging; ECG = electrocardiogram; echo = echocardiogram; FDG = ¹⁸F-fluorodeoxyglucose; ICD = implantable cardioverter defibrillator; LGE = late gadolinium enhancement; MPI = myocardial perfusion imaging; Rx=therapy † to identify coexistent inflammation; FDG PET/CT may be preferred first test in individuals with known systemic sarcoidosis where systemic sarcoidosis activity needs to be assessed. * If clinical suspicion is high or symptoms persist, FDG PET/CT and MPI may be considered in patients with normal CMR. ‡Immunosuppressive Rx may be considered taking into account the amount of inflammation. Patients with ICD are excluded for CMR.

Figure 1. Non-invasive imaging approach to initial evaluation of patients with suspected cardiac sarcoidosis.

tive inflammation. However, the relatively high sensitivity of the technique contributes to the exclusion of cardiac sarcoidosis.

Imaging to guide biopsy

In summary, abnormal cardiac findings on CMR and/or FDG PET are frequent and suggest localized areas of myocardial damage and/or inflammation in patients with cardiac sarcoidosis. In a clinical setting suggestive of cardiac sarcoidosis, 'hot' mediastinal or cervical lymph nodes on FDG PET provide a biopsy target that may improve the success rate of identifying sarcoid histopathology. The potential role of image-guided endomyocardial biopsy to improve the yield for histopathological diagnosis of cardiac sarcoidosis requires further evaluation.

Imaging to initiate and monitor therapy

In summary, in the absence of specific guidelines, in asymptomatic patients with cardiac sarcoidosis, echocardi-

graphy is useful to follow-up left ventricle ejection fraction and to evaluate for new wall motion abnormalities, wall thinning. A quantitative FDG PET with MPI may be useful to monitor progression of scar and inflammation and assess response to active immunosuppressive therapies (figure 2). Prospective randomized clinical trials of imaging guided management of immunosuppressive therapy are warranted.

Prognosis assessment in cardiac sarcoidosis

In summary, while there is a paucity of data in this regard, it seems plausible that the findings provided by echocardiography (providing an estimate of myocardial remodelling and function), CMR (providing an estimate of the extent of scar), PET imaging with FDG (providing an estimate of the overall magnitude and extent of myocardial inflammation), and MPI (providing an estimate of microvascular dysfunction and/or scar) may be complementary, both for diagnosing and treating di-

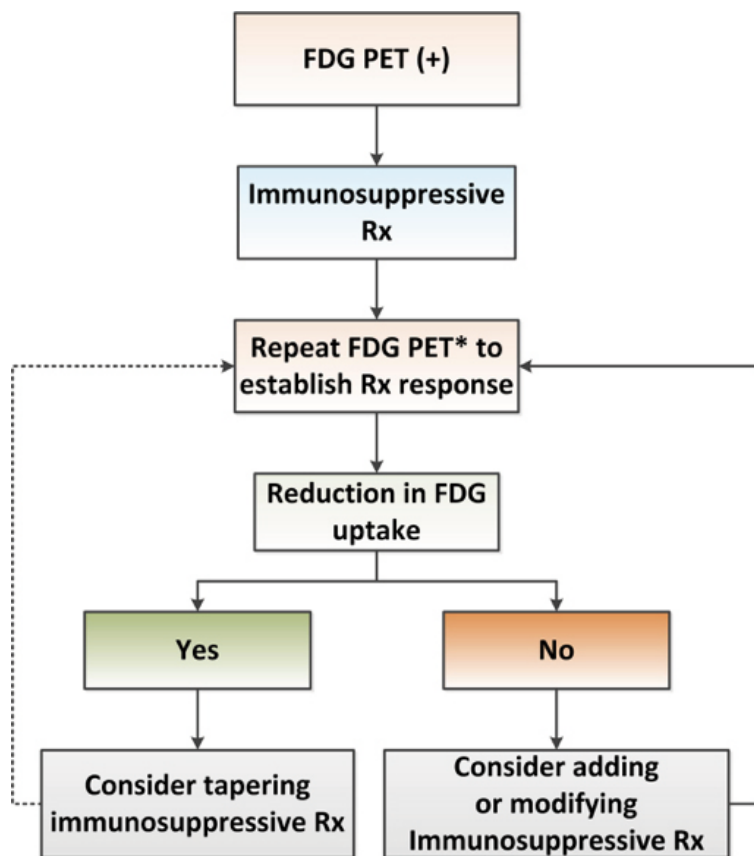
sease, as well as an estimation of the risk of future adverse events.

Conclusions

Sarcoidosis is a complex systemic disease that often requires multidisciplinary expertise and approach for diagnosis and management. Detection of cardiac sarcoidosis is important to prevent life-threatening arrhythmias and to preserve left ventricle function in affected individuals. A multi-imaging approach that can identify disease activity, prognosis and response to therapy is needed to improve further the management of patients with cardiac sarcoidosis. Optimal imaging based on standardized procedural guidelines for acquisition, interpretation, and quantification is paramount.

r.h.a.slart@umcg.nl ♦

Figure 2. Use of FDG PET imaging to guide immunosuppressive therapy in cardiac sarcoidosis. In cardiac sarcoidosis patients with positive FDG PET imaging, repeat FDG PET imaging can be repeated to judge treatment response, however whether the result of FDG PET can be used to taper immunosuppressive therapy is currently unclear and evidence is lacking to adjust treatment based on imaging. *The optimal timing of repeat FDG PET imaging is not well established, but approximately 4-6 months following treatment initiation is commonly employed, or when significant changes in therapy are being considered.



FDG = ¹⁸F-fluorodeoxyglucose; Rx=therapy.

References

1. Silverman KJ, Hutchins GM, Bulkley BH. Cardiac sarcoid: a clinicopathologic study of 84 unselected patients with systemic sarcoidosis. Circulation 1978;58(6):1204-11
2. Kim JS, Judson MA, Donnino R, et al. Cardiac sarcoidosis. Am Heart J 2009;157(1):9-21
3. Yazaki Y, Isobe M, Hiroe M, et al. Prognostic determinants of long-term survival in Japanese patients with cardiac sarcoidosis treated with prednisone. Am J Cardiol 2001;88(9):1006-10
4. Jpn Ministry Health Welfare. Diagnostic standard and guidelines for sarcoidosis. Jpn J Sarcoidosis and Granulomatous Disorders (Japanese) 2007;27:89-102
5. Birnie DH, Sauer WH, Bogun F, et al. HRS expert consensus statement on the diagnosis and management of arrhythmias associated with cardiac sarcoidosis. Heart Rhythm 2014;11(7):1305-23

¹⁸F-FDG PET/CT with clinical impact in infective endocarditis

A. Gomes, MD¹; S. van Assen, MD, PhD²; P.P. van Geel, MD, PhD³; Prof. B. Sinha, MD, PhD¹; Prof. R.H.J.A. Slart, MD, PhD^{4,5}; A.W.J.M. Glaudemans, MD, PhD⁵

Department of Medical Microbiology¹, Department of Cardiology³, Medical Imaging Center, Department of Nuclear Medicine and Molecular Imaging⁵, University of Groningen, University Medical Center Groningen, Groningen, the Netherlands; Department of Internal Medicine (Infectious Diseases)², Treant Zorggroep, Hoogeveen, the Netherlands; Department of Biomedical Photonic Imaging⁴, University of Twente, Enschede, the Netherlands.

Summary

Imaging modalities are of invaluable importance for the diagnosis of infective endocarditis. Historically, evidence for infective endocarditis by visualisation of structural intracardiac damage has been provided by echocardiography. Nowadays, technological advances enable visualisation of active infection with ¹⁸F-FDG PET/CT, even before ensuing structural damage. This imaging modality is increasingly validated for infective endocarditis. To illustrate this, we propose a change in paradigm by presenting an instructive case report. We suggest that physicians include this functional visualisation of intracardiac infection by ¹⁸F-FDG PET/CT complementary to the anatomical visualisation by echocardiography in the clinical reasoning process. Even with a lack of structural damage there can be a clear need to undergo cardiac surgery to prevent further deterioration, as effective treatment with antimicrobial treatment alone can be unsuccessful. A multidisciplinary endocarditis team should be implemented in every large hospital, as recommended by the European Society of Cardiology 2015 guideline. The nuclear medicine physician and radiologist should be part of this team, presenting the scan results in weekly team meetings, and informing the clinicians about the appropriate indication and interpretation of their imaging modalities.

Introduction

As the evidence for the added value on clinical impact of fluorine-18 fluorodeoxyglucose (¹⁸F-FDG) positron emission tomography with computed tomography (PET/CT) scanning in patients with suspicion of infective endocarditis is increasing (1), we promote a shift in paradigm for the management of these patients. In our opinion, the role of ¹⁸F-FDG PET/CT in infective endocarditis is clear and it should therefore be implemented in the diagnostic workup of every patient suspected of infective endocarditis, combined with a diagnostic cardiac CT angiography if indicated (1). We support the recommendation of ¹⁸F-FDG PET/CT in infective endocarditis by an illustrative case report.

Imaging in infective endocarditis

For the diagnosis of infective endocarditis, imaging has always played an important role. As definite diagnosis is difficult – both concerning sensitivity and specificity – there has always been much uncertainty, discussion, and falsely diagnosed patients with consequently suboptimal therapy and possible development of (fatal) complications. In order to structure and improve the diagnostic workup of patients suspected of endocarditis, the modified Duke criteria were introduced in 2000 (2). The two most important pillars of this scoring system are: 1) identification of the causative pathogen by microbiological methods, and 2) evidence of endocardi-

al involvement as site of destructive infection. Evidence for endocardial infection by visualisation of structural intracardiac damage has been provided thus far by both transthoracic (TTE) and transoesophageal (TEE) echocardiography. Nowadays, technological advances enable visualisation of active endocardial infection in the inflammatory phase with ¹⁸F-FDG PET/CT enabling early diagnosis. Thus also enabling earlier start of adequate therapy and prevention of on-going structural damage. Though the use of ¹⁸F-FDG PET/CT has already been validated for infective endocarditis (1), we experience various degrees of uncertainty and ambiguity about the implementation of this imaging modality and the use of its results in clinical practice. This is regrettable, as we believe that ¹⁸F-FDG PET/CT is clinically important and complementary to echocardiography, depending on the specific clinical situation of the individual patient. ¹⁸F-FDG PET/CT should therefore be strongly positioned in the diagnostic workup of patients with (suspected) infective endocarditis.

Echocardiography

Echocardiography is able to visualise anatomical changes of the heart with resulting changes in motility and flow, which develop after the initial inflammatory phase, in a later course of disease. Since echocardiography visualises and quantifies changes in blood flow dynamics, it is able to identify a valve aneurysm, fistula,

perforation, valve prolapse, and valve dehiscence by using colour Doppler. In addition, it informs about the size and mobility of vegetation and thereby embolism risk, and in the same investigation provides information about cardiac chamber function (3). Overall, TEE is superior to TTE in the visualisation of infective endocarditis, especially concerning perivalvular complications such as mycotic aneurysms and abscesses and in prosthetic valve endocarditis. TEE also has a major role in surgery: to determine the location and extent of infection, to guide surgery, to assess the result, and for early postoperative follow-up (4). However, superiority of either one of these modalities also depends on the location of the infection. TTE generally allows a better view of the right heart (excluding infection at the pulmonary valve and unusual locations such as the Eustachian tube or Chiari network), and of small anterior abscesses of the aortic valve (3,4). Unfortunately, echocardiography fails to detect infectious complications in 30% of patients, especially in those with intracardiac prosthetic material *in situ* as these patients present with perivalvular complications at a particularly high rate (1). Therefore, alternative imaging modalities, providing complementary information are needed.¹⁸F-FDG PET/CT may play a pivotal role here for optimal detection of cardiac infection complications in patients with intracardiac prosthetic material as well as extracardiac foci in all patients with infective endocarditis. Echocardiography will continue to be the first line imaging tool, and seems to be especially meaningful in the intracardiac diagnosis of native valve endocarditis, as well as for the visualisation of (especially smaller size) vegetation (1).

¹⁸F-FDG PET/CT

¹⁸F-FDG PET/CT provides functional data on the intracardiac extent of

infection before structural damage takes place, as well as extracardiac information about metastatic and embolic sites of infection, including the port of entry of the inflicting microorganism.

The added diagnostic value of ¹⁸F-FDG PET/CT has been demonstrated for intracardiac infections in patients with intracardiac prosthetic material after an appropriate post-surgical interval of 1-3 months (1,4). Important for optimal diagnostic accuracy is to prepare the patient adequately before the acquisition of the scan by fasting for at least 6 hours and a low carbohydrate, fat-allowed diet for at least 24 hours. It is important to identify intracardiac sites of infection early as it might enable treatment of the infection in the inflammatory phase before development of structural damage and further related complications. Perivalvular complications and valve dehiscence require urgent cardiac surgery and therefore prevention of this sudden occurrence is of invaluable importance. Important anatomical information can be provided in this regard by ECG-triggered diagnostic cardiac CT angiography, especially concerning perivalvular extension of infection (abscesses, pseudo-aneurysms, fistulas, and valve dehiscence with paravalvular leakage). If correctly indicated, the additional use of this diagnostic cardiac CT can further increase the impact of the ¹⁸F-FDG PET/CT on the therapeutic regimen.

The added diagnostic value of ¹⁸F-FDG PET/CT for extracardiac infection concerns all patients with a proven intracardiac infection (both native and prosthesis-related) (1). Extracardiac sites of infection are important to identify as they may require separate active treatment and follow-up to eliminate them as potential persistent sources of pathogen seeding (with possible reinfection of newly implanted prosthetic material).

A drawback of imaging with ¹⁸F-FDG PET/CT is the limited specificity for infection, as it is positive for all tissues with avid glucose uptake, such as malignant tumors and inflammation by other causes. Consequently, in order to limit the rate of false-positive results it is important to interpret a scan with sufficient information about the clinical situation of a patient. Scanning with ¹⁸F-FDG PET/CT may produce unwanted knowledge about metabolically active sites in the body that need additional follow-up to assort their nature and might require therapy.

The interpretation of a ¹⁸F-FDG PET/CT scan as either negative or positive for infective endocarditis is based on the intensity, distribution and pattern of ¹⁸F-FDG uptake as diagnostic criteria. To improve the reliability of clinical applicability and interpretation of ¹⁸F-FDG PET/CT, criteria need to be developed that become incorporated into guidelines.

Furthermore, the extent to which this scan has immediate therapeutic consequences depends on the specific clinical situation of the individual patient. Visualisation of infectious complications providing an indication for cardiac surgery are historically critically important in all patients with infective endocarditis: abscess, false aneurysm, fistula, and a large/growing vegetation (4). However, in patients with intracardiac prosthetic material *in situ*, evidence of an infected prosthesis can nowadays be sufficient to trigger surgical intervention, even without the visualisation of further structural damage. Prosthetic valve endocarditis can be adequately treated with antimicrobial therapy alone under specific conditions (5-8). However, presence of infection of implanted prosthetic material is generally an indication for removal of this material, as it is considered a source of ongoing infection that often cannot be controlled with antimicrobial therapy alone (4,5,9). Visualisation of

intracardiac structural damage was historically required for the decision to operate, but nowadays visualisation of infected prosthetic material prior to structural damage should be taken into consideration as an indication for early surgical intervention. ¹⁸F-FDG PET/CT should become an important additional tool in the multidisciplinary decision making process on the optimal therapy for an individual patient, taking comorbidity and risks of surgical consequences into account.

Paradigms

It involves a change in paradigm to start including the functional visualisation of intracardiac infection by ¹⁸F-FDG PET/CT as complement to the structural visualisation by echocardiography in the therapeutic decision making process. This change in paradigm has been put forward most clearly in the guideline of the European Society of Cardiology (4), and is also mentioned in that of the American Heart Association (9).

We experience that this change in paradigm represents a revolution in daily clinical practice for clinicians taking care of patients with infective endocarditis. Furthermore, we experience uncertainty and ambiguity about the reliability of image interpretation, especially a lack of confidence in the (positive) predictive value. Cardiothoracic surgeons might perceive it as bold to proceed to surgery without visual proof of mechanical reasons to correct cardiac anatomy in the course of this disease. A further, potentially complicating, matter is the perceived threshold by cardiothoracic surgeons in the use of mortality rate of their elective procedures as an indication for their quality. Unfortunately, this obstructs good clinical care if the patients' individual context and stratification is not taken into consideration. Therefore, in our view, the inclusion of the functional information provided by ¹⁸F-FDG PET/CT in the therapeutic decision making process can be justi-

fied in several cases since delayed intervention may often increase severe morbidity and mortality.

We are convinced that the additional use of ¹⁸F-FDG PET/CT for the diagnosis of infective endocarditis is supported by the following arguments: 1) visualisation of structural damage usually occurs late in the disease process; 2) false negative results with echocardiography alone occur in an important percentage of patients; and 3) in the decision to proceed to cardiac surgery or not, the decision is not only about current haemodynamic cardiac function, but also about future opportunities for the patient to undergo surgery. Delay of surgery may decrease the prognosis of the patient or result in the development of physical conditions in which the patient is no longer eligible for cardiac surgery - these may be e.g. cardiac, pulmonary, cerebral, or renal. Furthermore, the development of extracardiac infectious foci may jeopardise the prognosis due to their ability to re-infect the freshly implanted prosthetic material without adequate antimicrobial therapy. Of course, the lack of specificity of the ¹⁸F-FDG PET/CT should also be taken into account in the clinical decision making process, as unnecessary surgery is a burden to the patient and healthcare system.

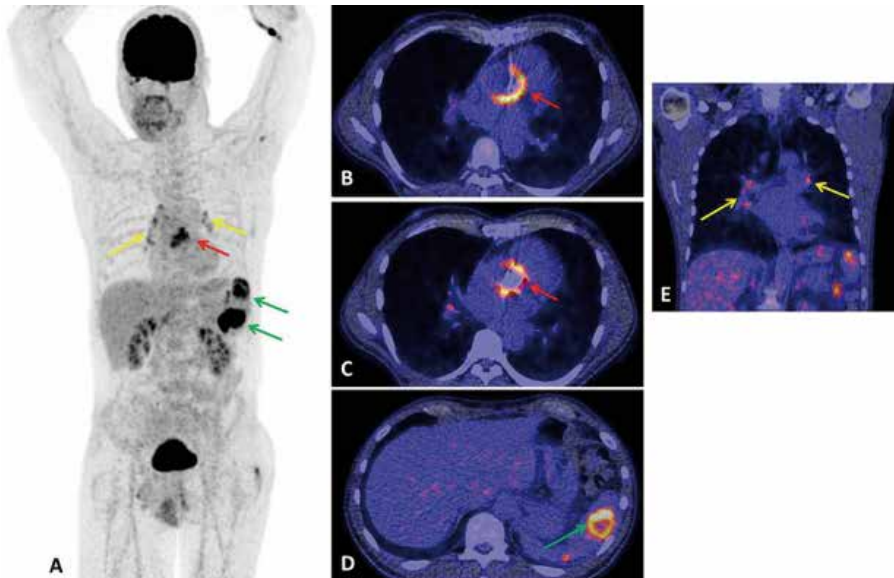
Multidisciplinary workup

Ultimately, the optimal therapeutic regimen should be determined by a multidisciplinary team carefully considering the information provided by the modified Duke criteria and new diagnostic modalities on the one hand and their potential pitfalls on the other hand, always in light of the specific clinical situation for the individual patient. Therefore, starting the formalisation of a multidisciplinary endocarditis meeting and team to discuss the optimal diagnostic workup and therapeutic regimen of individual patients is important, as

well as the inclusion of experienced nuclear medicine physicians and radiologists (imagers). The knowledge about false positive and false negative ¹⁸F-FDG PET/CT scans is currently incomplete, but this modality gives us the opportunity for more focused treatment, earlier in the course of disease and for possible prevention of new complications. Nevertheless, we need to increase our knowledge about sources of false results with the use of this imaging modality in clinical practice and future scientific studies need to clarify this topic.

Case report

In this illustrative case report, ¹⁸F-FDG PET/CTA was performed in a 57 year old male patient with non-specific symptoms of stiff joints (with previous Reiter's syndrome), possible Raynaud's disease and unexplained high inflammatory parameters. His clinical history mentioned a Bentall procedure in two stages. First, his aortic valve was replaced by a mechanical prosthetic valve 7 years ago, because of significant stenosis. Second, replacement of his aortic root and ascending aorta with re-implantation of the coronary arteries was performed 2 years ago, because of an ascending aorta aneurysm. His clinical history also included a transient ischaemic attack 6 months ago. ¹⁸F-FDG PET/CTA with appropriate dietary preparation showed paravalvular uptake of FDG on the left side of the aortic prosthetic valve with a large contrast filled cavity, indicating active infective endocarditis with a paravalvular abscess and some pannus on the left side (see figure). Additionally, increased FDG uptake was shown in enlarged mediastinal lymph nodes and in multiple spleen abscesses. A following TTE did not reveal any vegetation, nor did TEE. However, at the same time-point, TEE did show a paravalvular cavity around the aortic valve communicating with the left ventricular outflow tract, and a mild aortic valve insufficiency. After taking blood



[A] Coronary MIP FDG-PET image showing increased FDG uptake at the site of the prosthetic valve (red arrows), at multiple mediastinal and hilar lymph nodes (yellow arrows) and in the spleen (green arrows), suggestive of multiple spleen abscesses. [B-C] fused transaxial FDG-PET/CT slices showing the increased uptake at the site of the prosthetic valve. [D] fused transaxial FDG-PET/CT slice showing one of the spleen abscesses. [E] fused coronal FDG-PET/CT slice showing increased uptake at mediastinal and hilar lymph nodes.

cultures, intravenous vancomycin (1500 mg loading dose, and thereafter 2500 mg/24 hours continuously) and gentamicin (250 mg once daily) were simultaneously started as empirical therapy for prosthetic valve infective endocarditis. Blood cultures remained negative. The patient was deemed eligible for surgery, but only after eradication of his spleen abscesses. Therefore, the patient first underwent splenectomy. Microscopy of pus from the splenic abscesses showed Gram-positive rods, after which gentamicin was replaced by intravenous ceftriaxone (2000 mg once daily). Finally, the patient underwent another Bentall procedure 1 month after the initial visualisation of the aortic prosthetic valve infective endocarditis on ¹⁸F-FDG PET/CTA. As molecular testing on the explanted material during cardiac surgery showed *Propionibacterium acnes* as pathogen, the patient was treated with ceftriaxone for another 6 weeks after his surgery. At follow-up 3 months after surgery, and 6 weeks after stopping his antibiotic treatment, this patient showed good clinical recovery from his aggressively treated infective endocarditis, which was initially diagnosed on ¹⁸F-FDG PET/CTA.

This successful case illustrates the importance of both the ¹⁸F-FDG PET and CTA scan in the diagnostic workup and therapeutic decision-making process for patients suspected of infective endocarditis. This case also emphasises the importance of ¹⁸F-FDG PET/CT in the identification of extracardiac infectious foci which may complicate a case of infective endocarditis.

Our recommendation

To further stimulate the described change in paradigm and include molecular imaging results in the multidisciplinary decision making process for endocarditis patients, we would like to make some suggestions. First, we must start to rely on molecular imaging tools and interpretation concerning the diagnosis of endocarditis, considering the increased sensitivity for early stages of infective endocarditis on the one hand and the limited specificity for infection on the other hand. There is sufficient evidence for this concept. If an experienced nuclear medicine physician concludes that a PET scan is positive for infective endocarditis based on intensity, distribution and pattern of ¹⁸F-FDG uptake as

diagnostic criteria for infection, we should include this result in the multidisciplinary decision making process for the optimisation of the individual therapeutic regimen. This is supported by the ESC 2015 modified criteria for the diagnosis of infective endocarditis (4): *major* criteria include 1) abnormal activity around the site of prosthetic valve implantation detected by ¹⁸F-FDG PET/CT (if implanted more than 3 months previously) and 2) definite paravalvular lesions by cardiac CT; *minor* criteria include vascular phenomena that are not detected by clinical examination but are detected by imaging only. Second, we need to start translating imaging with ¹⁸F-FDG PET/CT into a change in the therapeutic regimen if infective endocarditis is suspected. The antimicrobial regimen should be adapted to treat intravascular infection with biofilm formation, which is formed in the infection process of prosthetic material as well as in native valve endocarditis (10). Biofilm demands special antimicrobial agents as they contain bacteria with an altered phenotype in comparison to their free-floating planktonic form, causing them to be challenging to culture and

eradicate (10). A surgical plan needs to be discussed in an early phase of disease with the cardiothoracic surgeon as core member of the multidisciplinary endocarditis team. In this meeting, the consequences of a positive ¹⁸F-FDG PET/CT should be (or become) clear to all team members, as well as the chances of successful treatment with antimicrobial therapy alone.

Conclusion

Infective endocarditis remains a complex disease, though there is no magic bullet, we see room for improving diagnosis. We should make more use of ¹⁸F-FDG PET/CT(A) and integrate positive results in the diagnosis of infective endocarditis, based on the currently available evidence and the growing experience of imaging specialists in clinical practice. Even without visualisation of anatomical damage, the need to undergo (early) cardiac surgery should be considered as effective treatment to prevent further deterioration, as opposed to antimicrobial treatment alone. Current challenges with the use of ¹⁸F-FDG PET/CT(A) that remain to be resolved include the lack of standardised criteria for interpretation, sources of false positive and negative results, and discussions about the post-surgical interval in which imaging can be reliably performed. Imaging specialists should promote the value of ¹⁸FDG PET/CT for the visualisation of infective endocarditis and provide clear criteria for scan interpretation with a translation in clear results. This will help to convince clinicians that ¹⁸F-FDG PET/CT deserves a prominent position in the workup of suspected endocarditis to prevent serious complications.

a.gomes@umcg.nl ♦

Financial support

INTERREG project EurHealth-1Health, project number 202085; <http://www.eurhealth-1health.eu/nl/nieuws/>

References

1. Gomes A, Glaudemans AW, Touw DJ, et al. Diagnostic value of imaging in infective endocarditis: a systematic review. *Lancet Infect Dis* 2017;17(1):e1-e14.
2. Li JS, Sexton DJ, Mick N, et al. Proposed modifications to the Duke criteria for the diagnosis of infective endocarditis. *Clin Infect Dis* 2000;30(4):633-638.
3. Habib G, Badano L, Tribouilloy C, et al. Recommendations for the practice of echocardiography in infective endocarditis. *Eur J Echocardiogr* 2010;11(2):202-219.
4. Habib G, Lancellotti P, Antunes MJ, et al. 2015 ESC Guidelines for the management of infective endocarditis: The Task Force for the Management of Infective Endocarditis of the European Society of Cardiology (ESC) Endorsed by: European Association for Cardio-Thoracic Surgery (EACTS), the European Association of Nuclear Medicine (EANM). *Eur Heart J* 2015;36(44):3075-3128.
5. Utili R, Durante-Mangoni E, Tripodi MF. Infection of intravascular prostheses: how to treat other than surgery. *Int J Antimicrob Agents* 2007 Nov;30 Suppl 1:S42-50.
6. Hill EE, Herregods MC, Vanderschueren S, et al. Management of prosthetic valve infective endocarditis. *Am J Cardiol* 2008;101(8):1174-1178.
7. Attaran S, Chukwuemeka A, Punjabi PP, Anderson J. Do all patients with prosthetic valve endocarditis need surgery? *Interact Cardiovasc Thorac Surg* 2012;15(6):1057-1061.
8. Bonow RO, Carabello BA, Chatterjee K, et al. 2008 focused update incorporated into the ACC/AHA 2006 guidelines for the management of patients with valvular heart disease: a report of the American College of Cardiology/American Heart Association Task Force on Practice Guidelines (Writing Committee to revise the 1998 guidelines for the management of patients with valvular heart disease). Endorsed by the Society of Cardiovascular Anesthesiologists, Society for Cardiovascular Angiography and Interventions, and Society of Thoracic Surgeons. *J Am Coll Cardiol* 2008 Sep 23;52(13):e1-142.
9. Baddour LM, Wilson WR, Bayer AS, et al. Infective Endocarditis in Adults: Diagnosis, Antimicrobial Therapy, and Management of Complications: A Scientific Statement for Healthcare Professionals From the American Heart Association. *Circulation* 2015 Oct 13;132(15):1435-1486.
10. Donlan RM. Biofilm formation: a clinically relevant microbiological process. *Clin Infect Dis* 2001;33(8):1387-1392.

Diagnostic workup of giant cell arteritis; role of imaging

E. Brouwer, MD, PhD^{1,2}; K.S.M. van der Geest, MD, PhD^{1,2}; Prof. R.H.J.A. Slart, MD, PhD^{1,3,4}; A.W.J.M. Glaudemans, MD, PhD^{1,3}; D.J. Mulder, MD, PhD^{1,5}; A. Rutgers, MD, PhD; M. Sandovici, MD, PhD^{1,2}

Vasculitis Expertise Center Groningen¹, Department of Rheumatology and Clinical Immunology², Department of Nuclear Medicine and Molecular Imaging³, Department of Biomedical Photonic Imaging, University of Twente, Enschede, the Netherlands⁴, Department of Internal Medicine⁵ University Medical Center Groningen, Groningen, the Netherlands

Abstract

Giant cell arteritis (GCA) and polymyalgia rheumatica (PMR) belong to a disease spectrum.

In order to diagnose GCA and PMR classification criteria are used. These include age, clinical signs and symptoms, an elevated ESR and in GCA, a biopsy of the temporal artery (TAB). Unfortunately, using these classification criteria the diagnosis GCA can be missed. For this reason new classification criteria that combine a clinical dataset consisting of cranial GCA, systemic GCA and PMR symptoms with laboratory testing (ESR and/or CRP), a temporal artery biopsy and/or imaging were developed. Ultrasound (US), [¹⁸F]-fluorodeoxyglucose (FDG) positron emission tomography (PET)/CT and MRI play an emerging role in visualizing arterial wall inflammation in GCA.

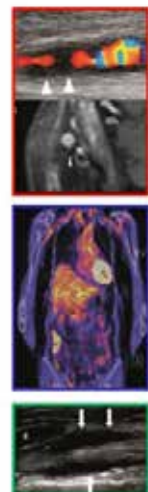
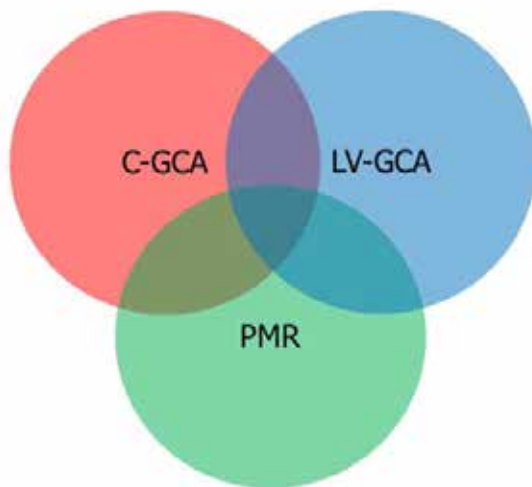


Figure 1. Disease spectrum and imaging modalities in Giant Cell Arteritis (GCA): Cranial (C)-GCA (ultrasound top picture and MRI bottom picture in the red box; white arrows indicate wall oedema/'halo' sign), Large Vessel (LV)-GCA (PET/CT picture in the blue box) and PMR (PET/CT, uptake surrounding shoulders in the blue box and ultrasound in the green box; arrows indicate biceps tenosynovitis, the asterix depicts subdeltoid bursitis) adapted from Dejaco et al (2).

Introduction

Giant cell arteritis (GCA) is an immune mediated vasculitis characterized by inflammation of the large and medium sized arteries (1). GCA is closely linked to polymyalgia rheumatica (PMR) and both diseases occur only in persons older than 50 (2). The diagnostic work up and treatment of both GCA and PMR is rapidly changing. The present paper highlights the role of imaging in the current diagnostic work up of GCA and PMR. Furthermore, it discusses the

emerging imaging modalities, their diagnostic potential and their possible pitfalls in GCA and PMR.

Clinical spectrum and pathogenesis of GCA and PMR

GCA and PMR can present separately but can also co-occur. PMR is observed in 50% of GCA patients and 30% of PMR patients have underlying vessel inflammation. Fifteen per cent of patients with PMR may develop GCA (3,4). GCA is a granulomatous vasculitis

that mainly affects the vascular wall of medium and large arteries. GCA is not solely a "headache disease" (cranial GCA (C-GCA)) but can also present itself as systemic vessel inflammation (large vessel GCA (LV-GCA)) or PMR (2) (figure 1). Symptoms such as jaw claudication (facial artery), diplopia (vaso nervorum; cranial nerves III (oculomotorius), IV (trochlearis) or VI (abducens)), sight loss (ophthalmic, retinal and posterior ciliary arteries) and headache (temporal artery), are caused

Table 1. Giant cell arteritis (GCA) 1990 classification criteria and symptoms (30).

ACR GCA 1990 criteria (3 of 5 required)
age at onset ≥ 50 years
ESR ≥ 50 mm (by Westergren method)
new or new type headache
temporal artery abnormalities (tenderness, decreased pulsation, unrelated to arteriosclerosis of cervical arteries)
abnormal artery biopsy (vasculitis characterized by a predominance of mononuclear cell infiltration or granulomatous inflammation, usually with multinucleated giant cells)

cranial symptoms
new or different headache
scalp tenderness
temporal artery tenderness and/or swelling
loss of pulse of the temporal artery
ischaemia-related sight loss/diplopia
jaw claudication/ tongue pain
TIA/CVA
systemic symptoms
fever
weight loss
malaise
night sweats
loss of pulse / bruits
arm claudication
leg claudication
PMR clinic

Table 2. Combined cranial and systemic signs and symptoms of GCA.

by involvement of the supplying cranial arteries and are seen in patients with C-GCA. Persistent inflammation of the cranial arteries can lead to occlusion of the vascular lumen and/or chronic damage. Involvement of systemic vessels (thoracic and abdominal aorta and its branches) may lead to loss of pulse with limb claudication and aortic aneurysms (5). The clinical hallmark of PMR is pain and stiffness of both shoulders and hips which quickly resolves on treatment in most patients. The immune pathogenesis of both GCA and PMR is complex and not yet well understood. There is consensus, however, that GCA pathology is initiated by local dendritic cell activation followed by infiltration of the vessel wall by CD4+ T-cells and monocytes/macrophages via the vaso vasorum (6). PMR pathology is characterized by inflammation of bursae, synovium and tendons. Although the target organs are different in GCA and PMR (i.e. arteries

versus bursal/joint synovium, tendons), at the systemic level both GCA and PMR patients show raised pro-inflammatory markers such as interleukin-6, CRP and ESR. General symptoms such as weight loss, malaise, night sweats and low grade fever reflect the systemic inflammatory burden.

Treatment of GCA

Treatment with glucocorticoids is currently the first choice for the clinical management of GCA and PMR. However, long-term glucocorticoid treatment is associated with severe side effects. Good alternatives are therefore highly needed (7). There is some evidence for a glucocorticoid-sparing effect of methotrexate (RCT's) (8), leflunomide (case series) (9) and abatacept (10) in GCA and PMR. The major breakthrough in the treatment of GCA came with the recent open label study with tocilizumab, which is an interleukin-6 receptor blocker, followed by the double blind four

arm RCT with tocilizumab in GCA, the GiACTA study (11,12).

Diagnostic Work up of GCA

The fact that GCA is perceived as a headache disease and also called temporal arteritis results from the 1990 ACR classification criteria which solely focus on cranial signs and symptoms and the temporal artery biopsy (TAB) as diagnostic tool (table 1). According to the ACR 1990 criteria, a TAB is desirable in every case of suspected GCA and a positive TAB is diagnostic for GCA. There is no role for imaging in this set of criteria.

For GCA patients with involvement of the aorta and its branches (LV-GCA) and PMR patients with underlying LV-GCA (table 2 and 3) these criteria are clearly not sufficient.

New classification criteria covering the C-GCA, LV-GCA and PMR spectrum are currently used in international multicentre clinical trials. These criteria combine a clinical dataset consisting of

Chuang and Hunder criteria (all required)
age at onset 50 years
ESR 40 mm (by Westergren method)
bilateral pain or tenderness > 1 month, 2 girdles
exclusion of other diagnosis
EULAR/ACR 2012 criteria (without US: a score of 4 or more is categorised as PMR; with US: score of 5 or more is categorised as PMR)*
age at onset 50 years (required)
bilateral shoulder aching (required)
abnormal CRP or BSE (required)
morning stiffness > 45 min (2 points)
hip pain/limited range of motion (1 point)
absence of RF or ACPA (2 points)
absence of other joint involvement (1 point)
US: at least one shoulder with subdeltoid bursitis and/or biceps tenosynovitis and/or glenohumeral synovitis (either posterior or axillary) and at least one hip with synovitis and/or trochanteric bursitis (1 point)
US: both shoulders with subdeltoid bursitis, biceps tenosynovitis or glenohumeral synovitis (1 point)

Table 3. Chuang Hunder and EULAR/ACR 2012 Provisional Classification Criteria for PMR.

*RF, rheumatoid factor; ACPA, anticitrullinated protein antibody; ESR, erythrocyte sedimentation rate; CRP, C-reactive protein; PMR, polymyalgia rheumatica; US, ultrasound.

both cranial, systemic symptoms and PMR symptoms of GCA (table 1, 2 and 3) with laboratory testing (not only ESR but also the more widely used CRP), a TAB and/or imaging as diagnostic tools (12). A drawback is that these new criteria are not yet validated.

Imaging in GCA

Imaging plays a central role in the new classification criteria for GCA used in international multicentre clinical trials and it is increasingly used in daily clinical practice when GCA is suspected. Several studies have demonstrated the limited diagnostic value of TAB in LV-GCA patients presenting with systemic and PMR symptoms in the absence of cranial symptoms (13–16). For LV-GCA, the [¹⁸F]-Fluorodeoxyglucose (FDG) positron emission tomography (PET) combined with a low dose CT ([¹⁸F]-FDG PET/CT) is the diagnostic modality of choice. TAB may also be of limited diagnostic value in C-GCA patients with limited cranial involvement, who

present with sight loss or diplopia, without involvement of the temporal arteries. Ultrasound (US) and/or Magnetic Resonance Imaging (MRI) are the imaging modalities of choice in C-GCA. Of utmost importance is that imaging is performed before or, in case of immediate need of treatment to prevent sight loss, within 3 days of starting glucocorticoids (16,17) (table 4).

Ultrasound

Ultrasound (US) of the cranial and axillary arteries is an emerging diagnostic tool for GCA. Colour Doppler ultrasound can detect wall oedema, known as a 'halo' sign, throughout the length of the vessel. This is the most important finding suggesting GCA and it showed higher sensitivity compared to the TAB in the recent TABUL study (18). Specificity reaches 100% in case of bilateral 'halo' sign (19). Other vasculitis features, such as increased intima-media vessel wall thickness, are diagnosed

with greyscale ultrasound. A positive compression sign has been demonstrated to be a robust marker with excellent inter-observer agreement (20–22). The assessment of other large vessels, particularly the axillary arteries, is recognized to further increase the sensitivity for detection of GCA. Nevertheless, US use is still not widespread in daily clinical practice and requires up to date US machines and skilled sonographers (21).

[¹⁸F]-Fluorodeoxyglucose (FDG) positron emission tomography (PET)/CT

FDG-PET/CT is a functional imaging technique used for identifying the presence of large vessel involvement in patients with GCA (23). It can also detect inflammation of articular and extra-articular synovial structures in case of co-existing PMR (24). A recent paper demonstrated that one third of patients with PMR show LV uptake on FDG PET/CT (4). In addition, the PET/

Table 4. Overview of the imaging diagnostic modalities in addition to temporal artery biopsy (TAB) in Giant Cell Arteritis (GCA). Ideally, patients are evaluated in a fast track setting (31) with immediate access to state of the art ultrasound (US), ¹⁸F-FDG PET/CT and/or MRI imaging. Currently there is insufficient evidence to recommend a specific imaging test as primary assessment when suspecting GCA. The imaging modality used is very much dependent on the local availability and expertise besides the clinical signs and symptoms of the patient. In patients without visual symptoms, imaging should preferably be performed before start of glucocorticoids (GC). Patients with visual symptoms consistent with GCA should be evaluated by an ophthalmologist in the fast track setting and (i.v.) glucocorticoids should be started immediately to prevent sight loss.

	US	¹⁸ F-FDG PET/CT	MRI	TAB
timing	before or within 3 days after start of GC	before or within 3 days after start of GC	unknown	before or within 2 weeks after start of GC
vascular bed	temporal, facial, carotid, subclavian and axillary artery	aorta and its branches, including the carotid arteries	branches of the internal and external carotid artery	temporal artery

CT may also reveal alternative diagnoses such as rheumatoid arthritis, spondyloarthritis, malignancy or infection. A limitation of FDG PET/CT is the lack of an internationally accepted standard and definition of vascular inflammation (16).

MRI

MRI of the cranial and systemic large arteries is an excellent emerging diagnostic tool in patients with GCA. Stenosis, dilatation or vessel wall oedema can be observed. Preferably a 3, 5 or even 7 Tesla scanner is used for the optimal detection of vessel wall inflammation in GCA (25). The MRI is an excellent tool for visualizing the central retinal artery and the posterior ciliary artery, which cannot be visualized by US or PET/CT. Besides, MRI is superior to the CT (26,27) with regards to soft tissue contrast and exposure to radiation.

Combined fluorodeoxyglucose (FDG) positron emission tomography (PET)/MRI in GCA

PET/MRI not only offers a sensitive evaluation of the inflammatory processes in large vessels but also provides a detailed morphological analysis of both cranial and systemic large vessels in a

single examination. Moreover, the radiation dose may be reduced as compared to PET/CT by limiting the injected radiotracer activity while increasing PET acquisition duration (matching the longer time needed for MRI data acquisition) (28). A recent paper elegantly demonstrated the excellent possibilities of the combined use of PET and a 7-TESLA-MRI (29). Clear limitations are currently the availability and lack of standardization.

Key messages

- GCA and PMR belong to a disease spectrum.
- There is a huge unmet need for a fast diagnostic work up including state of the art imaging in GCA and PMR.
- Glucocorticoid treatment interferes with imaging but should be started as early as possible to prevent irrevocable damage, such as blindness, in GCA.

e.brouwer@umcg.nl ♦

References

1. Weyand CM, Goronzy JJ. Immune mechanisms in medium and large-vessel vasculitis. Nat Rev

Rheumatol [Internet]. Nature Publishing Group; 2013;9(12):731–40. Available from: <http://www.ncbi.nlm.nih.gov/pmc/articles/PMC4277683/>&tool=pmcentrez&rendertype=abstract

2. Dejaco C, Duftner C, Buttgereit F, Matteson EL, Dasgupta B. The Spectrum of Giant Cell Arteritis and Polymyalgia Rheumatica: Revisiting the Concept of the Disease. *Rheumatology (Oxford)*. 2016;(in revision).
3. Prieto-Gonzalez S, Arguis P, Garcia-Martinez, et al. Large vessel involvement in biopsy-proven giant cell arteritis: prospective study in 40 newly diagnosed patients using CT angiography. *Ann Rheum Dis* [Internet]. 2012;71(7):1170–6. Available from: <http://www.ncbi.nlm.nih.gov/pubmed/22267328>
4. Lavado-Pérez C, Martínez-Rodríguez I, Martínez-Amador N, et al. ¹⁸F-FDG PET/CT for the detection of large vessel vasculitis in patients with polymyalgia rheumatica. *Rev Esp Med Nucl Imagen Mol* [Internet]. 2015;34(5):275–81. Available from: <http://linkinghub.elsevier.com/retrieve/pii/>

- S2253654X15000694
5. Muratore F, Kermani TA, Crown CS, Green AB, Salvarani C, Matteson EL, et al. Large-vessel giant cell arteritis: a cohort study. *Rheumatology (Oxford)* [Internet]. 2015;54(3):463-70. Available from: <http://rheumatology.oxfordjournals.org/content/54/3/463>. long
 6. Weyand CM, Asia S, America IN. Medium- and Large-Vessel Vasculitis. 2003;(c):160-9.
 7. Buttgereit F, Dejaco C, Matteson EL, Dasgupta B. Polymyalgia Rheumatica and Giant Cell Arteritis. *Jama* [Internet]. 2016;315(22):2442. Available from: <http://www.ncbi.nlm.nih.gov/pubmed/27299619%0A>
 8. Mahr AD, Jover JA, Spiera RF, et al. Adjunctive methotrexate for treatment of giant cell arteritis: An individual patient data meta-analysis. *Arthritis Rheum*. 2007;56(8):2789-97.
 9. Adizie T, Christidis D, Dharmapaliyah C, Borg F, Dasgupta B. Efficacy and tolerability of leflunomide in difficult-to-treat polymyalgia rheumatica and giant cell arteritis: A case series. *Int J Clin Pract*. 2012;66(9):906-9.
 10. Langford CA, Monach PA, Specks U, Seo P, Cuthbertson D, Mclear CA, et al. An open-label trial of abatacept (CTLA4-IG) in non-severe relapsing granulomatosis with polyangiitis (Wegener's) for the Vasculitis Clinical Research Consortium. *Ann Rheum Dis*. 2014;73:1376-9.
 11. Villiger PM, Adler S, Kuchen S, et al. Tocilizumab for induction and maintenance of remission in giant cell arteritis: A phase 2, randomised, double-blind, placebo-controlled trial. *Lancet* [Internet]. Elsevier Ltd; 2016;387(10031):1921-7.
 12. J.H. Stone, K. Tuckwell, S. Dimonaco, et.al. Trial of Tocilizumab in Giant-Cell Arteritis. *N Engl J Med* [Internet]. 2017;3774377:317-28. Available from: <http://www.nejm.org/doi/pdf/10.1056/NEJMoa1613849>
 13. Blockmans D, Stroobants S, Maes A, Mortelmans L. Positron emission tomography in giant cell arteritis and polymyalgia rheumatica: evidence for inflammation of the aortic arch. *Am J Med*. 2000;108(3):246-9.
 14. Besson FL, Parienti J-J, Bienvenu B, et al. Diagnostic performance of (18)F-fluorodeoxyglucose positron emission tomography in giant cell arteritis: a systematic review and meta-analysis. *Eur J Nucl Med Mol Imaging*. 2011;38:1764-72.
 15. Lensen KDF, Comans EFI, Voskuyl AE, et al. Large-Vessel Vasculitis : Interobserver Agreement and Diagnostic Accuracy of 18 F-FDG-PET / CT. *Biomed Res Int*. Hindawi Publishing Corporation; 2015;2015(Lvv).
 16. Stellingwerff MD, Brouwer E, Lensen K-JDF, et al. Different Scoring Methods of FDG PET/ CT in Giant Cell Arteritis: Need for Standardization. *Medicine (Baltimore)* [Internet]. 2015;94(37):e1542. Available from: <http://www.ncbi.nlm.nih.gov/article/1542>
 17. Dalsgaard Nielsen B, Tønder Hansen I, Krarup Keller K, et al. Attenuation of Fluorine-18-Fluorodeoxyglucose Uptake in Large Vessel Giant Cell Arteritis after Short-Term High-Dose Steroid Treatment - a Diagnostic Window of Opportunity. 2016;
 18. Luqmani R, Lee E, Singh S, et al. The Role of Ultrasound Com-
 - pared to Biopsy of Temporal Arteries in the Diagnosis and Treatment of Giant Cell Arteritis (TABUL): a diagnostic accuracy and cost-effectiveness study. *Health Technol Assess* [Internet]. 2016;20(90):1-238. Available from: <http://www.ncbi.nlm.nih.gov/pubmed/27925577>
 19. Arida A, Kyriyanou M, Kanakis M, Sfikakis PP. The diagnostic value of ultrasonography-derived edema of the temporal artery wall in giant cell arteritis: a second meta-analysis. *BMC Musculoskeletal Disorders* [Internet]. 2010;11(1):44. Available from: <http://bmcmusculoskeletaldisorders.biomedcentral.com/articles/10.1186/1471-2474-11-44>
 20. Schäfer VS, Juche A, Ramiro S, Krause A, Schmidt WA. Ultrasound cut-off values for intima-media thickness of temporal, facial and axillary arteries in giant cell arteritis. *Rheumatology* [Internet]. 2017;3:232. Available from: <https://academic.oup.com/rheumatology/article-lookup/doi/10.1093/rheumatology/kex143>
 21. Terslev L, Diamantopoulos AP, Døhn UM, Schmidt WA, Torp-Pedersen S. Settings and artefacts relevant for Doppler ultrasound in large vessel vasculitis. *Arthritis Res Ther* [Internet]. *Arthritis Research & Therapy*; 2017;19(1):167. Available from: <http://arthritis-research.biomedcentral.com/articles/10.1186/s13075-017-1374-1>
 22. Aschwanden M, Imfeld S, Staub D, et al. The ultrasound compression sign to diagnose temporal giant cell arteritis shows an excellent interobserver agreement. *Clin Exp Rheumatol*. 2015;33(2):3-5.
 23. Fuchs M, Briel M, Daikeler T, et al. The impact of 18F-FDG PET on the management of patients with suspected large vessel vasculitis. *Eur J Nucl Med Mol Imaging*.

- 2012;39(2):344-53.
24. Camellino D, Paparo F, Morbelli S, et al. Interspinous bursitis is common in polymyalgia rheumatica, but is not associated with spinal pain. *Arthritis Res Ther*. 2014;16(492):1-6.
 25. Einspieler I, Thürmel K, Pyka T, et al. Imaging large vessel vasculitis with fully integrated PET/MRI: a pilot study. *Eur J Nucl Med Mol Imaging*. 2015;42(7):1012-24.
 26. Bley TA, Reinhard M, Hauenstein C, et al. Comparison of duplex sonography and high-resolution magnetic resonance imaging in the diagnosis of giant cell (temporal) arteritis. *Arthritis Rheum*. 2008;58(8):2574-8.
 27. Veldhoen S, Klink T, Geiger J, et al. MRI displays involvement of the temporalis muscle and the deep temporal artery in patients with giant cell arteritis. *Eur Radiol*. 2014;24:2971-9.
 28. Oehmigen M, Ziegler S, Jakoby BW, et al. Radiotracer Dose Reduction in Integrated PET/MR: Implications from National Electrical Manufacturers Association Phantom Studies. *J Nucl Med* [Internet]. 2014;55(8):1361-7. Available from: <http://jnm.snmjournals.org/cgi/doi/10.2967/jnumed.114.139147>
 29. Goll C, Thormann M, Hofmuller W, et al. Feasibility study: 7 T MRI in giant cell arteritis. *Graefe's Arch Clin Exp Ophthalmol* [Internet]. Graefe's Archive for Clinical and Experimental Ophthalmology; 2016;254(6):1111-6. Available from: <http://dx.doi.org/10.1007/s00417-016-3337-7>.
 30. Hunder GG. Giant Cell (Temporal) Arteritis - 1990_Completed Article.pdf. 1990. p. 8.
 31. Patil P, Williams M, Maw WW, et al. Fast track pathway reduces sight loss in giant cell arteritis: results of a longitudinal observational cohort study. *Clin Exp Rheumatol* [Internet]. 2015;33(2 Suppl 89):103-6. Available from: <http://www.ncbi.nlm.nih.gov/pubmed/26016758>



Contents

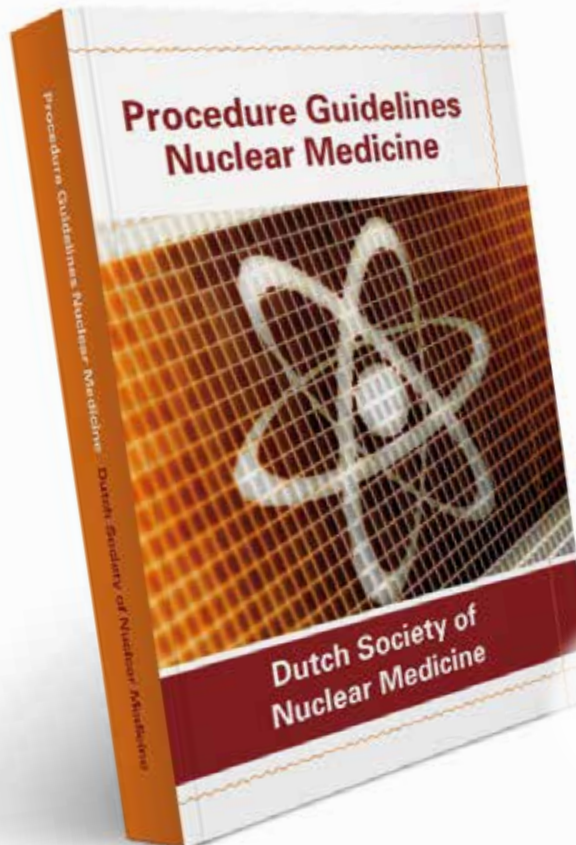
These procedure guidelines describe almost all common patient investigations and therapies that are carried out by a department of nuclear medicine.

The emphasis is on the quality of the procedures as well as the necessary equipment, radiopharmaceuticals and describes physical and pharmaceutical aspects used in nuclear medicine.

[read the introduction »](#)

guidelinesnuclearmedicine.com

Vanaf 2018 digitaal beschikbaar
voor leden van NVNG



ISBN:	ISBN 978-90-78876-09-0
Uitgever:	Kloosterhof Neer B.V.
Omvang:	780 pagina's
Uitvoering:	garengenaaid
Prijs:	€ 53 (leden NVNG excl. verzendkosten) € 79,50 (excl. verzendkosten)

€ 53

(voor leden NVNG)



VANDERWILT techniques is a development and manufacturing company, specialised in products for nuclear medicine such as patient positioning products, phantoms and shielding products.

Contact

T +31 (0)411 68 60 19 | www.for-med.nl



Diagnose en behandeling geïnfecteerde vaatprothesen, handvatten voor de kliniek

M. Wouthuyzen-Bakker, MD, PhD¹; M. van Oosten, MD, PhD¹; prof. C.J. Zeebregts, MD, PhD²; prof. R.H.J.A. Slart, MD, PhD³; E. Kloeze, MD⁴; R. Winter, MD¹; P. van Schaik, MD, PhD²; B.R. Saleem, MD, PhD²; A.W.J.M. Glaudemans, MD, PhD³

Afdelingen ¹Medische Microbiologie en Infectiepreventie, ²Chirurgie, onderafdeling Vaatchirurgie, ³Medical Imaging Center, afdeling Nucleaire Geneeskunde en Moleculaire Beeldvorming, en ⁴Interne geneeskunde / infectieziekten, Rijksuniversiteit Groningen, Universitair Medisch Centrum Groningen, Groningen, Nederland

Voorwoord

Een geïnfecteerde vaatprothese is een ernstige aandoening en kent een hoge morbiditeit en mortaliteit; afhankelijk van de anatomische locatie variërend tussen de 15 en 75% (1-2). Het diagnosticeren en behandelen van een geïnfecteerde vaatprothese is complex en vergt om deze reden een multidisciplinaire aanpak van vaatchirurgen, infectiologen, arts- microbiologen, radiologen en nucleair geneeskundigen. Onderstaand artikel illustreert de complexiteit van de aandoening en biedt handvatten voor de klinische praktijk.

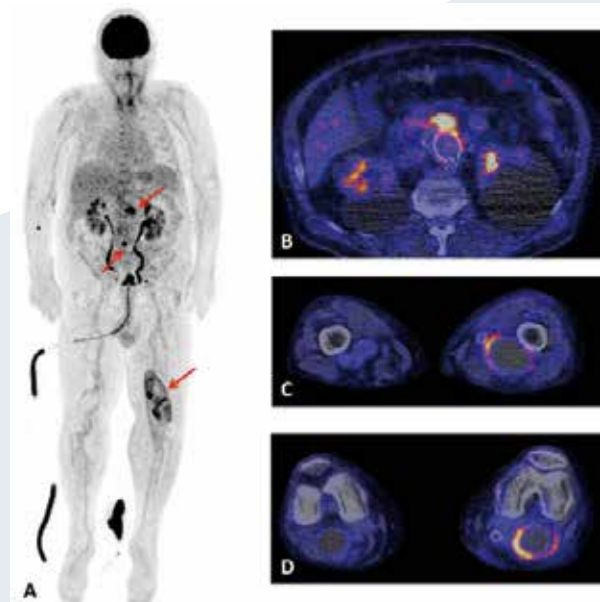
Casus

Een 81-jarige patiënt presenteerde zich met sinds twee weken bestaande koorts en milde roodheid en warmte van de linkerknieholte. De patiënt was bekend met aneurysmatische verwijding van de aorta en arteriae poplitea beiderzijds, waarvoor enkele jaren voor presentatie een endovasculaire aneurysma repair (EVAR), en een veneuze bypass in de rechterknie en een kunststof bypass in de linkerknie werden geplaatst. Onder verdenking van een urineweginfectie was een aantal dagen eerder door de huisarts gestart met ciprofloxacin, maar vanwege een forse CRP stijging werd de patiënt doorverwezen naar het ziekenhuis. Bij opname in het ziekenhuis

werd, na afname van bloedkweken en een urinekweek, gestart met meropenem, onder initiële verdenking van een gecompliceerde urineweginfectie bij bekende kolonisatie met extended-spectrum bèta-lactamase (ESBL)-positieve micro-organismen. Helaas werden van lokaal in de knie geen kweken verkregen. Er werd tijdens de opname een ¹⁸F-FDG PET/CT verricht die opname liet zien ter plaatse van het aneurysma in de linkerknie en ter plaatse van de bifurcatie en het proximale gedeelte van de EVAR bij een bekende endoleak (figuur 1). De opnamepatronen waren suggestief voor infectie. Onder meropenem hield de patiënt koorts en koude rillingen en het CRP daalde langzaam van

250 mg/L naar 150 mg/L. De bloedkweken bleven negatief. Na een week werd een punctie verricht van het aneurysma in de rechterknie voor kweek, maar de kweek en 16S-PCR waren negatief. Kort daarop werd een chirurgisch débridement verricht van de knie. Hierbij bleef de kunststof bypass in situ vanwege het ontbreken van alternatieve revascularisatie mogelijkheden. Peroperatief werd een vijftal kweken afgenoemd, die een dag later allen groei lieten zien van een Gram-positief staafje, wat bij determinatie bleek te gaan om *Listeria monocytogenes*. Bij resistantiebepaling bleek deze slechts intermediair gevoelig voor meropenem, wat mede zou kunnen verklaren waarom de patiënt koorts bleef

Figuur 1. (A) MIP coronaal van de ¹⁸F-FDG PET, de pijlen markeren de pathologische FDG opname verdacht voor infectie; (B) Transversale doorsneden van de ¹⁸F-FDG PET/CT met pathologisch verhoogde opname ter plaatse van proximale gedeelte EVAR; (C en D) Transversale doorsneden van de ¹⁸F-FDG PET/CT met heterogeen verhoogde opname in de randen van het aneurysma in de linkerknie.



houden tijdens behandeling. Het antibiotische regime werd omgezet naar amoxicilline met cotrimoxazol voor een behandelduur van minstens vier weken, waarna gecontinueerd werd met cotrimoxazol suppressie therapie. De ongebruikelijke verwekker werd gemeld bij de Gemeentelijke gezondheidsdienst (GGD), conform protocol.

Deze casus illustreert het belang van algemeen onderzoek, beeldvorming en microbiologisch onderzoek om de respectievelijke foci van infectie en de veroorzakende micro-organismen vast te stellen, cruciaal voor een juiste diagnose en therapie.

Klinische aspecten

Er wordt klinisch onderscheid gemaakt tussen een vroege en een late vaatprothese-infectie (3). Een vroege infectie wordt gedefinieerd als een infectie die binnen drie maanden na het plaatsen van de vaatprothese optreedt. Dit betreft meestal een infectie met een virulent micro-organisme dat via de operatiewond het lichaam binnen is gekomen. Het klinisch beeld omvat dan ook vaak kenmerken van lokale infectie en inflammatie. Een late infectie wordt gedefinieerd als een infectie die later dan drie maanden na het plaatsen van de vaatprothese optreedt. Net als bij een vroege infectie, is de porte d'entrée van deze infectie meestal de operatie(wond). Het betreft hier echter over het algemeen minder virulente micro-organismen, waardoor de infectie vaak een indolent / chronisch karakter heeft en lastiger te herkennen is.

Onderscheid maken tussen een vroege en late infectie is onder andere van belang voor het diagnostisch traject en het kiezen van de juiste empirische antimicrobiële behandeling (4).

Een geïnfecteerde vaatprothese kan ook ontstaan ten gevolge van een bacteriëmie of per continuitatem vanuit een andere infectiefocus (bijvoorbeeld de urinewegen, de darmen, een flebitis, enzovoort). De grootste kans op een secundair geïnfecteerde vaatprothese vanuit een bacteriëmie ligt in de periode waarin endothelialisatie van de

vaatprothese nog moet optreden (tot ongeveer zes weken postoperatief). Bij sommige patiënten blijft endothelialisatie echter onvolledig, en kan zelfs jaren na het plaatsen van de vaatprothese nog een secundaire infectie optreden. Een bacteriëmie met een *Staphylococcus aureus* (*S. aureus*) is hiervoor het meest berucht vanwege zijn adhesieve eigenschappen aan (onregelmatige) oppervlakten. Bij een patiënt met een vaatprothese in situ en een *S. aureus* bacteriëmie dient men dus altijd bedacht te zijn op een secundair geïnfecteerde vaatprothese, met name bij persisterende positieve bloedkweken, persisterende koorts en/of persisterende inflammatieparameters ondanks adequate antibiotische behandeling (5).

Definitie vaatprothese-infectie

In de literatuur bestaat geen duidelijke consensus over de diagnostische criteria van een vaatprothese-infectie. Een geïnfecteerde vaatprothese wordt als zeer waarschijnlijk geacht indien minimaal twee van de drie criteria aanwezig zijn die *niet* op een andere manier verklaard kunnen worden (3):

Microbiologische criteria:

Eén positieve peri-prothetische kweek en/of één positieve bloedkweek. Indien het een commensaal, laagvirulent micro-organisme betreft (bv. coagulase-negatieve stafylokokken (o.a. *S. epidermidis*, *S. haemolyticus*), *Propionibacterium acnes* of corynebacteriën) dan dienen minimaal twee kweken positief te zijn met hetzelfde micro-organisme en hetzelfde resistentiepatroon. *Coxiella burnetii* anti-fase I IgG-antistof-titer $\geq 1:800$.

Radiologische of biochemische criteria:

CRP $> 10 \text{ mg/L}$ of leukocytose $> 10 \times 10^9/\text{L}$, en/of radiologische tekenen van een infectie van de vaatprothese (zie beeldvormend onderzoek voor criteria).

Klinische criteria:

Lokale en/of systemische tekenen van een infectie zoals beschreven in tabel

1 (presentatie onder andere afhankelijk van lokalisatie prothese).

Diagnostiek

Bij iedere patiënt met een verdenking op een geïnfecteerde vaatprothese dient uitgebreide diagnostiek plaats te vinden, bestaande uit anamnese (inclusief in kaart brengen van medische voorgeschiedenis), lichamelijk onderzoek, laboratorium & microbiologisch onderzoek en beeldvormend onderzoek.

Anamnese en lichamelijk onderzoek

Patiënten met één van de volgende risicofactoren hebben een verhoogde kans op het ontwikkelen van een vaatprothese-infectie: 1) plaatsing van de prothese gedurende een spoedoperatie; 2) inadequate perioperatieve antibiotische profylaxe; 3) excisie via de lies; 4) een bacteriëmie gedurende de opnameperiode na het plaatsen van de prothese; 5) een voorgeschiedenis van multipele interventies voor en/of na het plaatsen van de vaatprothese; 6) een slechte wondgenezing; 7) een infectie in het gebied rondom de vaatprothese; 8) comorbiditeit (diabetes mellitus, chronische nierinsufficiëntie, obesitas, gestoorde immuniteit) (2,7). Kenmerkende symptomen voor een geïnfecteerde vaatprothese zijn samengevat in tabel 1. Alhoewel een vroege prothese-infectie zich meestal (per)acuut呈teert, en een late prothese-infectie een meer chronisch/slimerend karakter kent, kunnen veel (lokale) symptomen overeen komen. De symptomen zijn mede afhankelijk van de lokalisatie van de prothese.

Laboratorium en microbiologisch onderzoek

Naast het bepalen van ontstekingsparameters, dienen tevens nierfunctie en leverwaarden bij iedere patiënt te worden bepaald voor het kiezen van de juiste (dosering) antibiotica en voor het monitoren van eventuele bijwerkingen van de therapie. Het opsporen van het ver-

Tabel 1. Symptomen van een vaatprothese-infectie.

koorts (50-75%)
koude rillingen
pijn ter plaatse van, of distaal van de vaatprothese
lekkende operatiwond
inflammatie van de huid ter plaatse van de vaatprothese
dehiscentie van het operatielitteken
lymfocele / abces rondom het operatielitteken
palpabele massa ter hoogte van de vaatprothese
fistel van de huid
(acute) ischemie ledemaat
hoge of lage tractus digestivus bloeding (bij aortoduodenale fistel)
ileus (bij geïnfecteerde aortaprothese)

NB: Bij systemische tekenen van een infectie (koorts, koude rillingen) dient tevens gezocht te worden naar een mogelijke alternatieve verklaring (focusonderzoek).

oorzakende micro-organisme is essentieel voor een succesvolle behandeling. Om deze reden dienen alle kweken te worden afgenoemt onder antibiotica. Indien de patiënt reeds wordt behandeld met antibiotica, dient bij voorkeur (indien de kliniek dit toelaat) het antibioticum te worden gestaakt en dienen er nieuwe kweken te worden afgenoemt bij koorts ($T > 38,5$ graden) of twee weken na staken van de antibiotica.

Bloedkweken

Bij iedere patiënt met verdenking op een vaatprothese-infectie dienen minimaal twee sets (4 flesjes) bloedkweken te worden afgenoemt (ook bij afwezigheid van koorts). Daarbij dient opgemerkt te worden dat de opbrengst van bloedkweken klein is indien alleen het extra-luminale oppervlak van de vaatprothese betrokken is (6,8).

Kweken aspiraat

Naast de afname van bloedkweken dienen (indien mogelijk) intra-operatief of via een radiologische punctie, minimaal 3 aspiraties rondom de geïnfecteerde

vaatprothese te worden afgenoemt voor een banale kweek. Een fistel of oppervlakkige wondkweek wordt bij voorkeur niet afgenoemt. De kans op een foutpositieve uitslag door kolonisatie van de huid is bij fistels groot en kweekuitslagen kunnen om deze reden niet goed worden geïnterpreteerd. Indien de patiënt reeds wordt behandeld met antibiotica kunnen de kweken, naast reguliere kweekmethoden, in overleg met de arts-microbioloog, nog worden ingezet voor een 16S-PCR of gerichte PCRs. Hiermee kan bacterieel DNA worden gedetecteerd, ook van dode micro-organismen. Een belangrijk nadeel van de 16S-PCR is dat deze methode minder sensitief is en bij PCR - in tegenstelling tot de kweekresistentie van de betreffende bacterie niet kan worden bepaald (9). Het heeft dus absoluut de voorkeur om het betreffende antibioticum te staken en twee weken nadien alsnog kweken in te sturen, zoals boven beschreven.

Serologie *Coxiella burnetii*

Indien kweken negatief blijven en/of er

twijfel bestaat over de kweekuitslagen in relatie tot het klinisch beeld, dient Q-koorts te worden overwogen. Hiervoor kan serologisch onderzoek worden ingezet op *Coxiella burnetii*. Een anti-fase I IgG-antistoftiter $\geq 1:800$ is bewijzend voor een chronische infectie.

Beeldvormend onderzoek

Bij een klinische verdenking op een geïnfecteerde vaatprothese dient onderstaand beeldvormend onderzoek te worden verricht.

Echo-doppler

Bij een vaatprothese ter plaatse van de extremitelen wordt een echo-doppler verricht. Indien valse aneurysmata, trombose, en/of peri-prothetische collecties worden gezien kan direct echografisch worden gepunteerd voor microbiologisch onderzoek (zie kweken biopt) (10-13). Bij een positieve echo wordt aansluitend een CT-angiografie of ^{18}F -FDG PET met low dose CT (zie onder) verricht om de uitgebreidheid van de infectie in kaart te brengen. Vanwege de kans op een fout-negatieve uitslag wordt bij een negatieve echo-doppler en blijvende verdenking op een vaatprothese-infectie tevens aanvullende beeldvorming gedaan (zie onder).

CT-angiografie (CTA)

Bij verdenking op een vroege vaatprothese-infectie (≤ 3 maanden postoperatief) is het advies een CTA met contrast te verrichten. De sensitiviteit en specifieiteit van een CTA bij een vroege infectie is hoog: respectievelijk 95% en 85%. Een ^{18}F -FDG PET-scan kan tot circa twee maanden postoperatief foutpositief zijn, en wordt om deze reden bij verdenking op een vroege vaatprothese-infectie afgeraden. Zeer suggestieve radiologische tekenen voor een vaatprothese-infectie zijn: peri-prothetische infiltratie, (vocht)collecties, luchtbellen, valse aneurysmata, en lokale intestinale wandverdikking bij aortale vaatprothesen. Deze tekenen kunnen echter ook postoperatief voorkomen, zonder dat er sprake is van infectie. Het is niet

bekend hoe lang dit postoperatief kan blijven bestaan. Het is beschreven dat vocht rondom de vaatprothese nog tot ruim twee maanden na de operatie aanwezig kan zijn. Luchtbellen zijn over het algemeen in minder dan een week na operatie verdwenen, maar kunnen echter tot zeven weken postoperatief blijven bestaan (14-17).

¹⁸F-FDG PET met low dose CT

Bij een verdenking op een late / chronische infectie (≥ 3 maanden postoperatief) wordt een gecombineerde ¹⁸F-FDG PET met een *low dose* CT-scan geadviseerd. De sensitiviteit van een CTA is in dit stadium van infectie laag ($\pm 55\%$) en wordt om deze reden afgeraad. De positief en negatief voorspellende waarde van een ¹⁸F-FDG PET met een *low dose* CT bij verdenking op een late / chronische infectie is hoog; respectievelijk 89% en 84%. Een focale of heterogene opname van FDG langs de vaatprothese is zeer suggestief voor een infectie (20-26). Een homogene opname langs de vaatprothese past bij fysiologische opname en kan tot vele jaren na het plaatsen van de prothese aanwezig blijven, afhankelijk van het gebruikte materiaal. Heterogene opname in een deel van de prothese of uitbreiding van FDG opname buiten de prothese is verdacht voor infectie (zie figuur 2). Een bijkomend voordeel van een ¹⁸F-FDG PET is dat tevens naar eventuele strooihaarden van een gedissemineerde infectie en/of een alternatief focus van infectie gekeken kan worden.

Behandeling

De behandeling van een geïnfecteerde vaatprothese bestaat uit een combinatie van chirurgische interventie en langdurige antibiotische behandeling. Indien de infectie vroeg (< 4 weken) postoperatief ontstaat en/of secundair is aan een bacteriëmie vanuit een ander focus, kan worden getracht de prothese middels chirurgisch débridement en antibiotische therapie te behouden. Een langer bestaande geïnfecteerde vaatprothese is echter, ten gevolge van

de biofilm formatie, antibiotisch niet 'schoon te krijgen' (4). Het volledig verwijderen van de vaatprothese in combinatie met antibiotische behandeling is dan de enige manier voor het bereiken van curatie. Is het verwijderen van de vaatprothese vanwege comorbiditeit en/of beperkte revascularisatie mogelijkheden niet haalbaar dan behoort chirurgisch débridement (indien mogelijk) met een inductiefase met intraveneuze antibiotica en aansluitend levenslange antibiotische suppressietherapie tot de mogelijkheden. Bij infra-inguinale infecties is het soms noodzakelijk de ledemaat te amputeren. Voor welke behandeling uiteindelijk wordt gekozen, dient multidisciplinair te worden besloten.

Chirurgische behandeling

Bij de behandeling van vaatprothese-infectie speelt de locatie een belangrijke rol. Er wordt onderscheid gemaakt tussen centraal en perifeer gelegen prothesen. Indien het een prothese is voor de behandeling van centrale vaatreconstructies (EVAR of dacron prothese; buis of broekprothese) is de explantatie een dusdanig grote ingreep met hoge morbiditeit en mortaliteit dat een eventuele operatie zorgvuldig, in overleg met patiënt en behandelteam, overwogen moet worden (27). Conservatieve behandeling bij een vaatprothese-infectie moet beperkt worden tot patiënten met hoge comorbiditeit. Indien de patiënt klinisch achteruitgaat ondanks optimale antibiotische behandeling kan een explantatie alsnog overwogen worden. Er zijn dan meerdere opties mogelijk om toch de circulatie naar distaal te behouden. Extra-anatomische bypass werd tot kort gezien als de gouden standaard. Deze prothese wordt net onder de huid geplaatst en loopt meestal van een slagader onder het sleutelbeen tot de slagader in de lies. Deze zogenaamde extra-anatomische bypass heeft echter een grote kans om op termijn op te stollen dan wel te infecteren. Daarbij is de plaatsing van een extra-anatomische bypass geassocieerd met een grote kans op amputatie van een ledemaat.

Tegenwoordig gaat de voorkeur uit naar een in-situ reconstructie. Een in-situ reconstructie kan met verschillende soorten materialen: autologe vene, cryopreserved allograft en een met rifampicine doordrenkte prothese (28-30). Recent zijn er nieuwe ontwikkelingen met betrekking tot prothesematerialen van runderpericard (31). Voor perifere vaatprotheses heeft een redo-bypass met autologe vene de voorkeur. Een redo-bypass met kunststof materiaal is minder wenselijk aangezien de kans op reïnfectie vrij groot is.

Antibiotische behandeling

De meest voorkomende verwekkers van een geïnfecteerde vaatprothese worden weergegeven in tabel 2 (32). Mogelijk vanwege het gebrek aan studies, bestaat er in de literatuur geen duidelijk correlatie tussen de locatie van de prothese-infectie en het veroorzakende micro-organisme. Bij empirische antibiotische therapie moet rekening worden gehouden met het onderscheid tussen vroege en/of acute infecties en late en/ of chronische infecties. Tevens dient er rekening gehouden te worden met eventuele resistentie micro-organismen waar de patiënt mee gekoloniseerd kan zijn. De keuze, dosering en duur van de antibiotische therapie dient altijd te worden overlegd met de arts-microbioloog en/of infectioloog. Bij bekend worden van kweken kan de antibiotische behandeling dan worden versmald of aangepast.

Antibiotische therapie na volledig débridement en verwijdering van kunstmateriaal

Indien de geïnfecteerde prothese in zijn geheel is verwijderd en volledig / adequaat chirurgisch débridement heeft plaatsgevonden, volstaat waarschijnlijk zes weken intraveneuze antibiotische therapie voor het bereiken van curatie. Eventuele aanvullende orale antibiotische therapie voor een periode van drie tot zes maanden dient multidisciplinair worden besloten. Dit zal onder andere mede worden bepaald door

Tabel 2. Meest voorkomende verwekkers geïnfecteerde vaatprothese.

Coagulase negatieve stafylokokken	33%
<i>Staphylococcus aureus</i>	30%
<i>Escherichia coli</i>	15%
<i>Pseudomonas aeruginosa</i>	8%
<i>Enterococcus</i> species	5%
<i>Klebsiella pneumoniae</i>	2%
<i>Candida</i> species	2%
<i>Streptococcus</i> species	1%
Kweek negatief	4%

Deze gegevens zijn gebaseerd op kweekresultaten van 119 patiënten, waarvan 68 met een aorta-iliofemorale en 51 met een extracavitaire prothese-infectie (32); 20-30% van geïnfecteerde vaatprothesen zijn polymicrobieel (33).

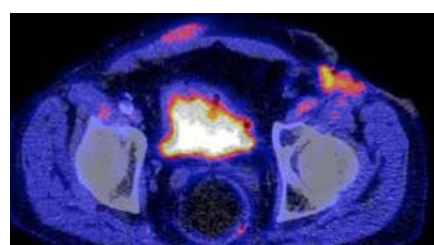
het type chirurgische reconstructie dat is uitgevoerd (in situ reconstructie versus extra-anatomische bypass), het type prothese dat wordt geplaatst (veneuze/ arteriële graft versus kunstmateriaal), de klinische respons, en het veroorzakend micro-organisme.

Antibiotische therapie bij sub-optimaal débridement en/of achterblijven van kunstmateriaal

Indien het kunstmateriaal niet kan worden verwijderd dient minimaal twee tot vier weken inductie behandeling plaats te vinden middels intraveneuze antibiotische behandeling. Deze behandeling wordt gevolgd door levenslange antibiotische suppressie-therapie. Bij een vroege infectie (< 4 weken) en/of bij het ontstaan van een bacteriëmie in de vroeg postoperatieve fase, kan in sommige gevallen worden getracht de prothese te behouden en het conservatief met antibiotica te behandelen. Indien echter geen débridement heeft plaatsgevonden, dan is de kans groot dat de infectie chronisch wordt, en de patiënt behandeld zal moeten worden met levenslange antibiotische suppressie-therapie.

m.wouthuizen-bakker@umcg.nl ♦

Figuur 2. 76-jarige man met sinds een half jaar een axillobifemorale bypass vanaf links. Nu opgenomen in verband met blootliggende bypass in linkerlies. Patiënt wordt opgewerkt voor revisie prothese, waarbij waarschijnlijk een gedeelte van de prothese verwijderd zal worden. Welk gedeelte van de prothese is geïnfecteerd? ¹⁸F-FDG PET: Heterogene opname met enige uitbreiding richting weke delen en de huid van het distale tweederde deel linker femorale poot (A, B), verdacht voor en passend bij bestaande infectie. De overige delen van de axillobifemorale bypass vertonen homogeen, normale reactieve opname (B), derhalve niet verdacht voor infectie. Elders in het lichaam geen aanwijzingen voor infectie. Kweek pus/weefsel insteek lies links: *Staphylococcus aureus*.



ReferentieS

1. Leroy O, Meybeck A, Sarraz-Bourret B, et al. Vascular graft infections. *Curr Opin Infect Dis.* 2012;25(2): 154-8
2. Antonios VS, Noel AA, Steckelberg JM, et al. Prosthetic vascular graft infection: a risk factor analysis using a case-control study. *J Infect.* 2006;53(1):49-55
3. Fitzgerald SF, Kelly C, Humphreys H. Diagnosis and treatment of prosthetic aortic graft infections: confusion and inconsistency in the absence of evidence or consensus. *J Antimicrob Chemother.* 2005;56(6): 996-9
4. Lebeaux D, Ghigo JM, Beloin C. Biofilm-related infections: bridging the gap between clinical management and fundamental aspects of recalcitrance toward antibiotics. *Microbiol Mol Biol Rev.* 2014;78(3):510-43
5. Shanani L. Vascular graft infections and role of PET/CT in patients with persistent bacteraemia. *BMJ Case Rep.* 2015 Mar 16;2015.
6. Legout L, Sarraz-Bourret B, D'Elia PV, et al. Characteristics and prognosis in patients with prosthetic vascular graft infection: a prospective observational cohort study. *Clin Microbiol Infect.* 2012;18:352-8
7. Siracuse JJ, Nandivada P, Giles KA, et al. Prosthetic graft infections involving the femoral artery. *J Vasc Surg.* 2013;57:700-5
8. Saleem BR, Meerwaldt R, Tielliu IF, et al. Conservative treatment of vascular prosthetic graft infection is associated with high mortality. *Am J Surg.* 2010;200(1): 47-52
9. Harris KA, Hartley JC. Development of broad-range 16S rDNA PCR for use in the routine diagnostic clinical microbiology service. *J Med Microbiol.* 2003;52:685-91
10. Hodgkiss-Harlow KD, Bandyk DF. Interpretation of arterial duplex testing of lower-extremity arteries and interventions. *Semin Vasc Surg.* 2013;26(2-3):95-104
11. Cook T, Nolting L, Barr C, et al. Diagnostic ultrasonography for peripheral vascular emergencies. *Crit Care Clin.* 2014;30(2):185-206
12. Khoo SW, Han DC. The use of ultrasound in vascular procedures. *Surg Clin North Am.* 2011;91(1):173-84
13. Mennitt K, Deol M, Gao J. Emergency color doppler sonography of the extremity artery: a pictorial essay. *Clin Imaging.* 2017;42:240-8
14. Low RN, Wall SD, Jeffrey RB, et al. Aortoenteric fistula and perigraft infection: evaluation with CT. *Radiology* 1990;175(1):157-62
15. Qvarfordt PG, Reilly LM, Mark AS, et al. Computerized tomographic assessment of graft incorporation after aortic reconstruction. *Am J Surg* 1985;150:227-31
16. O'Hara PJ, Borkowski GP, Herzer NR, et al. Natural history of periprosthetic air on computerized axial tomographic examination of the abdomen following abdominal aortic aneurysm repair. *J Vasc Surg* 1984;1:429-33
17. Orton DF, LeVeen RF, Saigh JA, et al. Aortic prosthetic graft infections: radiologic manifestations and implications for management. *Radiographics.* 2000;20:977-93
18. Gotthardt M, Bleeker-Rovers CP, Boerman OC, Oyen WJ. Imaging of inflammation by PET, conventional scintigraphy, and other imaging techniques. *J Nucl Med Technol.* 2013;41:157-69
19. Modrall JG, Clagett GP. The role of imaging techniques in evaluating possible graft infections. *Semin Vasc Surg* 1999;12:339-47
20. Saleem BR, Berger P, Vaartjes I, et al. Modest utility of quantitative measures in (18)F-fluorodeoxyglucose positron emission tomography scanning for the diagnosis of aortic prosthetic graft infection. *J Vasc Surg.* 2015;61(4): 965-71
21. Fukuchi K, Ishida Y, Higashi, et al. Detection of aortic graft infection by fluorodeoxyglucose positron emission tomography: comparison with computed tomographic findings. *J Vasc Surg.* 2005;42(5):919-25
22. Keidar Z, Engel A, Hoffman A, et al. Prosthetic vascular graft infection: the role of 18F-FDG-PET/CT. *J Nucl Med.* 2007;48(8): 1230-6
23. Spacek M, Beloholavek O, Votrubova J, et al. Diagnostics of non-acute vascular prosthesis using 18F-FDG-PET/CT: our experience with 96 prostheses. *Euro J Nucl Med Mol Imaging.* 2009;36(5): 850-8
24. Bruggink JL, Glaudemans AW, Saleem BR, et al. Accuracy of FDG-PET-CT in the diagnostic work-up of vascular graft infection. *Eur J Vasc Endovasc Surg.* 2010;40(3):348-54
25. Tokuda Y, Oshima H, Araki Y, et al. Detection of thoracic aortic prosthetic graft infection with 18F-fluorodeoxyglucose positron emission tomography/computed tomography. *Eur J Cardiothorac Surg.* 2013;43(6):1183-7
26. Sah BR, Husmann L, Mayer D, et al. Diagnostic performance of 18F-FDG-PET/CT in vascular graft infection. *Eur J Vasc Endovasc Surg.* 2015;49:455-64
27. Khashram M, Williman JA, Hider PN. Systematic Review and Meta-analysis of Factors Influencing Survival Following Abdominal Aortic Aneurysm Repair. *Eur J Vasc Endovasc Surg.* 2016;51(2):203-15
28. Mertens RA1, O'Hara PJ, Hertzler NR, et al. Surgical management of infringuinal arterial prosthetic

- graft infections: review of a thirty-five-year experience. *J Vasc Surg.* 1995 May;21(5):782-90
29. Szcot M, Meybeck A, Legout L, et al. Vascular graft infections in the intensive care unit: clinical spectrum and prognostic factors. *J Infect.* 2011;62 (3): 204-11
30. Chaufour X, Gaudric J, Goueffic Y, et al. A multicenter experience with infected abdominal aortic endograft explantation. *J Vasc Surg.* 2017;65(2):372-80
31. Lindsey P, Echeverria A, Cheung M, et al. Lower Extremity Bypass Using Bovine Carotid Artery Graft (Artegraft): An Analysis of 124 Cases with Long-Term Results. *World J Surg.* 2017 Aug [Epub ahead of print].
32. Bandyk DF, Novotney ML, Back MR, et al. Expanded application of in situ replacement for prosthetic graft infection. *J Vasc Surg.* 2001;34:411-20
33. Calligaro KD, Veith FJ, Schwartz ML, et al. Differences in early versus late extracavitory arterial graft infections. *J Vasc Surg.* 1995;22(6):680-5

▼ Dit geneesmiddel is onderworpen aan aanvullende monitoring. Verkorte Productinformatie Xofigo® 1100 kBq/ml oplossing voor injectie

Samenstelling: Werkzame stof: radium Ra-223 dichloride (radium-223 dichloride, 1100 kBq/ml, op de referentiedatum overeenkomend met 0,58 ng radium-223). Elke injectieflacon bevat 6 ml oplossing (op de referentiedatum 6,6 MBq radium-223 dichloride). **Hulstoffen:** Water voor injecties, natriumcitraat, natriumchloride, zoutzuur verdunt. **Indicatie:** Behandeling van volwassenen met castratiereistent prostaatcarcinoom, symptomatiche botmetastasen en geen bekende viscerale metastasen. Xofigo dient alleen te worden toegediend door personen die bevoegd zijn om met radioactieve geneesmiddelen te werken binnen een hier toe aangewezen klinische setting. **Contra-indicaties:** Er zijn geen contra-indicaties bekend. **Bijzondere waarschuwingen en voorzorgen bij gebruik:** Beenmergsuppressie, met name trombocytopenie, neutropenie, leukopenie en pancytopenie, is gemeld. Hematologische evaluatie van patiënten moet uitgevoerd worden bij aanvang van de behandeling en vóór elke volgende dosis. Indien er binnen 6 weken na de laatste toediening van Xofigo geen herstel van het absolute aantal neutrofieren (ANC) en de hemoglobine is opgetreden, ondanks het ontvangen van standaard zorg, mag de behandeling met Xofigo alleen worden voortgezet na een zorgvuldige afweging van de voordelen en risico's. Voorzichtigheid is geboden bij de behandeling van patiënten met tekenen van verminderde beenmergreserve, bijv. na een eerder cytotoxische chemotherapie en/of radiotherapie (EBRT, *external beam radiation therapy*) of patiënten met gevorderde diffuse infiltratie van het bot (EO4; 'superscan'), aangezien er een verhoogde incidentie van hematologische bijwerkingen zoals neutropenie en trombocytopenie is waargenomen. Beperkte beschikbare gegevens geven aan dat patiënten die chemotherapie krijgen nadat ze met Xofigo zijn behandeld, een vergelijkbaar hematologisch profiel hadden vergeleken met patiënten die chemotherapie kregen na placebo. Ziekte van Crohn en colitis ulcerosa, omdat Xofigo via de feces wordt uitgescheiden, kan straling leiden tot een verergering van acute inflammatoire darmziekten. Daarom dient Xofigo alleen te worden toegediend na zorgvuldige afweging van de voordelen en risico's bij deze patiënten. Bij patiënten met onbehandelde, dreigende of al aanwezige ruggenmergcompressie dient behandeling met standaardzorg volgens klinische indicatie te worden voortgezet voordat de behandeling met Xofigo wordt gestart of hervat. Bij patiënten met botfracturen dienen de fracturen orthopedisch te worden stabiliseerd voordat de behandeling met Xofigo wordt gestart of hervat. Bij patiënten die behandeld werden met bisfosfonaten en Xofigo kan een verhoogd risico op de ontwikkeling van osteonecrose van de kaak (ONJ) niet uitgesloten worden. In de fase III-studie zijn gevallen van ONJ gemeld bij 0,67% van de patiënten (4/600) in de Xofigo-arm in vergelijking met 0,33% van de patiënten (1/301) in de placebo-arm. Alle patiënten met ONJ waren echter eerder of gelijktijdig aan bisfosfonaten blootgesteld en hadden eerder chemotherapie gehad. Xofigo draagt bij aan de totale cumulatieve hoeveelheid straling waarvan patiënten op de lange termijn worden blootgesteld en kan daar ook gepaard gaan met een verhoogd risico op kanker en erfelijke defecten. Er zijn geen gevallen gemeld van Xofigo-geïnduceerde kanker in de klinische studies met een follow-upperiode tot en met drie jaar. Afhankelijk van het toegediende volume kan dit geneesmiddel tot maximaal 2,35 mmol (54 mg) natrium per dosis bevatten. **Bijwerkingen:** Zeer vaak: trombocytopenie, diarree, braken, misselijkheid; Vaak: neutropenie, pancytopenie, leukopenie, injectieplaatsreacties; Soms: lymphopenie. **Handelsvorm:** Injectieflacon met 6 ml oplossing voor injectie. **Nummer van de vergunning:** EU/1/13/873/001. **Vergunninghouder:** Bayer AG, 51368 Leverkusen, Duitsland. **Verdere informatie beschikbaar bij:** Bayer B.V., Energieweg 1, 3641 RT Mijdrecht, tel. 0297 280 666. **Afleverstatus:** UR. **Datum goedkeuring/herziening van de SmPC:** 08/2017. **Versie:** september 2017. Uitgebreide informatie (SmPC) is op aanvraag beschikbaar.

Referenties: 1. Mohler JL, et al. NCCN Clinical Practice Guidelines in Oncology (NCCN Guidelines®) Prostate Cancer. Version 2.2016. NCCN; 2016:1-108. 2. Mottet N, et al. Guidelines on Prostate Cancer. EAU; 2016:1-146. 3. SmPC Xofigo® (radium Ra-223 dichloride), 04/2016. 4. Prostaatcarcinoom, Landelijke richtlijn, Versie 2.1, 2016, IKNL.



Xofigo®
radium Ra 223 dichloride

Future perspective: where is cardiovascular nuclear imaging heading?

F.M. Bengel, MD, FAHA

Department of Nuclear Medicine, Hannover Medical School, Hannover, Germany

As the field of cardiovascular medicine is evolving towards an ever increasing plethora of therapeutic options, diagnostic techniques such as cardiovascular imaging are evolving alongside with it in order to meet the changing demands of therapeutic decision making. By facing such novel challenges, nuclear cardiology has also evolved in recent years and it will continue to do so in the future. New imaging technologies, new radiotracers and new disease targets have been implemented, and the entire field of nuclear imaging (outside of cardiology) is benefitting from these developments.

The articles of this issue of the journal comprehensively summarize the major trends that will shape cardiovascular imaging in the future: the quest for absolute quantification, the development of multi-modality (interdisciplinary) imaging strategies, and the reach beyond imaging of anatomy and physiology, towards true molecular and cellular imaging techniques.

The management of coronary artery disease (CAD) remains the biggest challenge for cardiovascular medicine, and the role of ischemia in guiding therapeutic management is now generally accepted. Nuclear cardiology has been the leading technique in defining ischemia, but there is increasing availability and success of alternative techniques such as echocardiography, cardiac computed tomography (CT) or cardiac magnetic resonance imaging (MRI). On the one hand, this has triggered an evolution of radionuclide based perfusion imaging approaches, which includes an increasing utilization

of PET, the development of sensitive solid-state detector SPECT systems, and an increasing implementation of absolute myocardial blood flow quantification for refined diagnostic and prognostic workup (1,2). On the other hand, this emphasizes the need for cardiac imaging experts to go beyond a single modality and understand the benefits and challenges of a majority of (or even all) available imaging techniques, in order to be able to select the best test for each individual situation. For the nuclear physician, this means that personal knowledge and/or close interdisciplinary interaction with experts in clinical cardiac CT and cardiac MRI is needed – which also is a requirement for optimal utilization of high-end hybrid PET/CT and PET/MRI systems (3, 4). The future of CAD imaging will likely consist of multi-modality algorithms which include a step-wise implementation of different techniques based on clinical scenario and available prior test results, and which include a choice between available techniques based on individual patient characteristics such as age, gender, and risk factors (5).

Knowledge of multi-modality imaging becomes even more important with an increasing implementation of molecular targeted tracers, which may yield a weak signal from a circumscribed region such as vessel wall or valve and thus require accurate co-registration with a morphologic imaging technique and with a technique that enables concomitant interpretation of function and motion. Disease targets outside of CAD such as infiltrative cardiomyo-

pathies, device infection, inflammatory conditions and heart failure progression / ventricular remodelling have led to a rapid increase of clinical molecular imaging in the cardiovascular system. The recent implementation of FDG PET/CT and leukocyte SPECT/CT into guidelines for infective endocarditis (6), along with the rapid growth of cardiac sarcoidosis and amyloidosis imaging (7-9) are prime examples of this trend, where radionuclide imaging provides sensitivity and specificity and CT or MRI provide spatial resolution and localization. This trend toward new molecular imaging applications in the cardiovascular system has just begun. New tracers will accelerate its growth. Accordingly, the future of radionuclide cardiovascular imaging is very promising, but it will come with changes that need to be recognized and internalized by those active in the field.

bengel.frank@mh-hannover.de ♦

References

- Acampa W, Buechel RR, Gimelli A. Low dose in nuclear cardiology: state of the art in the era of new cadmium-zinc-telluride cameras. Eur Heart J Cardiovasc Imaging. 2016;17:591-5
- Bengel FM, Higuchi T, Javadi MS, Lautamaki R. Cardiac positron emission tomography. J Am Coll Cardiol. 2009;54:1-15
- Gaemperli O, Bengel FM, Kaufmann PA. Cardiac hybrid imaging. Eur Heart J. 2011;32:2100-8
- Rischpler C, Nekolla SG, Dregely I, Schwaiger M. Hybrid PET/

- MR imaging of the heart: potential, initial experiences, and future prospects. *J Nucl Med.* 2013;54:402-15
5. Task Force M, Montalescot G, Sechtem U, et al. 2013 ESC guidelines on the management of stable coronary artery disease: the Task Force on the management of stable coronary artery disease of the European Society of Cardiology. *Eur Heart J.* 2013;34:2949-3003
6. Habib G, Lancellotti P, Antunes MJ, et al. 2015 ESC Guidelines for the management of infective endocarditis: The Task Force for the Management of Infective Endocarditis of the European Society of Cardiology (ESC). Endorsed by: European Association for Cardio-Thoracic Surgery (EACTS), the European Association of Nuclear Medicine (EANM). *Eur Heart J.* 2015;36:3075-128
7. Bengel FM. The non-invasive biopsy: molecular imaging for the detection of cardiac involvement in systemic disease. *Eur Heart J Cardiovasc Imaging.* 2014;15:1299-1300
8. Bengel FM, George RT, Schulter KH, Lardo AC, Wollert KC. Image-guided therapies for myocardial repair: concepts and practical implementation. *Eur Heart J Cardiovasc Imaging.* 2013;14:741-51
9. Schatka I, Bengel FM. Advanced imaging of cardiac sarcoidosis. *J Nucl Med.* 2014;55:99-106

Team Kloosterhof dankt je voor je bijdrage en fijne samenwerking. Op naar een groeizaam 2018!

Eric, Yvonne, Annemieke, Marie-José, Loes,
Janet, Liesbeth, Anuska en Jorg

Tijdschrift voor Coaching | LoopbaanVisie | Tijdschrift Positieve Psychologie |
Tijdschrift voor Ontwikkeling in Organisaties | PsychoSociaal digitaal | TA Magazine |
De Nieuwe Meso | Examens | Tijdschrift voor Nucleaire Geneeskunde



Tijdschrift voor Nucleaire Geneeskunde
ISSN 1381-4842, nr. 4, december 2017
Uitgever



Kloosterhof acquisitie services - uitgeverij
 Napoleonsweg 128a
 6086 AJ Neer
 T: 0475 59 71 51
 F: 0475 59 71 53
 E: info@kloosterhof.nl
 I: www.kloosterhof.nl

Hoofdredacteur
 dr. B.F. Bulten
 benbulten@gmail.com
 dr. R.A. Valdés Olmos
 r.a.valdes_olmos@lumc.nl

Redactie
 dr. J.J.M. Balink
 dr. M. Bauwens
 drs. B. Bosveld
 dr. N. Bouwmans
 drs. J. Emmering
 dr. A.W.J.M. Glaudemans
 J.A.C. van Osch
 drs. E.C. Owers
 A. Reniers
 dr. O. de Winter

Bureauredactie
 drs. Anuska Muijres
 T: 0475 600589
 E: anuska@kloosterhof.nl

Advertentie-exploitatie
 Kloosterhof Neer B.V.
 acquisitie services - uitgeverij
 Eric Vullers
 T: 0475 597151
 E: eric@kloosterhof.nl

Vormgeving
 Kloosterhof Vormgeving
 Marie-José Verstappen
 Annemieke Peeters

Abonnementen
 Leden en donateurs van de aangesloten Leden en
 donateurs van de aangesloten beroepsverenigingen
 ontvangen het Tijdschrift voor Nucleaire Geneeskunde
 kosteloos. Voor anderen geldt een abonnementsprijs
 van € 45,00 per jaar; studenten betalen € 29,00 per jaar
 (incl. BTW en verzendkosten).
 Voor buitenlandse abonnementen gelden andere
 tarieven.
 Opgave en informatie over (buitenlandse)
 abonnementen
 en losse nummers (€ 13,50) bij Kloosterhof acquisitie
 services - uitgeverij, telefoon 0475 59 71 51.
www.tijdschriftvoornucleairegeneeskunde.nl

Verschijningsdata, jaargang 40
 Nummer 1: 27 maart 2018
 Nummer 2: 26 juni 2018
 Nummer 3: 25 september 2018
 Nummer 4: 27 december 2018

Aanleveren kopij, jaargang 40
 Nummer 1: 1 januari 2018
 Nummer 2: 1 april 2018
 Nummer 3: 1 juli 2018
 Nummer 4: 1 oktober 2018

Kloosterhof acquisitie services - uitgeverij
 Het verlenen van toestemming tot publicatie in dit
 tijdschrift houdt in dat de auteur aan de uitgever
 onvooraardelijker aanspraak overdraagt op de door
 derden verschuldigde vergoeding voor kopiëren, als
 bedoeld in Artikel 17, lid 2, der Auteurswet 1912 en
 in het KB van 20-71974 (stb. 351) en artikel 16b der
 Auteurswet 1912, teneinde deze te doen exploiteren
 door en overeenkomstig de Reglementen van de
 Stichting Reprorecht te Hoofddorp, een en ander
 behoudend uitdrukkelijk voorbehoud van de kant van
 de auteur.

Cursus- en congresagenda

2018

EANM FOCUS 1 – The International Conference on Molecular Imaging and Theranostics in Prostate Cancer

1-3 February, Valencia, Spain
<http://focusmeeting.eanm.org>

ECR 2018 - European Congress of Radiology Annual Meeting

February 28 – March 4, 2018. Vienna, Austria.
<http://www.myesr.org/congress>

Eight International Symposium on Sentinel Node Biopsy in Head and Neck Cancer - Consensus Conference

20-21 April 2018, Royal College of Physicians, London, UK.
<https://eighthsnb.com>

WFNMB 2018 - 12th Congress of the World Federation of Nuclear Medicine and Biology

20 - 24 April, 2018, Melbourne, Australia
<http://wfnmb2018.com>

5th European IRPA Congress "Encouraging Sustainability in Radiation Protection".

4 - 8 June, 2018, The Hague, The Netherlands
<https://irpa2018europe.com/>

SNMMI 2018 - Annual Meeting of the Society of Nuclear Medicine and Molecular Imaging

23 - 27 June, 2018, Philadelphia, Pennsylvania, USA
<http://www.snmmi.org/MeetingsEvents/EventDetail.aspx?EventID=23027>

ISNS 2018 - International Sentinel Node Society Biennial Meeting

11 - 13 October 2018, Kioi Conference, Tokyo Garden Terrace, Japan
<http://www2.convention.co.jp/isns2018>

EANM 2018 - 31st Annual Congress of the European Association of Nuclear Medicine

13 - 17 October, 2018, Düsseldorf, Germany
<http://www.eanm.org/congresses-events/future-congress/>

Adreswijzigingen

Regelmatig komt het voor dat wijzigingen in het bezorgadres voor het Tijdschrift voor Nucleaire Geneeskunde op de verkeerde plaats terechtkomen. Adreswijzigingen moeten altijd aan de betreffende verenigingssecretariaten worden doorgegeven. Dus voor de medisch nucleair werkers bij de NVMBR, en voor de leden van de NVNG en het Belgisch Genootschap voor Nucleaire Geneeskunde aan hun respectievelijke secretariaten. De verenigingssecretariaten zorgen dan voor het doorgeven van de wijzigingen aan de Tijdschrift adresadministratie. Alleen adreswijzigingen van betaalde abonnementen moeten rechtstreeks aan de abonnementenadministratie van Kloosterhof Neer B.V. worden doorgegeven: Kloosterhof Neer B.V., t.a.v. administratie TvNG, Napoleonweg 128a | 6086 AJ Neer of per E-mail: nucleaire@kloosterhof.nl



Overweeg start met kuur Xofigo® bij patiënten progressief op 2^e generatie hormoontherapie^{1,2}



LNLNKTSM01.2017.1394

XOFIGO® is geïndiceerd voor de behandeling van volwassenen met castratieresistent prostaatcarcinoom, symptomatische botmetastasen en geen bekende viscerale metastasen.³

* De mediane overlevingswinst van Xofigo® vs placebo in de ALSYMPCA bedraagt 3,6 maanden

Zie voor referenties en productinformatie elders in dit blad.

 **Xofigo®**
radium Ra 223 dichloride

**XOFIGO® IS AANBEVOLEN
IN DE LANDELIJKE RICHTLIJN
PROSTAATCARCINOOM 2016 ALS
EEN VAN DE BEHANDELOPTIES IN:**

- 1^e lijn (chemo-fit & niet chemo-fit)
- 2^e lijn (post-docetaxel)
bij mCRPC-patiënten met symptomatische
botmetastasen en geen bekende viscerale
metastasen⁴



The gold standard in diagnosing Bile Acid Diarrhoea (BAD)¹

SeHCAT test remains the clinical gold standard in diagnosing BAD

- A review article published by Gastroenterologists at Sahlgrenska University Hospital (Sweden) concludes: *BAD is common, and likely under-diagnosed. BAD should be considered relatively early in the differential diagnosis of chronic diarrhoea.*¹
- A pathway from Coventry University Hospital (UK) shows SeHCAT testing featuring early in the investigatory pathway in younger patients with normal faecal calprotectin.²

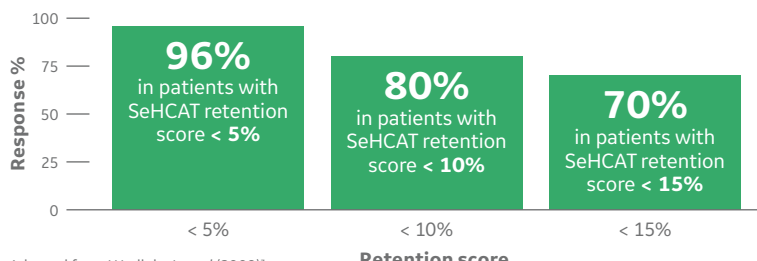
The types of bile acid diarrhoea¹

Diarrhoea caused by bile acids has historically been referred to as bile acid malabsorption; this description is, however, not entirely correct.

- **Type 1: bile acid malabsorption. In ileal disease,** there is true malabsorption of bile acids. This was the original mechanism to be identified, and was initially referred to as cholerheic enteropathy.
- **Type 2: idiopathic bile acid diarrhoea,** discovered in the 1970s and termed "**idiopathic bile acid catharsis**". Now known to be associated with **defective feedback inhibition** instead of malabsorption. This type is also known to be highly represented in patients with diarrhoea predominant irritable bowel syndrome (IBS-D).
- **Type 3: bile acid-induced diarrhoea** in association with **other** gastro-intestinal pathology which may or may not contribute to its pathogenesis, most prominently postcholecystectomy and in combination with microscopic colitis.

Studies have shown there is a relationship between the severity of the SeHCAT retention and the response to therapy³

Response to therapy in relation to SeHCAT retention score



Open the door
to freedom from
chronic diarrhoea



References:

1. Mottacki N, Simrén M, Bajor A et al. Aliment Pharmacol Ther 2016; 43 (8): 884-98.
2. Arasaradnam RP, Cullis J, Nwokolo C et al. Nuclear Medicine Communications 2012; 33: 449-51.
3. Wedlake L, A'hern R, Russell D et al. Aliment Pharmacol Ther 2009; 30 (7): 707-17.

See for product information elsewhere in this journal.

SeHCAT™
Tauroselcholic [⁷⁵Se] acid